CHARACTERIZATION OF SRC FAMILY KINASES AS POTENTIAL TARGETS FOR INTERVENTION IN VASCULAR ENDOTHELIAL GROWTH FACTOR -MEDIATED RETINAL NEOVASCULARIZATION

By

Xiang Qi Werdich

Dissertation

Submitted to the Faculty of the

Graduate School of Vanderbilt University

in partial fulfillment of the requirements

for the degree of

DOCTOR OF PHILOSOPHY

in

Cell and Developmental Biology

May, 2005

Nashville, Tennessee

Approved:

David M. Miller (Chair)

Ann Richmond

Jin Chen

Franco M. Recchia

John S. Penn

ACKNOWLEDGMENTS

I truly cherish my time in graduate school, when almost every part of my world was spinning around research. It is not just about earning the degree. It is more about how much I have learned. I am proud of what I have accomplished and deeply appreciate all those who have helped me enormously.

I own a tremendous debt of gratitude to my mentor Dr. John S. Penn. He helped me to build up my knowledge about molecular and cellular aspects of ocular angiogenesis. He guided me along my academic path during the last five years and his advice has been, and is continuing to be, essential for my success. I enjoyed very much the many opportunities which he created for me, whether it was to communicate with leading scientists, or to pursue my own ideas. He is a very kind and caring person, also giving me a lot of support in my personal life. I enjoy very much working with him, and my thanks to him will go beyond graduate school.

I want to thank my other committee members, Dr. David M. Miller, Dr. Ann W. Richmond, Dr. Jin Chen, Dr. Franco M. Recchia, and Dr. J. Donald M. Gass. I have benefited from their scientific and clinical knowledge and expertise during their lectures, even before they joined my committee. Their advice not only had a great impact on my research, but also shaped my views about science in general.

My experiments would have been more difficult, and sometimes even impossible if I did not have the help and support from many other people. First, I want to thank all current and former members of the Penn laboratory, especially Dr. Gary W. McCollum, Dr. Rong Yang, Dr. Lawrence E. Bullard, Kathleen A. Haddix, Jesse D. Kay, Jessica A.

Fowler, Joshua M. Barnett. I appreciate very much their assistance, and their companionship and friendship bringing many joyful and exciting moments into my daily "laboratory" life. Even a lot of people from outside of our lab also helped me during my time in graduate school, such as Dr. Abboud J. Ghalayini, Dr. Dawn M. Kilkenny, Mr. Richard D. Robinson, Dr. Vijay P. Sarthy, Dr. Robbert J. Slebos, Dr. Derya Unutmaz, and Dr. Sam K. Wells.

Graduate school is not only about science. I am enjoying every minute with my loving husband, Andreas. I still consider it a miracle that coming from opposite sides of this planet, we eventually found each other here at Vanderbilt University. With him by my side, my research has progressed much less stressful and more efficient. I always remember the night of Feb. 14, 2004 when Andy went with me to develop a Western blot. At that night, the result showed for the first time that RNA interference worked, and that was a great relief for me after trying so hard for such a long time. I was jumping and screaming! That was the best Valentine's-Day present that I ever had! So, graduate school is still all about science.

I owe my deepest thanks to my parents for their love and dedicated care from the moment when I was born. Their faith and wisdom have nurtured and guided me ever since. I also thank my sister and brother and their families for being with me always.

I am very grateful to my good friends who pulled me out of the lab in difficult times when nothing seemed to work. They have enriched my days at Vanderbilt with happiness and sunshine. Though being thousands of miles away from home, I have never felt lonely when they were around. We had a lot of fun, and I would like to thank them all for the good time and hope that the friendship will go on!

This dissertation was supported by National Institutes of Health (NIH) grants EY07533 and EY08126 (JSP), and a grant from Research to Prevent Blindness, Inc.

TABLE OF CONTENTS

LIST OF TABLES

LIST OF FIGURES

LIST OF ABBREVIATIONS

ANOVA	analysis of variance
BrdU	5-bromo-2'-deoxy-uridine
DAPI	4',6-diamidino-2-phenylindole
DNA	deoxyribonucleic acid
EDTA	ethylenedinitrilotetraacetic acid
ELISA	enzyme-linked immunosorbent assay
EST	expressed sequence tag
flk-1	fetal liver kinase-1
flt-1	fms-like tyrosine kinase-1
HRP	horseradish peroxidase
IgG	immunoglobulin-G
KDR	kinase-insert-domain-containing receptor
MEK	MAPK/Erk kinase
mRNA	messenger ribonucleic acid
PMSF	phenylmethylsulfonyl fluoride
SD	standard deviation
SEM	standard error of the mean

CHAPTER I

BACKGROUND AND SIGNIFICANCE

Pathological retinal angiogenesis (retinal neovascularization) is the leading cause of severe vision loss and irreversible blindness in developed countries, affecting people of all ages (1). It is the characteristic pathological event of diverse retinal diseases, such as diabetic retinopathy, retinopathy of prematurity (ROP), retinal vein occlusion, and sickle cell retinopathy. Gaining the ability to control retinal angiogenesis does not only benefit clinical therapy, but also has an enormous scientific appeal. Despite tissue specific aspects, retinal neovascularization shares many common features with other pathological angiogenic conditions, such as in tumorigenesis, rheumatoid arthritis and atherosclerosis (2). The eye, *per se*, constitutes an ideal model to study the molecular mechanisms of both physiological and pathological blood vessel growth. There exist various reliable animal models of ocular angiogenesis. Retinal vasculature can be accessed easily *in vivo* for manipulation and visualization. More importantly, genes can be selectively expressed in the retina (3). As a result, interest in ocular neovascularization is growing rapidly.

In 1950s, professor I. C. Michaelson pioneered the research of the development and pathophysiology of the retinal vasculature, and laid the groundwork for generations of ophthalmic scientists. The retina is nourished by two independent circulatory systems: retinal vasculature and choroidal vasculature. The inner (vitreous) half of the retina receives blood supply directly from the retinal vasculature. Arterioles and venules permeate the inner retina, forming a superficial capillary network just beneath the surface

of the retina and a deep network at the level of the inner nuclear layer. The outer (scleral) retina is completely avascular and receives oxygen and nutrients from the underlying choroidal circulation by diffusion (4). In infants born prematurely, retinal vascular development may be arrested by oxygen supplementation. In diseases, such as diabetes and sickle cell disease, normal retinal circulation may be interrupted by vessel atrophy or occlusion. These pathophysiological courses are often followed by proliferative retinal blood vessel growth. The new blood vessels can be either intraretinal or preretinal (i.e. growing into the vitreous cavity). The preretinal vessels are abnormal. They lack lumina and are prone to leak, which can result in vitreous hemorrhage, scarring, and tractional retinal detachment, leading to severe and permanent vision loss (3). The correlation of retinal ischemia and hypoxia of the nonperfused retinal tissue and the subsequent retinal neovascularization points to the presence of possible hypoxia-induced retinal angiogenic factor(s) (5,6).

During the last four-decades of research, vascular endothelial growth factor (VEGF, also referred to as VEGF-A) was defined as a primary candidate for driving ocular neovascularization, despite other factors which may also contribute (2). VEGF expression can be induced by hypoxia (7) in retinal cells (8,9). Its expression is both temporally and spatially correlated with ocular angiogenesis in animal models (10,11). Increased VEGF levels were found in ocular fluids from patients with various forms of retinal angiogenic conditions (12). Overexpression of VEGF in the mouse retina was shown to be sufficient to induce neovascularization (13).

During ischemia and hypoxia, the retina uses a common response pathway which is employed by most, if not all, tissues to activate specific genes to deal with the crisis and

restore oxygen homeostasis, for example, by restructuring blood supply. Deregulation of this pathway can lead to retinal neovascularization (14). Reduced oxygen tension is sensed possibly by a cytosolic membrane bound heme protein (15), which activates transcription factor hypoxia inducible factor-1 (HIF-1) (16) via a signaling cascade involving protein phosphorylation (17,18). HIF-1 is an α/β heterodimer, which serves as a central regulator of hypoxic gene expression. By binding to the targeted genes, it stimulates the transcription of multiple genes that are upregulated under hypoxia, including VEGF (14).

VEGF (or VEGF-A) belongs to a gene family which also includes VEGF-B, VEGF-C, VEGF-D, and placental growth factor (PLGF). As the prototype member of this gene family, VEGF is a key regulator of blood vessel growth. VEGF-C and VEGF-D regulate lymphatic angiogenesis (19). VEGF is a heparin-binding homodimeric glycoprotein of 45 kDa (20). It exists in at least six isoforms (121-, 145-, 165-, 183-, 189-, and 206-amino acid isoforms) in human (19,21,22), and three isoforms (120-, 164-, 188-amino acid isoforms) in the rodent (23). These isoforms are generated via alternative splicing from a single VEGF gene. While $VEGF_{121/120}$ is freely diffusible, $VEGF_{189/188}$ and $VEGF_{206}$ are primarily associated with the cell surface and the extracellular matrix (ECM). $VEGF_{165/164}$ has both properties, as a fraction is diffusible while some is sequestered (24). The ECM-bound VEGF isoforms may be released to generate bioactive fragments (25). Different VEGF isoforms possess distinct functions in vascular development (26-28). $VEGF_{165/164}$ may play an important role in pathogenesis of retinal neovascularization (29,30).

In endothelial cells, the biological effects of VEGF are mediated through its high

affinity receptors, VEGFR-1 (flt-1) and VEGFR-2 (KDR in human/flk-1 in the rodent) (31-34). VEGF receptors belong to the superfamily of tyrosine kinase receptors. Both receptors have seven immunoglobulin-like domains in the extracellular region, a single transmembrane domain, and a split intracellular tyrosine kinase domain (35-37). VEGFR-2 is the major mediator of biologically-relevant VEGF signaling in endothelial cells (19,38-40). Stimulation of endothelial cells with VEGF leads to receptor dimerization and autophosphorylation. Activated VEGF receptors subsequently initiate intracellular signal transduction cascades which consist of a battery of signal molecules, such as phospholipase C-γ (PLC-γ), phosphoinositide 3′-kinase (PI 3-kinase), Ras GTPase-activating protein (GAP), and mitogen-activated protein kinase (MAPK), and focal adhesion kinase (FAK), among others. Initially identified as a vasopermeability factor, VEGF exerts profound impact on multiple facets of endothelial cell function, such as proliferation, chemotaxis, survival and differentiation (Figure 1.1) (41,42).

As membrane-attached nonreceptor protein tyrosine kinases, broadly expressed Src family kinases (SFKs) link a variety of extracellular cues to intracellular signal pathways (43). Family members Src, Fyn and Yes are often coexpressed, such as, in vascular endothelial cells (43-45). Recent studies revealed that SFKs were involved in both hypoxia-induced VEGF expression in cancer cells (18) and VEGF signaling in endothelial cells (46-48). However, their roles in pathological angiogenesis, such as VEGF-mediated retinal neovascularization, are unknown.

Src was first identified as the transforming protein (v-Src) of the oncogenic retrovirus, Rous sarcoma virus (RSV) (49). Its highly conserved cellular homologs (43) are ubiquitously expressed. So far, nine SFK members have been identified. Src, Fyn and

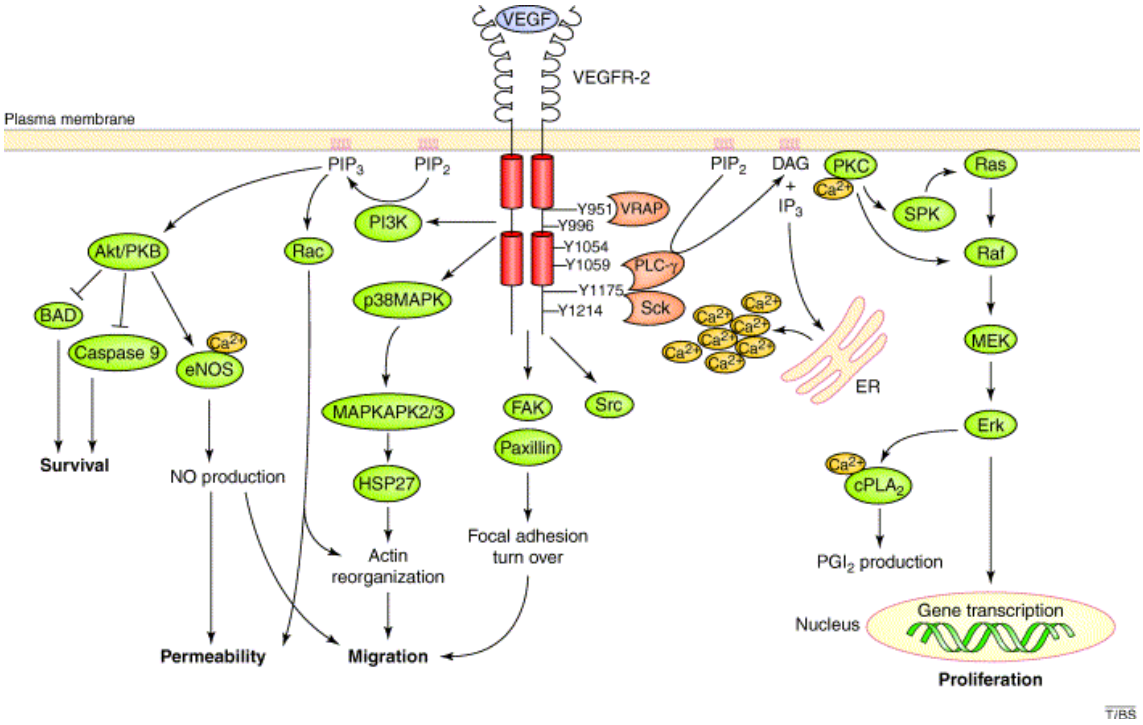

Figure 1.1. Schematic illustration of VEGFR-2 intracellular signaling. Downstream signal transduction molecules carry a propagating signal regulating several different endothelial cellular functions such as survival, permeability, migration and proliferation. Abbreviations: $cPLA_2$, cytosolic phospholipase A_2; eNOS, endothelial nitric oxide synthase; Erk, extracellular regulated kinase; HSP27, heatshock protein 27; MAPKAPK 2/3, MAPK-activating protein kinase-2 and 3; NO, nitric oxide; PGI_2, prostacyclin; PIP_3, phosphatidylinositol (3,4,5)-trisphosphate; Sck, Shc-like protein; SPK, sphingosine kinase. (Cross MJ et al. *Trends Biochem Sci* 2003, 28:488-494)

Yes are broadly expressed, while, others (e.g. Hck, Blk, Lck) have more restricted expression patterns and are present only in certain tissues. SFKs are 52 to 62 kDa proteins consisting of six distinct functional domains: a) a lipid modified Src homology (SH) 4 domain, which is involved in targeting SFKs to cellular membranes; b) a unique domain, which is distinct for each member; c) a SH3 protein-binding domain; d) a SH2 protein-binding domain; e) a catalytic domain, which possesses tyrosine-specific protein kinase activity; and finally f) a short negative regulatory carboxyl terminal tail. The kinases are maintained inactive by intramolecular interactions of SH3 and SH2 domains

with amino acids located within and adjacent to the catalytic domain. The association of the SH2 domain with phospho-Tyr527 in the negative regulatory tail is particularly important for suppressing kinase activity in some SFKs. These intramolecular interactions can be regulated by membrane-linked receptors and docking proteins. Once this “closed” configuration is "opened", the intrinsic SFK tyrosine kinase activity is activated by phosphorylation of a key tyrosine residue (Tyr416) in the catalytic domain (43). The phosphorylation state of Tyr416 is directly correlated with SFK catalytic activity (50). SFKs are involved in signal transduction pathways of a diversity of receptors, such as immune recognition receptors, integrin and other adhesion receptors, and receptor protein tyrosine kinases (RPTKs), and facilitate cross talk between these receptors. SFKs can also be activated in response to stress, such as during ultraviolet C irradiation, heat, or hypoxia. These kinases regulate a variety of cellular events, including cell growth, survival and differentiation, cytoskeletal arrangement, migration, gene transcription and other biological activities (43).

It is known that coexpressed SFKs (e.g. Src, Fyn and Yes) often play redundant roles; deficiency in one SFK member can be compensated by others (43,51). However, knockout mice deficient in one or more SFKs revealed that Src, Fyn or Yes was likely to possess unique functions as well (51). Particularly, Eliceiri and colleagues demonstrated that Src- or Yes-, but not Fyn-, deficient mice displayed impaired VEGF-induced vascular permeability (46). Systemic administration of PP1 (a broad spectrum SFK inhibitor) to mice showed the potential to prevent secondary tissue damage from increased VEGF-mediated vascular permeability [e.g. in the pathophysiolology of stroke (52)]. In the eye, VEGF-mediated vascular permeability is notoriously responsible for

extravasation in both proliferative retinopathy, and many nonproliferative pathological conditions, such as aphakic/pseudophakic cystoid macular edema, retinoblastoma, and ocular inflammatory disease (3,13,53,54). Thus, selective inhibition of Src or Yes in the eye may greatly reduce many types of ocular edema.

In summary, pathological retinal angiogensis shares many features with physiological retinal vascularization. Blocking common pro-angiogenic events would potentially endanger existing vasculature and compensatory intraretinal revascularization. Thus, ophthalmic scientists are eagerly searching for new therapeutic strategies that can selectively target pathological neovascularization. SFKs are involved in both the hypoxia-induced VEGF expression pathway and the VEGF downstream signaling pathway. Family members likely play differential roles in these cellular events. Thus, those SFK members which actively contribute to the pathogenesis of a disease may be selectively targeted for inhibition, while avoiding members that are essential for maintaining physiological functions. The goal of this dissertation is to dissect and characterize molecular mechanisms and biological functions that are regulated by SFKs and related to retinal neovascularization. Our intention is to contribute to the scientific and clinical knowledge of VEGF- and SFK-mediated biological events.

CHAPTER II

VARIABLE OXYGEN AND RETINAL VEGF LEVELS: CORRELATION WITH INCIDENCE AND SEVERITY OF PATHOLOGY IN A RAT MODEL OF OXYGEN-INDUCED RETINOPATHY

Xiang Q. Werdich, Gary W. McCollum, Veera S. Rajaratnam, and John S. Penn

Department of Ophthalmology and Visual Sciences

Department of Cell and Developmental Biology

Vanderbilt University School of Medicine, Nashville, TN 37232

This manuscript has been published in:

Experimental Eye Research

Vol. 79, pp. 623-630, November 2004

2.1. Abstract

Retinal capillary quiescence is regulated by a delicate balance between proangiogenic and anti-angiogenic factors. Pathological angiogenesis is the result of a shift in this balance towards proangiogenic influences. Retinal neovascularization is produced in a rat model of oxygen-induced retinopathy (OIR) by exposing newborn rat pups to alternating periods of hyperoxia and hypoxia. Based upon previous work, two similar exposure paradigms were investigated and compared, exposure of rat pups to alternating periods of 45 and 12.5% oxygen, and to alternating periods of 40 and 15% oxygen. The resulting retinal pathology was assessed by measurement of retinal clock hours with pathological blood vessel growth and the percentage of the retina that is avascular. The 45 and 12.5% exposure produced significantly greater incidence and severity of pathology than the 40 and 15% protocol. To explain the difference in pathology between these two very similar exposure protocols, retinal levels of proangiogenic VEGF and VEGFR-2 and anti-angiogenic pigment epithelium-derived factor (PEDF) were measured by ELISA and western blot analysis at 0, 2, and 6 days post-exposure. In whole retinal lysates, there were no significant differences in VEGFR-2 and PEDF levels. However, VEGF levels were approximately 48 and 78% higher on post-oxygen exposure day 0 and 2, respectively, in the group treated with alternating periods of 45 and 12.5% oxygen compared to the group treated with alternating periods of 40 and 15% oxygen. There was no significant difference in VEGF levels between these two groups on day 6 post-exposure. Therefore, the difference in pathology observed between these two experimental paradigms is associated with differences in whole retinal VEGF levels, but not changes in whole retinal VEGFR-2 or PEDF levels. The results of this study suggest

the existence of a threshold in the rat model of OIR, such that a small change in blood oxygen profile triggers a disproportionate increase in subsequent neovascularization, which is accompanied by more dramatic changes of retinal VEGF level than VEGFR-2 or PEDF level. If a similar threshold exists for humans, it could explain why some oxygen-treated premature infants develop retinopathy and others do not, despite similar gestational ages, birth weights and clinical courses.

2.2 Introduction

Several lines of evidence indicate that the progression of pathologic and physiologic angiogenesis is tightly controlled by a balance of pro-angiogenic and anti-angiogenic stimuli (55,56). VEGF stimulates endothelial cell proliferation and tube formation *in vitro* and is a major pro-angiogenic factor *in vivo* (57-60). Elevated levels of VEGF have been associated with animal models of, as well as humans affected with, ocular vasoproliferative disease (12,55,58,61). VEGF binds and activates two receptor tyrosine kinases, VEGFR-1/Flt-1 and VEGFR-2/KDR/Flk-1 (60). Experimental evidence suggests that VEGFR-2 contributes to the angiogenic phenotype by stimulating the MAP kinase pathway necessary for endothelial cell proliferation, an essential component of angiogenesis (62).

PEDF, originally isolated from the conditioned media of retinal pigment epithelial cells, displays neurotropic activity and is one of the most potent naturally occurring inhibitors of angiogenesis (63-65). PEDF inhibits endothelial cell proliferation *in vitro* and blood vessel growth in the eye (56). PEDF inhibits VEGF induced corneal neovascularization (65) and pathologic retinal angiogenesis in ischemia-induced

retinopathy of the mouse (66). Evidence to date suggests that PEDF manifests its anti-proliferative effects by promoting endothelial cell apoptosis (67).

ROP is a potentially blinding disease generally restricted to low birth weight infants sustained by oxygen therapy (6,68). The pathogenesis of human ROP is biphasic, starting with vasoattenuation related to hyperoxygenation of the neonatal retina, followed by retinal vasoproliferation (69). Dysregulated angiogenesis is constitutive of the vasoproliferative phase leading to the growth of retinal blood vessels through the inner limiting membrane into the vitreous cavity. This preretinal growth of vessels can lead to vitreous hemorrhage and tractional retinal detachment (70). A rat model has been developed that approximates the pathology of ROP and is reliable in terms of the development of this vasoproliferative response (71). The model consists of exposing newborn rat pups to alternating periods of hyperoxia and hypoxia. In a previous study, several exposure protocols were investigated and resulted in variable levels of disease incidence and severity (72). In particular, two very similar exposure protocols yielded widely disparate pathologic outcomes. One protocol involved exposing newborn rat pups to alternating periods of 45% oxygen (hyperoxia) and 12.5% oxygen (hypoxia), and in the other the oxygen levels were alternated between 40 and 15% (Figure 2.1). The '45/12.5%' exposure led to significantly greater disease incidence and severity than the '40/15%' treatment, despite the modest difference in the oxygen concentrations between the two exposure protocols.

In this study we repeated these two oxygen treatments, and again observed highly significant differences in pathology between the two groups of rats. We then measured the VEGF, VEGFR-2 and PEDF retinal protein levels over time post-exposure to

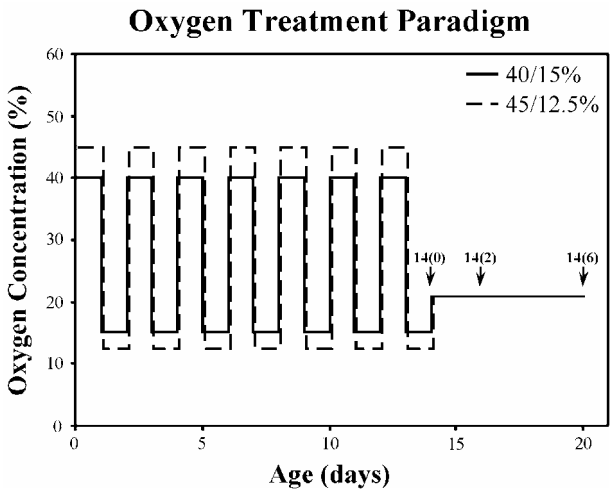

Figure 2.1. A real-time plot of the 45/12.5 and 40/15% oxygen exposure regimen. Arrows designate times at which rats were sacrificed and analyzed.

determine if the disproportionate differences in pathology between these two exposure paradigms could be related to differences in protein levels of the pro-angiogenic VEGF and VEGFR-2 and/or the anti-angiogenic PEDF.

2.3 Materials and Methods

Oxygen treatment

Within 4 hr after birth, normalized litters of 16 Sprague-Dawley rat pups each were placed with nursing dams in Isolette® infant incubators, and subjected to one of two similar variable oxygen exposure protocols. The first was performed by cycling newborn rats between 40% oxygen for 24 hr and 15% oxygen for 24 hr for seven cycles and is referred to as the 40/15% protocol. The second protocol was similar except the hyperoxic episodes were 45% oxygen and the hypoxic episodes were 12.5% oxygen and is referred

to as the 45/12.5% protocol (Figure 2.1). The term ΔFiO_2 used in Tables 2.1 and 2.2 designates the difference in the two oxygen concentrations to which a treatment group was subjected, applying the units of fraction of inspired oxygen (i.e. $\Delta FiO_2 = 0.25$ for exposure to alternating 40 and 15% oxygen). Use and treatment of animals conformed to the Declaration of Helsinki principles.

Table 2.1. Body weights of newborn rat pups after variable oxygen treatment.
* Significantly different between 40/15 and 45/12.5% treatments, $p < 0.05$.
** Significantly different between room air and both oxygen-treated groups, $p < 0.05$.

		Body weights (g) (mean ± SD)		
Treatment (sample size)	**ΔFiO_2**	**Day 14(0)**	**Day 14(2)**	**Day 14(6)**
40/15% (n = 20)	0.250	21.7 ± 3.2	29.6 ± 2.7	35.3 ± 5.0
45/12.5% (n = 24)	0.325	19.8 ± 1.3	26.0 ± 2.1*	33.2 ± 5.3*
Room air (n = 8)		25.9 ± 2.3**	33.7 ± 1.6**	45.6 ± 3.2**

Table 2.2. Effects of variable oxygen treatments on retinopathy.
40/15 and 45/12.5% treatments were compared with each other. The percentages of the retina that is avascular were compared within each method, not between methods. * $p < 0.05$, ** $p < 0.005$.

Treatment (sample size)	ΔFiO_2	Method	Retinal avascular area (% of total retinal area) (mean ± SD)			Retinopathy		
			Day 14(0)	Day 14(2)	Day 14(6)	Incidence (%)	Severity (clock hours)	
40/15% (n = 68)	0.250	**ADPase**	8.3 ± 4.8	3.5 ± 3.5	0.1 ± 0.7	13.6	**Median**	0
		FITC	14.6 ± 6.6	6.6 ± 4.4	2.2 ± 1.5		**Range**	0 - 2
45/12.5% (n = 57)	0.325	**ADPase**	15.7 ± 6.1**	11.1 ± 7.4**	2.6 ± 4.3**	78.3**	**Median**	2**
		FITC	23.8 ± 4.7*	13.4 ± 7.2*	5.8 ± 3.0		**Range**	0 - 9

Tissue histochemistry

Animals from the 40/15 and 45/12.5% treatment groups were removed to room air after the 14th day of oxygen treatment, hereafter referred to as day 14(0). The degree of retinal avascularity of animals from the two exposure groups was measured at day14(0) and at 2 and 6 days post oxygen exposure, hereafter referred to as day 14(2) and 14(6), respectively. The retinal avascular areas were assessed by two methods: visualization of the retinal vasculature using infusion of fluorescein isothiocyanate (FITC)-conjugated dextran and adenosine diphosphatase (ADPase) staining (Figure 2.2). Animals from each

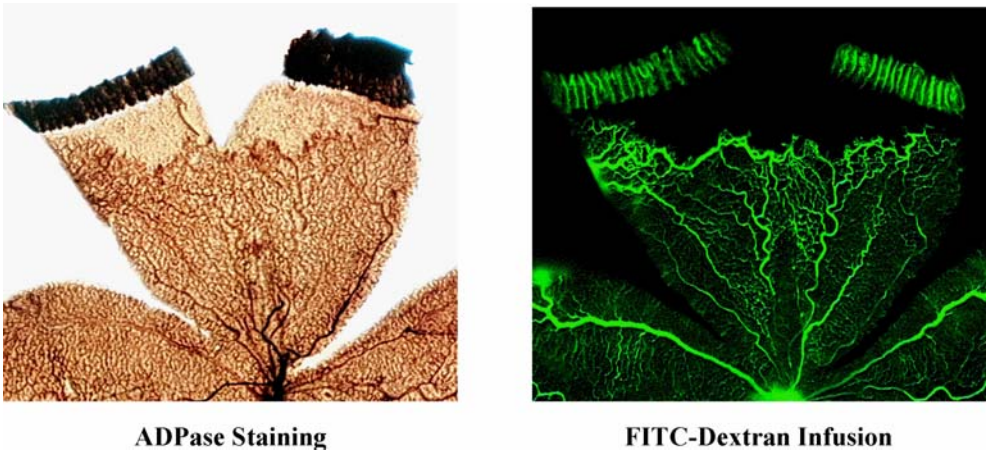

Figure 2.2. Demonstration of retinal avascular area assessed by ADPase staining and FITC-dextran infusion. The retina was harvested from the 45/12.5% oxygen-treated group on day 14(2).

exposure group were deeply anesthetized by isoflurane (Baxter, Deerfield, IL) inhalation. Right retinas were extruded for VEGF ELISA assay and Western blot analysis, and the central retinal artery and vein were clamped with hemostats. Then 40 µl of a calcium- and magnesium-free phosphate-buffered saline (PBS; Gibco, Rockville, MD) solution containing 9.0 mg of FITC-dextran, average molecular weight of 145 000 Da (Sigma, St.

Louis, MO), was infused through the left ventricle as previously described (71). The rats were sacrificed by decapitation and the left neural retinas were dissected and flat-mounted. After evaluation of the retinal avascular area (see below), the same retinas were then placed in 10% (v/v) neutral buffered formalin (NBF). The 10% (v/v) NBF solution was prepared by dissolving 50 ml of a 37% formaldehyde solution (Fisher, Fair Lawn, NJ) in PBS to a total volume of 500 ml. The vasculature of each retina was stained using a histochemical method for detecting ADPase, according to a previously described procedure (73) adapted for use here (74). The stained retinas were then whole-mounted onto slides.

Assessment of retinal avascularity and pathology

After FITC-dextran infusion, images of flat-mounted retinas were observed with an Olympus fluorescence microscope (Olympus, Melville, NY) and captured digitally with a Polaroid DMC digitizing camera (Polaroid, Cambridge, MA) coupled to a G4 Macintosh computer (Apple, Cupertino, CA) utilizing Adobe Photoshop 5.0 (Adobe, San Jose, CA). After ADPase staining, the retinal avascular areas were re-evaluated. Images of the ADPase-stained retinas were digitized and captured in the same format as described above, except that a zoom stereomicroscope with an illumination base (Olympus) was used. The vascularized retinal areas and the total retinal areas of all retinal images were traced on the computer monitor face with an interactive stylus pen (FT Data Systems, Stanton, CA). The operator was masked with respect to the treatment. The vascularized retinal areas and the total retinal areas were converted from pixels to mm^2 with image analysis software (Enhance 3.0; Microfrontier, Des Moines, IA). Then the retinal

avascular areas were calculated and the values are expressed as the percentage of total retina for each treatment group (mean ± SD) at each time point for each of the two staining methods. The retinas of age-matched room air controls were fully vascularized.

Abnormal preretinal neovascularization was assessed using the clock hour method previously described by others and us (62), using flat-mounted ADPase stained retinas dissected on day 14(6). Three trained observers evaluated the number of clock hours with abnormal blood vessel growth for each retina. The data were averaged from the three separate determinations for each retina and are expressed in values varying from 0 (no pathology) to 12 (involvement of entire retinal circumference). The retinas of age-matched room air rats showed no pathology.

VEGF enzyme immunoassay

Retinal tissues from the right eyes of animals sacrificed on day 14(0), 14(2) and 14(6) were frozen at -80°C immediately after extrusion. They remained frozen for 2-18 hr. The thawed retinas were sonicated in tris-buffered saline (TBS) containing protease and phosphatase inhibitors (50 mM Tris-HCl, 150 mM NaCl, 1 mM EDTA, 1 mM PMSF, 1 μg/ml aprotinin, 1 μg/ml leupeptin, 1 μg/ml pepstatin A, 1 mM Na_3VO_4, 1 mM NaF, PH 7.4) (Sigma). After centrifugation, supernatants were collected for experiments. The protein concentration of samples was measured by the bicinchoninic acid assay (BCA; Pierce, Rockford, IL). A VEGF colorimetric sandwich ELISA kit (R&D Systems, Minneapolis, MN) was used for retinal VEGF determination according to the manufacturer's instructions. The final mass of retinal VEGF was standardized to total retinal protein.

Western blot analysis

Polyclonal anti-VEGFR-2 antibody was purchased from Santa Cruz Biotechnology (Santa Cruz, CA). Polyclonal anti-PEDF antibody was purchased from BioProducts Maryland (Middletown, MD). Monoclonal antibody against β-actin, which was used as a gel loading control, was purchased from Sigma. Anti-rabbit or mouse HRP antibody (Promega, Madison, WI) was used as a secondary antibody. Retinal homogenates above were resolved by sodium dodecyl sulfate-polyacrylamide gel electrophoresis (SDS-PAGE) using 10% SDS-PAGE minigels (Bio-Rad, Hercules, CA). Proteins were then transferred to 0.2 μm nitrocellulose membrane (Bio-Rad). After incubation in the blocking buffer, TBS with 0.1% Tween-20 (Sigma) and 5% nonfat dry milk (Bio-Rad), for 30 min at room temperature, membranes were rinsed with TBS and incubated with the primary antibody in the blocking buffer overnight at 4°C. Then, membranes were washed with TBS and incubated with the secondary antibody in blocking buffer for 2 hr at room temperature. After thorough washing, the proteins were visualized with enhanced chemiluminescence (Amersham, Piscataway, NJ). Membranes were also stripped and reprobed for β-actin. Experiments were repeated three times.

Data analysis

Data were analyzed with Stat View software (Abacus Concepts, Berkeley, CA). The ANOVA statistical test was used to analyze parametric data of animal body weight and retinal VEGF concentration. Digitized images of Western blots were subjected to quantification with National Institutes of Health (NIH) Image software (Bethesda, MD). Raw densitometry values of VEGFR-2 and PEDF were normalized against that of β-

actin. These data were subsequently analyzed with the ANOVA test. The percentages of the retina that is avascular were converted with the arcsine transformation and subsequently analyzed with the Kruskal-Wallis statistical test. The retinopathy data assessed by the clock-hour method were analyzed with the non-parametric Mann-Whitney test. For each test, $p < 0.05$ was considered significant.

2.4 Results

Body weight

Room air animals had significantly higher body weight than either of the oxygen-treated groups at all three ages tested (Table 2.1). The body weight of the 40/15% group was significantly higher than that of the 45/12.5% group on day 14(2) and 14(6). However, there was no significant difference between them on day 14(0).

Retinal avascularity

As shown in Table 2.2, the average percentage of the retina that is avascular for the 45/12.5% treatment group was consistently and significantly higher ($p < 0.005$) than that of the 40/15% treatment group at each of the three time points examined using ADPase staining. Statistical significance was also achieved at day 14(0) and 14(2) using FITC-dextran infusion ($p < 0.05$). ADPase staining demonstrated a similar pattern of retinal avascular area as FITC-dextran infusion (Figure 2.2), but yielded values for the average percentage of avascular retinal area that were consistently lower than FITC-dextran infusion (Table 2.2). This is reasonable, as the FITC-dextran infusion technique assesses

retinal area associated only with the perfused vasculature, while the ADPase surface stain marks both perfused and non-perfused vessels. The retinas of rat pups raised in room air already reached complete vascularization on day 14(0).

Retinal neovascularization

Retinal neovascularization was assessed on day 14(6). A significant difference in incidence and severity between the 45/12.5 and 40/15% treatment groups was observed (Table 2.2, Figure 2.3). In the 45/12.5% treatment group, 78.3% of the rat pups displayed some level of preretinal neovascularization compared to 13.6% in the 40/15% treatment group. The level of severity, as measured by clock hours containing preretinal neovascularization, showed a range of 0 - 9 and a median of 2 for the 45/12.5% group

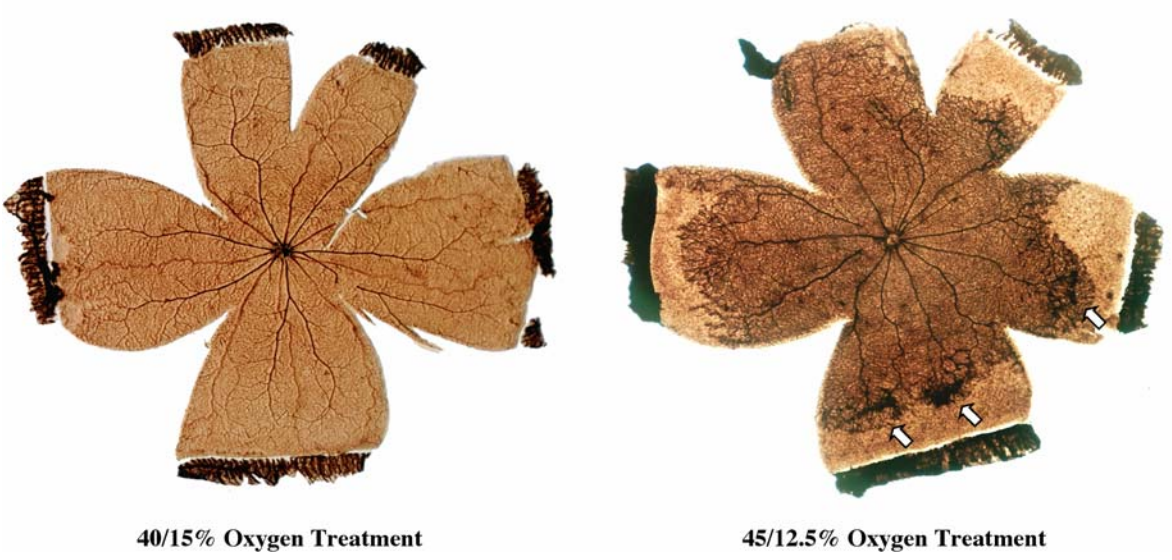

Figure 2.3. Comparison and demonstration of retinopathy in ADPase-stained retinas from rats treated with the 45/12.5 or the 40/15% oxygen exposure regimen. Retinas were harvested on day 14(6). The 45/12.5% rats had larger avascularity and more retinopathy (arrows) than 40/15% animals.

and a range of 0 - 2 and a median of 0 for the 40/15% group ($p < 0.005$). There was no retinal pathology observed in rat pups raised in room air.

Retinal VEGF concentration

As shown in Figure 2.4, on day 14(0), retinal VEGF level in the 45/12.5% group is as high as 1.5-fold of that in the 40/15% group ($p = 0.005$). Both are significantly higher than room air controls ($p < 0.005$). On day 14(2), retinal VEGF concentrations of both oxygen-treated groups decreased, compared to those of day 14(0). There was no significant difference between the 40/15% group and room air control. However, VEGF level in the 45/12.5% group remained significantly higher level, about 1.8-fold of that of

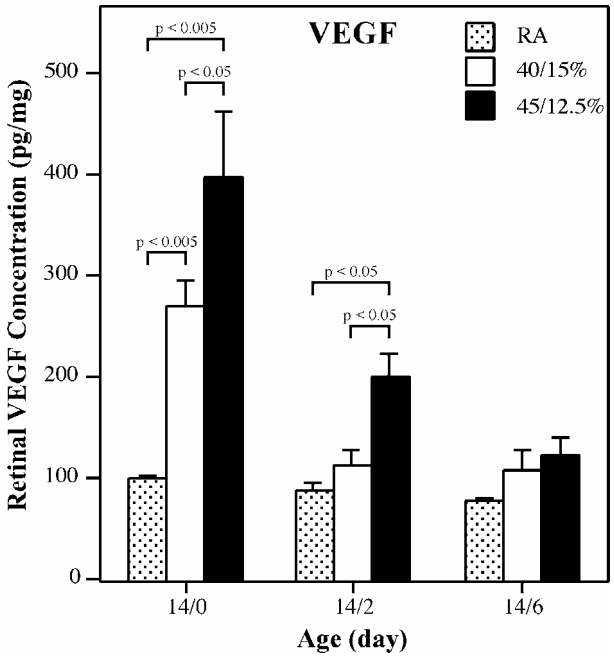

Figure 2.4. Retinal VEGF levels in rats treated with the 45/12.5 (n = 24) or the 40/15% (n = 20) oxygen exposure regimen, and in room air controls (n = 8). Data on each time point tested were compared between the 45/12.5 and 40/15% treatments, and between room air control and 45/12.5 or 40/15% treatment. Significant differences are demonstrated with *p* value.

the 40/15% group ($p < 0.05$). On day 14(6), there was no significant difference between any of the experimental groups. There was also no significant difference in retinal VEGF levels in room air rat pups over the time-course of this experiment.

Retinal VEGFR-2 and PEDF expression

Western blot analysis of whole retinal lysates shows that the VEGFR-2 levels in the 45/12.5 and 40/15% groups were not significantly different from each other at any of the time points tested, either by direct comparison of β-actin-normalized densitometry values (Figure 2.5, a and b) or after further normalization to retinal vascular area (data not shown). The latter method was based upon the notion that the greater the vascular area and density, the greater the expected level of VEGFR-2 in whole retinal lysate. Previous studies showed a significant increase of VEGFR-2 in OIR (75,76). In this study, whole retinal VEGFR-2 level in the room air group on day 14(0) was significantly higher than that in either oxygen-treated group, likely because the substantially greater vessel coverage and density in room air controls masked any of the local differences of VEGFR-2 in room air and oxygen-treated eyes. Retinal PEDF levels did not show significant differences among all three groups in the three tested points (Figure 2.5, a and c).

2.5 Discussion

The incidence and severity of ROP in premature human infants is highly correlated with variability in arterial blood oxygen levels during oxygen therapy (77-79). The partial pressure of oxygen in arterial blood can fluctuate rapidly in sick premature infants, leading to alternating episodes of severe and extended hyperoxemia and hypoxemia (79).

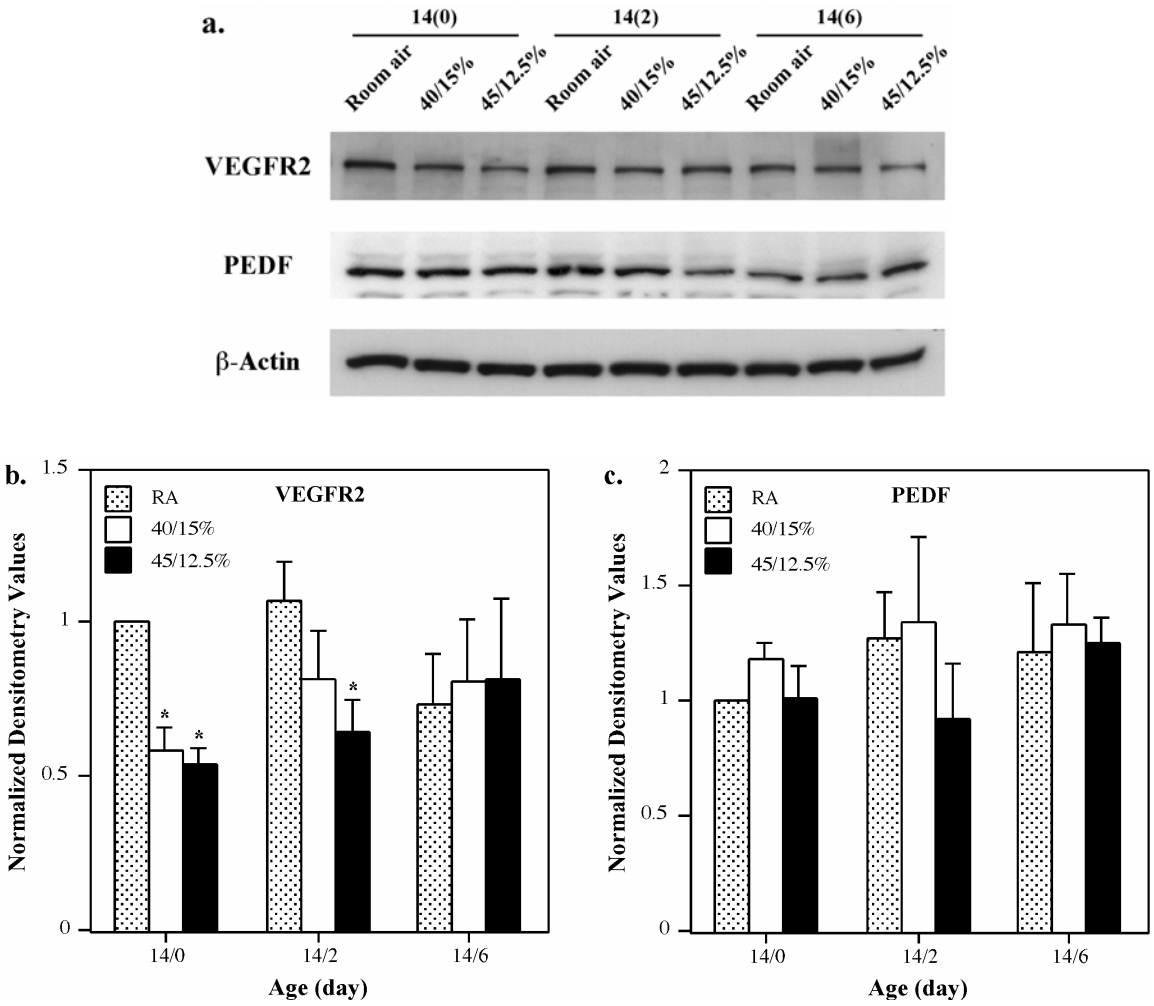

Figure 2.5. Retinal VEGFR-2 and PEDF protein expression levels in whole retinal lysates from rats treated with the 45/12.5 or the 40/15% oxygen exposure regimen, and from room air controls. a, Western blots demonstrate retinal VEGFR-2 and PEDF protein expression level. b, Densitometry analysis reveals no significant difference of VEGFR-2 levels between the 45/12.5 and 40/15% groups on day 14(0), 14(2), and 14(6). *, significantly different from room air control, $p < 0.05$. c, Densitometry analysis shows retinal PEDF levels of oxygen-treated rats and room air controls were not significantly different from each other at all three time points tested under ANOVA statistical test, $p > 0.05$.

Frequently, these events are related to the infant's underlying disease (e.g. patent ductus arteriosus, apnea, metabolic acidosis and bronchopulmonary dysplasia), but they may also be simply the result of routine medical and nursing intervention (79).

Mimicking these conditions, newborn rats that experience alternating cycles of ambient hyperoxia and hypoxia show a significant increase in the prevalence and consistency of the vasoproliferative response when compared to newborn rats that experience constant ambient hyperoxia or variable ambient hyperoxia (71,72,74). Furthermore, it has been previously shown that cyclic variation of 50 and 10% inspired oxygen translates into variable arterial blood oxygen levels in these rats which mimic the variable arterial blood oxygen levels of premature humans undergoing oxygen therapy in whom ROP is likely to develop (72). The results of these studies indicate that episodic ambient hypoxia during oxygen treatment promotes the production of a robust neovascular response in rats.

The two exposure paradigms that were repeated in this study, namely 40/15 vs. 45/12.5%, yielded disproportionate degrees of pathology despite the relatively small difference in oxygen concentrations used (Figure 2.1, Table 2.2). As before (72), the 45/12.5% protocol resulted in significantly higher incidence and severity of pathology when compared to the 40/15% exposure protocol (see Section 2.4). To investigate possible mechanisms that might explain the observed difference in pathological outcomes, we measured the retinal levels of pro-angiogenic VEGF and VEGFR-2 and anti-angiogenic PEDF in animals from these two treatment protocols over time post-oxygen exposure. The retinal VEGF levels of the 45/12.5% group were significantly higher on both day 14(0) (48%) and 14(2) (78%) than the 40/15% group. Although significant higher on day 14(0), retinal VEGF level in the 40/15% group on day 14(2) was not significantly different from that of the room air control. The VEGFR-2 and PEDF retinal levels of these two groups were not significantly different from each other

at any of the time points tested. Even though on day 14(2), PEDF in the 45/12.5% group trended towards difference from room air control and 40/15% animals, it is not significant under statistical test, $p = 0.250$ and 0.172 respectively. Based on these data, it is reasonable to suggest that the greater pathology observed in the 45/12.5% group is associated with a higher and longer retinal VEGF elevation observed post-oxygen exposure than in the 40/15% group. Additionally, VEGF, VEGFR-2, and PEDF were measured in whole retinal lysates. It is likely that although there may be significant local increase of retinal VEGF and VEGFR-2 levels (i.e. VEGFR-2 up-regulation in vascular tufts) (75,76) or possible local decrease of retinal PEDF level, in whole retinal lysates changes of VEGFR-2 or PEDF proved not as dramatic as that of VEGF. This may indicate a larger extent of global changes of retinal VEGF level than VEGFR-2 and PEDF levels.

VEGF is induced by hypoxia (58). It is possible that the higher retinal VEGF levels in the 45/12.5% treatment group at the time of removal of these animals to room air on day 14(0) are related to the episodes of more extreme ambient hypoxia (i.e. 12.5 vs. 15%) experienced by this group during oxygen treatment. The difference in retinal VEGF on day 14(2), however, may be related to the greater avascular area observed in the 45/12.5% treatment group. It has previously been hypothesized that the retinal avascular area becomes hypoxic on removal to normoxia, stimulating the synthesis of hypoxia-inducible factors such as VEGF (80-84). Therefore, the 45/12.5% group would likely produce more retinal VEGF post-oxygen exposure.

Investigators have proposed that the dominant neovascular stimulus in oxygen induced proliferative retinopathies is produced post-oxygen exposure by the avascular

retina (5,6,81,85). There are data that are consistent with this view. For example, in a mouse model of OIR, post-oxygen retinal VEGF mRNA levels were 50% compared to room air controls and increased six-fold by 24 hr post-exposure (86). However, in our rat model with variable oxygen exposure, it is obvious that both oxygen treatment and post-exposure retinal avascular area contribute to the onset of retinopathy. Although in this study it is not clear yet whether the high level of VEGF immediately after oxygen exposure is due to a cumulative effect of multiple episodes or simply one episode of hypoxia, robust neovascular stimulus is evident at the end of the oxygen treatment. This neovascular stimulus is even greater than the later one caused by retinal avascular area, since the retinal VEGF levels at 14(0) are about 2-fold of those at 14(2) in both 45/12.5 and 40/15% groups. It is important to note that 65% of preterm infants that receive oxygen therapy develop threshold ROP during the course of the therapy (Dale Phelps, personal communication, information derived from the STOP ROP trial; 2004). Clearly, a pro-angiogenic stimulus may develop before removal to room air and play a significant role in the pathogenesis of ROP.

In this study, similar oxygen exposure protocols resulted in significantly different pathologic outcomes that correlate with a difference in retinal VEGF levels in a rat model of OIR. Collectively, these data substantiate the notion that retinal VEGF levels may represent an index for the development of ischemia-induced retinal angiogenesis that may have bearing on human ROP. Furthermore, our studies suggest the existence of a threshold of variable oxygen concentrations in a rat model of OIR, which results in a disproportionate increase in subsequent neovascularization. Underlying the discrepancy, we observed a dramatic change of retinal VEGF level but not VEGFR-2 or PEDF level in

whole retinal lysates. If there is a similar event in human, this study may shed light on understanding why some premature infants develop ROP and others do not, even when the two experience similar clinical courses.

This work was supported by NIH grants EY07533 and EY08126 (JSP) and a grant from Research to Prevent Blindness, Inc.

CHAPTER III

VEGF INDUCTION BY HYPOXIA IN MÜLLER CELLS

Xiang Qi,[1] Vajay P. Sarthy,[2] and John S. Penn[1]

[1]Department of Ophthalmology and Visual Sciences

Department of Cell and Developmental Biology

Vanderbilt University School of Medicine, Nashville, TN 37232

[2]Department of Ophthalmology

Northwestern University School of Medicine, Chicago, IL 60611

Portions of this manuscript have been published in:

Investigative Ophthalmology and Visual Science

Vol. 45, pp. 1887, May 2004

3.1 Abstract

VEGF-mediated retinal angiogenesis includes both VEGF induction and signal transduction cascades. To date, much more effort has been spent on understanding and intervening in VEGF downstream signaling than on the upstream induction pathway. In order to study the mechanism of retinal VEGF induction by ischemia-induced hypoxia, we have developed an *in vitro* model of VEGF induction in primary rat Müller cells. Primary and transformed, immortalized Müller cells were compared under this condition. Exposure to hypoxia (0% oxygen) for 24 hr consistently and significantly induced VEGF protein production by two-fold in primary Müller cells. Only mild impact on cell growth was observed. The hypoxia treatment also increased VEGF production in the transformed rMC-1 cell culture. However, cell growth retardation and death were obvious. Both primary Müller cells and rMC-1 cells showed no increase of glial fibrillary acidic protein (GFAP) expression after 24 hr of hypoxia treatment. The results suggest a practical method of using primary rat Müller cells as an *in vitro* model to study the VEGF induction pathway in ischemia-induced retinal angiogenesis.

3.2 Introduction

Retinal or subretinal angiogenesis is the characteristic pathologic event of diverse retinal diseases. For most, if not all, ischemia-mediated angiogenic retinal conditions, VEGF is implicated as a critical factor. VEGF is a potent angiogenic growth factor and vasopermeability factor with high specificity for endothelial cells (19). The onset of VEGF-mediated retinopathy is composed of two main episodes: upstream VEGF induction by ischemia-induced hypoxia and downstream VEGF signaling in vascular

endothelial cells. For a decade, extensive efforts have been made to identify VEGF-related targets for pharmacologic intervention. Virtually all have been aimed at VEGF, its receptors or components of its signal transduction cascade. Much less effort has been spent on defining the retinal VEGF induction pathway or searching for potential therapeutic targets upstream from VEGF.

Müller cells are the most abundant glial cells in the vertebrate retina and play important roles in maintenance of retinal extracellular homeostasis and metabolic support of neurons, as do astrocytes, oligodendrocytes, or ependymal cells in other parts of the central nervous system (87). In the retina, Müller cells are the main storage site for glycogen, principally obtaining ATP through glycolysis and consuming little oxygen (88). They are highly resistant to hypoxia and hypoglycemia. Müller cells are also the predominant VEGF secreting cell type when the retina experiences hypoxia (11,89). Thus, Müller cells are an appropriate venue for studies of the molecular basis of retinal VEGF induction by hypoxia.

Recently developed methods for isolating and culturing Müller cells have provided better yield and purity allowing for their use in high throughput assays (90). Additionally, Dr. Vijay P. Sarthy and his colleagues successfully established an immortalized Müller cell line, rMC-1, which displays the Müller cell phenotype (91). rMC-1 cells were originally established and confirmed to facilitate gene expression studies in Müller cells. Their potential usage in studies of VEGF induction by hypoxia *in vitro* has not been defined.

Herein, we report an optimal condition for VEGF induction by hypoxia in primary rat Müller cell cultures, and compare primary Müller cells and rMC-1 cells under this

condition. This method of VEGF induction in primary rat Müller cell cultures is well controlled, reproducible and quantifiable. We believe the model can serve as a ready venue for studies of the molecular basis of retinal VEGF induction or as a method to screen potential inhibitors for future therapeutic applications.

3.3 Materials and Methods

Cell culture

All animals used in the study were cared for and handled according to the Association for Research in Vision and Ophthalmology (ARVO) Statement for the Use of Animals in Ophthalmic and Vision Research. Primary retinal Müller cell cultures were established from postnatal day 8 Long-Evans rat pups as previously described (90). Cells were grown in Dulbecco's modified eagle medium (DMEM; Gibco) supplemented with 10% fetal bovine serum (FBS; Hyclone, Logan, UT) and 1X antibiotic-antimycotic solution (Sigma). This medium will be known as "growth medium" in the experiments described below. Cultures were maintained at 37˚C in a 5% CO_2/95% air (20.9% oxygen) atmosphere (normoxic condition) in a humidified incubator. Passages from 3 to 5 were used for experiments. The identification of Müller cells was confirmed by immunocytochemical staining with a monoclonal antibody recognizing vimentin (DAKO, Carpinteria, CA), an intermediate filament protein normally expressed in Müller cells, and with polyclonal and monoclonal GFAP antibodies (DAKO).

The Müller cell line, rMC-1, was a kind gift from Dr. Vijay P. Sarthy. The cell line was established by transfecting primary rat Müller cell cultures, isolated from Sprague-

Dawley rats, with simian virus 40 (SV40). rMC-1 cells were reported to express both GFAP, a marker for reactive gliosis in Müller cells, and cellular retinaldehyde-binding protein, a marker for Müller cells in adult retina (91). rMC-1 cells were routinely cultured under the same condition as primary Müller cells.

Hypoxia exposure

Primary rat Müller cells or rMC-1 cells were seeded in 6 cm-Petri dishes at the same density and maintained at normoxic condition to 80% subconfluence with growth medium. On experiment day, cells were washed and supplemented with fresh culture medium, 4 ml per 6 cm-Petri dish. The cells were subjected to different hypoxic conditions for 24 hr. The anoxic condition (about 0% oxygen) with a CO_2-enriched environment was generated with BBL™ GasPak Pouch™ system (Becton Dickinson, Sparks, MD). Normoxic and other hypoxic conditions, oxygen concentrations ranging from 20.9% to 2.5%, were generated with an Isotemp laboratory CO_2 incubator with O_2 control (Kendro Laboratory, Asheville, NC). Appropriate humidity and 5% CO_2 were maintained at all times.

VEGF and protein quantification

Culture media from experimental dishes were collected and assayed for VEGF concentration with a colorimetric sandwich ELISA kit (R&D Systems) according to the manufacturer's instructions. The assay recognizes the 164 amino acid residue form of mouse VEGF, which shares 98% amino acid sequence identity with its rat homolog (92). Cells were washed with cold calcium- and magnesium-free PBS (Gibco) and lysed with

cold lysis buffer (50 mM Tris-HCl, 150 mM NaCl, 1% NP-40, 0.25% sodium deoxycholate, 1 mM EDTA, 1 mM PMSF, 1 μg/ml aprotinin, 1 μg/ml leupeptin, 1 μg/ml pepstatin A, 1 mM Na_3VO_4, 1 mM NaF, PH 7.4) (Sigma). Cell lysates were centrifuged at 5000 g for 15 min at 4˚C and protein concentrations were determined with a BCA protein assay kit (Pierce). The amount of VEGF (pg/ml) in culture media was normalized to total protein concentration (mg/ml) of cell lysates. Thus, it resolved the variation of VEGF production due to different cell densities. VEGF induction was designated as the ratio of normalized VEGF production (pg/mg) of hypoxia-treated cells to that of normoxia controls. Data were subjected to ANOVA statistical test using Stat View software (Abacus Concepts). All experiments were independently repeated at least three times.

Immunocytochemistry

Primary rat Müller cells or rMC-1 cells were seeded on coverslips for 2 days. Medium was freshly changed and cultures were then exposed to hypoxia with BBL™ GasPak Pouch™ system or maintained in normoxia for 24 hr. After washing with PBS, cells were fixed with 3% paraformaldehyde (Sigma) for 30 min, permeabilized in 0.1% Triton X-100 (Sigma) for 5min, and blocked in 1% bovine serum albumin (Jackson Immunoresearch Lab., West Grove, PA) for 10 min. Coverslips were incubated with primary antibodies at appropriate working dilutions for 30 min. FITC-conjugated goat anti-mouse IgG antibody and/or rhodamine red-X (RRX)-conjugated goat anti-rabbit IgG antibody (Jackson Immunoresearch Lab) were used as secondary antibodies. Samples were viewed with an Olympus fluorescence phdemicroscope (Olympus).

3.4 Results

The optimal hypoxic condition for VEGF induction in the primary rat Müller cell culture

Normoxic cell culture conditions constitute a higher oxygen concentration than that normally found in the retina (8). Primary rat Müller cells spontaneously secret VEGF, even in normoxia, at a level of 215.32 ± 56.47 pg/mg after 24 hr incubation. We did not detect VEGF using the ELISA assay in fresh DMEM growth medium. When oxygen concentration was reduced to about 0%, a two-fold increase in VEGF production over the normoxia control group was induced ($p < 0.05$) (Figure 3.1). Longer exposure periods augmented the magnitude of the difference, data not shown. Oxygen concentrations of 2.5% or higher failed to induce significantly higher VEGF protein production than normoxia by the 24-hour exposure regimen. Under the various hypoxic exposure conditions, there were no significant morphologic changes of primary Müller cell cultures observed by light microscopy.

Comparison of primary rat Müller cells and rMC-1 cells under the hypoxic condition

Under normoxic conditions, rMC-1 cells proliferated faster and displayed smaller cellular size than primary Müller cells. Like primary cells, rMC-1 cells also spontaneously secreted VEGF, at a level of 202.65 ± 39.71 pg/mg after 24 hr incubation, which was not significantly different from VEGF production by primary Müller cells in normoxia ($p > 0.05$).

rMC-1 cells appeared to be more susceptible to oxygen starvation than primary cultures. After hypoxia (0% oxygen) exposure for 24 hr, rMC-1 showed substantial cell

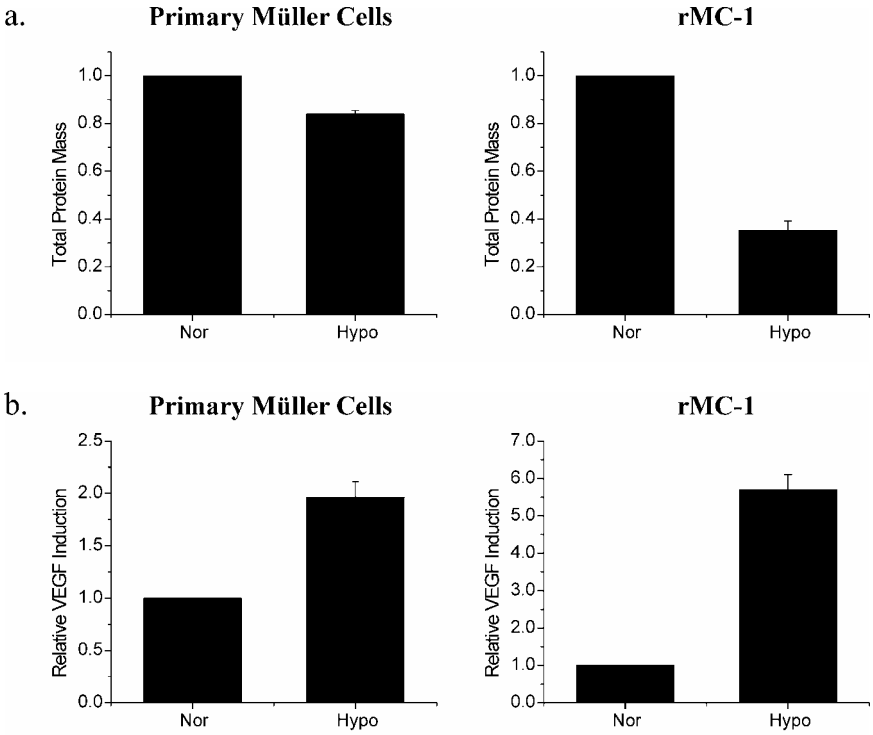

Figure 3.1. Comparison of primay rat Müller cells and rMC-1 cells under hypoxia. Cells were exposed to hypoxia (Hypo, 0% oxygen) or normaxia (Nor) for 24 hr. a, The impact of hypoxia on total protein mass. Results are the ratio of protein mass of hypoxia-treated samples to that of normoxia-maintained controls. b, VEGF induction by hypoxia.

growth retardation. Some cells rounded up and detached from the culture surface. The total protein mass of attaching cells, which is presumed to correlate with the amount of live cells, in hypoxia-treated rMC-1 cultures was 35.4% ($p < 0.05$) of that of normoxia-maintained controls. Primary Müller cell cultures were less affected by hypoxia; floating cells were rare. Total protein mass of hypoxia-treated samples was 84.0% ($p < 0.05$) of that of normoxic samples (Figure 3.1a).

Nevertheless, hypoxia did induce VEGF production in rMC-1 cells. After exposure to hypoxia (0% oxygen) for 24 hr, the amount of VEGF in the medium (pg/ml) of rMC-1 cultures significantly increased by about two-fold compared to that of normoxia-

maintained controls, despite the significantly smaller amount of live cells. When normalized to the total protein mass, VEGF production in hypoxia was 5.7-fold ($p < 0.05$) of that in normoxia, while a moderate increase of 2.0-fold ($p < 0.05$) was observed in primary cultures (Figure 3.1b).

A generalized increase of GFAP expression had been suggested to be a form of reaction in Müller cells to injuries *in vivo* (90). Thus, we further tested the impact of hypoxia (0% oxygen) on GFAP expression in primary Müller cells and rMC-1 cells. Consistent with previous reports (90), primary cultures were stained very weakly for the presence of GFAP by a polyclonal antibody. A stronger staining of nuclei was an apparent artifact of the polyclonal probe, since immunoreactivity was omitted when a monoclonal antibody was used. rMC-1 cells were also weakly stained by GFAP antibodies, as previously reported (91). After 24 hr exposure to hypoxia (0% oxygen), neither primary cultures nor rMC-1 cells showed a significant increase of the intensity in GFAP staining as compared to cells maintained in normoxia (Figure 3.2). Anti-vimentin staining showed no obvious morphology changes in either cell types.

3.5 Discussion

As predominant glial and VEGF secreting cells in the retina, Müller cells are superior to other retinal VEGF-secreting cell types for studying hypoxia-induced VEGF production pathways (93). Müller cells can respond to direct hypoxia insults by increasing VEGF production in monolayer cultures. Exposing primary rat Müller cells to oxygen concentrations of 0% for 24 hr consistently and significantly induces VEGF expression. The magnitude of the response can be potentially extended by longer

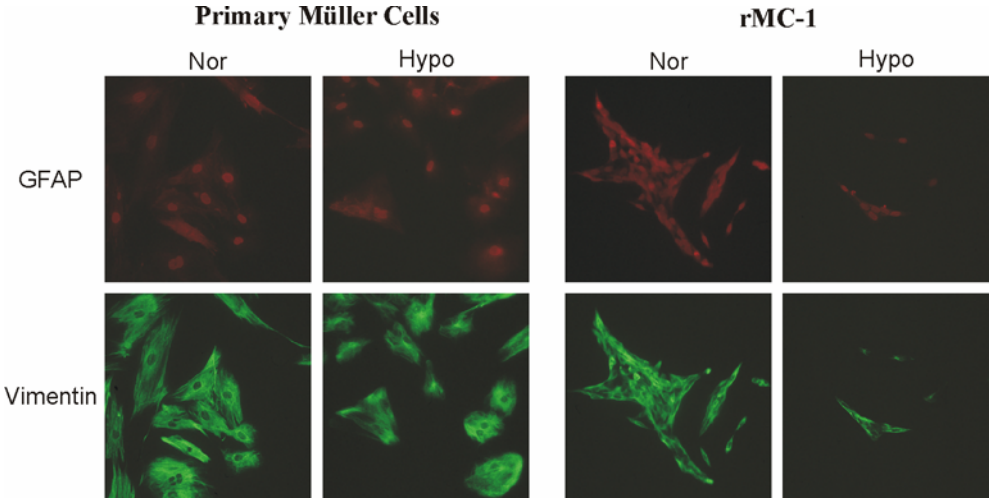

Figure 3.2. Immunocytochemistry analysis of GFAP expression in primary rat Müller cells and rMC-1 cells under hypoxia. Cells were exposed to hypoxia (0% oxygen) or maintained in normoxia for 24 hr. Cells were co-stained for GFAP and vimentin. GFAP is shown by RRX-labeling; vimentin is shown by FITC-labeling.

exposure periods, which will create an even greater window for characterizing or testing inhibitors of the process. Our finding that GFAP up-regulation was not induced by hypoxia exposure *in vitro* differs from published findings using *in vivo* models (90). This suggests that either the hypoxic condition is not stressful enough for GFAP expression, or that neuron-glial interactions are required for GFAP activation in Müller cells' response to hypoxia. Different from detecting VEGF messenger RNA by Northern blot, VEGF production in culture medium can be conveniently and accurately quantified by ELISA assay. Vulnerability of primary Müller cells to hypoxia is minimal under these exposure conditions. This assay can be utilized for quantitative studies of VEGF induction pathways by hypoxia, and as a venue to screen potential inhibitors for therapeutic applications.

In addition to its utility in gene expression studies, rMC-1 cells may be used for studying VEGF induction by hypoxia, particularly because secretion of VEGF by rMC-1

cells can be substantially induced by hypoxia. However, caution is warranted for several reasons. First, rMC-1 is an immortalized cell line derived from primary rat Müller cells by SV40 transfection. The phenotype of the cells is clearly different from that of primary cells. Secondly, rMC-1 cells are much more dependent on oxidative metabolism than primary cultures. Primary Müller cells obtain ATP principally from glycolysis and are highly resistant to oxygen starvation (88). However, rMC-1 cells display substantial cell growth retardation and even cell death upon exposure to a hypoxic condition which primary cells can tolerate well. In addition, the elevated capability of VEGF induction by hypoxia in rMC-1 also indicates the potential modifications of the molecular mechanism underlying the induction pathway.

As these cells become more widely used in scientific research, the advantages and disadvantages of both primary Müller cells and rMC-1 cells as experimental tools will be further characterized. Elucidation of the VEGF induction pathway and its utility in the development of therapeutic strategies will further improve the understanding and intervention of the onset of retina angiogenesis.

CHAPTER IV

DIFFERENTIATION OF THE ROLES OF SRC, FYN AND YES KINASES IN VEGF-MEDIATED ENDOTHELIAL CELL EVENTS BY RNA INTERFERENCE

Xiang Q. Werdich and John S. Penn

Department of Ophthalmology and Visual Sciences

Department of Cell and Developmental Biology

Vanderbilt University School of Medicine, Nashville, TN 37232

This manuscript has been submitted.

4.1 Abstract

Widely coexpressed SFK members Src, Fyn and Yes are involved in various cellular events, often acting downstream of receptor tyrosine kinases, such as VEGF receptors. They are well known for their functional redundancy; any unique features remain largely undefined. Utilizing RNA interference (RNAi), we have selectively knocked down Src, Fyn and Yes in human retinal microvascular endothelial cells (RMECs). Cells with single SFK knockdown showed that all three kinases were required for VEGF mitogenic signaling. VEGF-induced cell migration was significantly increased in Fyn-deficient cells and decreased in Yes-deficient cells. Selective interference of Fyn, but not Src or Yes, impaired VEGF-induced tube formation in human RMECs. Cells in which all three SFKs were targeted showed significant inhibition of all three cellular events. In addition, interference of Src, Fyn and Yes did not affect the anti-apoptotic effect of VEGF in human RMECs, as determined by DNA fragmentation analysis. These results provide direct evidence that Src, Fyn and Yes maintain distinct properties in the regulation of VEGF-mediated endothelial cell events.

4.2 Introduction

Angiogenesis is the process of new blood vessel formation from preexisting capillaries. It is not only fundamental to many physiological events, but also to the partial or characteristic pathology of a broad range of disease conditions, such as cancer, chronic inflammation (e.g. rheumatoid arthritis) and cardiovascular diseases (e.g. atherosclerosis) (94,95). Pathological retinal angiogenesis is the leading cause of severe vision loss and irreversible blindness in developed countries, affecting people of all ages (2,3). Despite

their tissue specificities, all types of angiogenesis share common features allowing for application of findings between systems.

VEGF has been shown to play a major role in the initiation and regulation of both physiological and pathological angiogenesis in various tissues (2,60). VEGF is a 45kDa heparin-binding growth factor (20,57). Initially known as vascular permeability factor (96), VEGF has a profound impact on multiple facets of endothelial cell function, such as promoting cell growth (57,97), migration (38), and survival (39,98). These biological effects are mediated through the high affinity tyrosine kinase receptors, VEGFR-1 (flt-1) and VEGFR-2 (KDR/flk-1) (32-34,99).

Eliceiri and colleagues reported that, *in vivo*, SFKs were selectively required in VEGF-, but not basic fibroblast growth factor-, mediated angiogenesis (46). Other groups demonstrated that SFKs signal upstream of important intermediates, such as PLC-γ (100) and FAK (47), and are involved in multiple VEGF-mediated endothelial cell events (46-48,101).

SFKs are nonreceptor membrane-attached protein tyrosine kinases. They form complexes with various receptors and intracellular substrates, influencing a broad spectrum of cellular events (43). The SFK members Src, Fyn and Yes are coexpressed in many tissues, including vascular endothelium (43-45). These closely related SFKs are well known for their functional redundancy. Deficiency in one SFK member can be compensated by other SFKs that are coexpressed (43,51). However, their unique features remain largely undefined. Eliceiri and colleagues showed that Src- or Yes-, but not Fyn-, deficient mice displayed impaired VEGF-induced vascular permeability (46). Systemic administration of PP1 (a broad spectrum SFK-inhibitor) to mice demonstrated the

potential to prevent secondary tissue damage due to increased VEGF-mediated vascular permeability [e.g. in the pathophysiology of stroke (52)]. In the eye, VEGF-mediated vascular permeability is notoriously responsible for extravasation in both neovascular and non-neovascular retinopathies (3,53,54). Thus, inhibition of SFKs in the eye may benefit the outcomes of many types of ocular edema. Before SFKs can be reasonably targeted for intervention in VEGF-mediated retinal angiogenesis and vascular permeability, the biological functions of the family members and their roles in pathological events must be defined. Optimal strategies will be aimed at those family members that actively contribute to the pathogenesis of a disease, while avoiding others that are essential for maintaining physiological functions.

Success of RNAi in mammalian cells (102) suggested that this method could be a reasonable approach to target the highly homologous Src, Fyn, or Yes for specific inhibition. RNAi is a process of sequence-specific, post-transcriptional gene silencing, which is widely recognized as a natural mechanism for cellular protection and cleansing in most eukaryotes (103). In mammalian cells, effective RNAi is mediated by double-stranded 21- or 22-nucleotide small interfering RNAs (siRNAs) (102). Although double knockdown of two proteins by siRNAs in mammalian cells was demonstrated (104), other studies showed that different siRNAs competed with one another when simultaneously introduced into cells, reducing the silencing effect of either individual sequence (105,106). The implication is that the RNAi machinery may be saturable (107). Thus, to achieve a successful multiple knockdown, careful titration and control of siRNA concentration is necessary.

Here, we demonstrate that human RMECs are susceptible to specific-gene RNAi.

Synthetic siRNA-mediated interference of Src, Fyn and Yes result in clear phenotypic changes in VEGF-induced endothelial cell events. Our results provide direct evidence of the differential properties of Src, Fyn and Yes in the regulation of VEGF signal cascades. Further characterization may facilitate selective targeting of individual SFK member(s) for intervention in VEGF-mediated pathological angiogenesis and vascular permeability.

4.3 Materials and Methods

Cell culture

Primary cultures of human RMECs (Cell Systems, Kirkland, WA) from the 5th to the 6th passages were used in all experiments. Culture vessels were coated with 0.1% gelatin (Sigma) in calcium- and magnesium-free PBS (Gibco). Cells were incubated at 37˚C with 5% CO_2 in endothelial growth medium (EGM; Cambrex, East Rutherford, NJ), supplemented with 10% FBS (Hyclone), referred to as growth medium. When experimental conditions required a serum and growth factor-free (SF) medium, MCDB-131 medium (Sigma) containing 1X antibiotic-antimycotic solution (Sigma) was used.

siRNA transfection

Upon 80% confluence, human RMECs were trypsinized with the ReagentPack™ subculture kit (Cambrex). For each transfection, siRNAs were electroporated into 5 x 10^5 cells using a human lung microvascular endothelial cell Nucleofector™ kit (Amaxa, Gaithersburg, MD) and a Nucleofector™ device (Amaxa) according to the manufacturer's instructions. Immediately after electroporation, cells were resuspended in

prewarmed antibiotics-free EGM containing 10% FBS. Cells were seeded simultaneously to analyze protein levels and VEGF-induced cellular events. Cells began to attach to culture vessels within one hour after electroporation and, 24 hours later, about 80% of the seeded cells were viable.

Four siRNAs targeting human Src mRNA were designed in conformity with *The siRNA User Guide* (108) utilizing Whitehead Institute's siRNA search engine. The sequences corresponding to Src cDNA were: the 5′ untranslated region (UTR), AAGCAACTTGCCCAGCTATGA; the SH2 domain, AAAGTGAGACCACGAAAGGTG; a region of the tyrosine kinase domain, AAGCTGGTGCAGTTGTATGCT; and a region surrounding tyrosine 419 of the tyrosine kinase domain, AAGACAATGAGTACACGGCGC. Each siRNA duplex was BLAST-searched against EST libraries to ensure that only one gene was targeted. Then, siRNAs were chemically synthesized by Qiagen (Valencia, CA) with symmetric 3′ dTdT overhangs. Four additional siRNA duplexes with symmetric 3′ UU overhangs targeting human Src mRNA were purchased from Dharmacon (Lafayette, CO). These were siRNAs targeting the conjunctional region between the SH2 domain and the tyrosine kinase domain, CGTCCAAGCCGCAGACTCA, and three regions of the tyrosine kinase domain, TGCCTCAGCTGGTGGACAT, CCTCAGGCATGGCGTACGT and GAGAACCTGGTGTGCAAAG (Figure 4.1a).

The Fyn siRNA duplex (109) with symmetric 3′ dTdT overhangs, corresponding to the SH2 domain of Fyn cDNA, AAAGATGCTGAGCGACAGCTA, was chemically synthesized by Qiagen (Figure 4.1a). Validated synthetic Yes siRNA (Figure 4.1a), β-actin siRNA, and nonsense control siRNA were purchased from Ambion (Austin, TX).

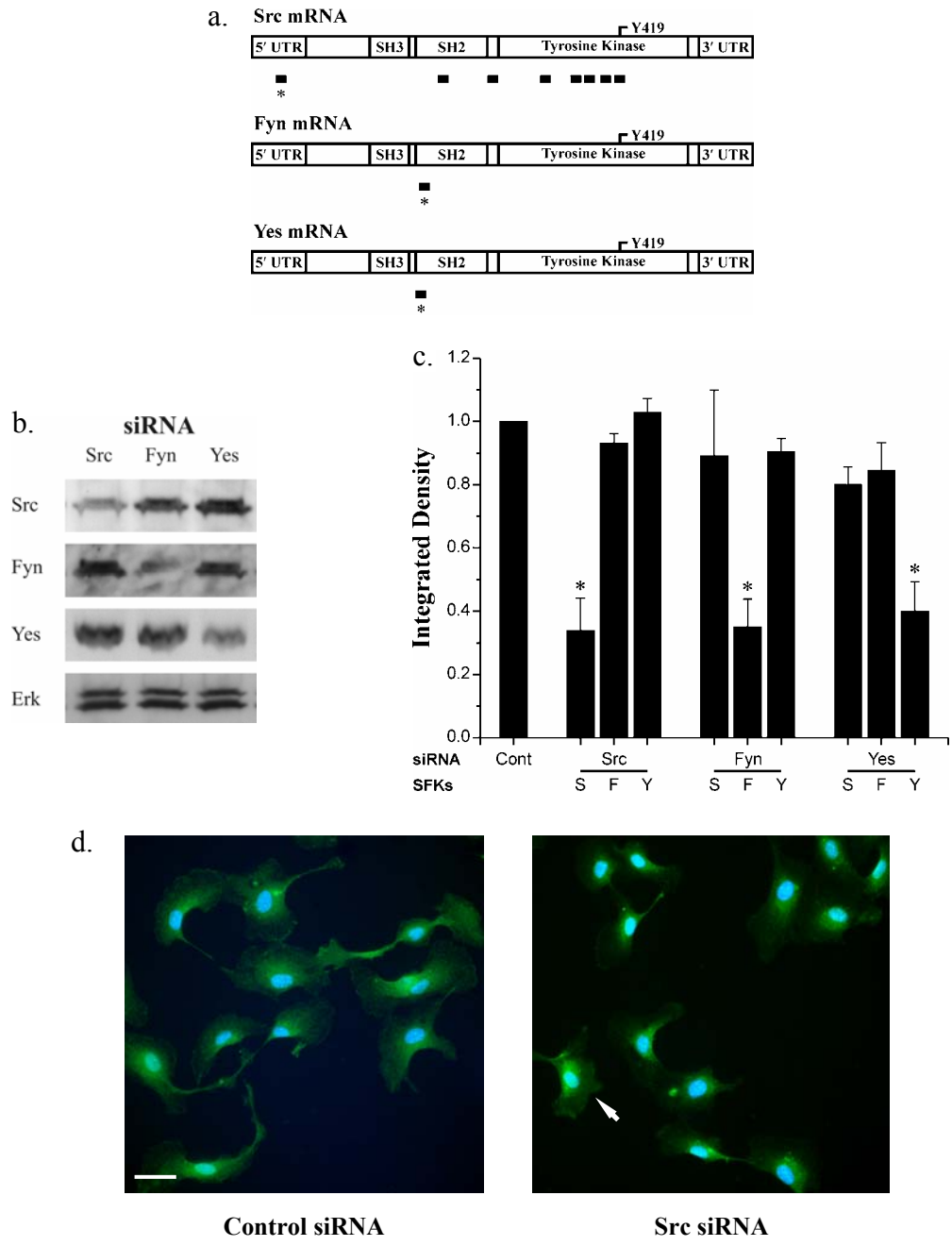

Figure 4.1. siRNAs mediate specific gene-downregulation of Src, Fyn or Yes in human RMECs. a, Schematic of the domain structure of Src, Fyn and Yes mRNAs. Small black bars indicate the relative target locations of siRNAs. *, siRNAs used for cell assays. b, Western blot analysis (24 hr post-transfection). c, Densitometric analysis of the protein expression (mean ± SEM). *, significantly different from nonsense control siRNA-transfected cells, $p < 0.001$. Cont, nonsense control siRNA; S, Src; F, Fyn; Y, Yes. d, Immunocytochemical staining of Src in human RMECs. Nuclei were counterstained with DAPI. Arrow indicates a cell which failed to undergo RNAi in a Src siRNA-transfected cell population. Bar, 40 μm.

To study SFKs in VEGF-mediated endothelial cell events, Src, Fyn, or Yes siRNA each was used at a concentration of 300 nM for transfection in single or triple knockdowns. Nonsense siRNA was used at 300 nM or 900 nM serving as controls in all experiments. We did not observe any significant differences in VEGF-mediated endothelial cell events between the two concentrations of nonsense control siRNA.

Western blot analysis

Following siRNA-transfection, human RMECs were immediately cultured in 12-well plates at equal quantities. At harvest time, about 80% confluence, cells were washed with PBS and lysed with boiling 2X Laemmli SDS sample buffer (Sigma). Proteins were resolved by 10% SDS-PAGE minigels (Bio-Rad) and transferred to 0.2 μm nitrocellulose membranes (Bio-Rad). After incubation in blocking buffer, TBS (Sigma) with 0.1% Tween-20 (Sigma) and 5% nonfat dry milk (Bio-Rad), for 30 min at room temperature, blots were incubated with the primary antibody overnight at 4°C and with the secondary antibody for 2 hr at room temperature. Following thorough washing, proteins were visualized with enhanced chemiluminescence (Amersham). Blots were routinely stripped and reprobed for other proteins to obtain loading controls. Every experiment was repeated at least three times independently.

Antibodies specifically recognizing individual Src, Fyn, or Yes were purchased from Upstate (Waltham, MA) and Santa Cruz Biotechnology. The Erk1/2 antibody was purchased from Cell Signaling (Beverly, MA). The β-actin antibody was purchased from Sigma. HRP-conjugated anti-rabbit or anti-mouse antibodies (Promega) were used as secondary antibodies.

Digitized images of Western blots were quantified using Image J software (NIH). Raw densitometric values of proteins were normalized against those of internal controls (i.e. untargeted proteins) and then used for statistical analysis.

Immunocytochemistry

Human RMECs were cultured on coverslips for 24 hr post-transfection. Cells were then washed with PBS, fixed with 3% paraformaldehyde (Sigma) for 30 min, permeabilized in 0.1% Triton X-100 (Sigma) for 5 min, and blocked in 1% bovine serum albumin (Jackson Immunoresearch) for 10 min. Coverslips were incubated with the primary antibody at appropriate working dilutions for 30 min. FITC-conjugated goat anti-rabbit IgG antibody (Jackson Immunoresearch) was used as a secondary antibody. Nuclei were counterstained with DAPI (Sigma). Samples were viewed with a Zeiss fluorescence Axiophot upright microscope (Carl Zeiss Microimaging, Thornwood, NY), and images were taken using a MicroMax CCD camera (Princeton Instruments, Trenton, NJ).

Cell proliferation assay

Cell growth was quantified with a colorimetric cell proliferation immunoassay recognizing BrdU incorporation (Roche Applied Science, Indianapolis, IN). Following siRNA-transfection, human RMECs were immediately seeded in 96-well plates at 4×10^3 cells per well. Twenty-four hours later, after washing with SF medium, cells were treated for 45 hr with either SF medium containing 1% FBS or SF medium containing 1% FBS and 25 ng/ml recombinant human VEGF 165 (R&D Systems). Five repeats were made per treatment. Cells were then labeled with BrdU *in situ* for 3 hr at 37˚C. The amount of

BrdU incorporation was measured according to the manufacturer's instructions. The experiment was repeated six times independently.

Apoptosis assay

The enrichment of cytoplasmic mono- and oligonucleosomes due to DNA fragmentation was determined with a photometric cell death immunoassay (Roche Applied Science). Following siRNA-transfection, human RMECs were immediately seeded in 48-well plates at 8 x 10^3 cells per well. Twenty-four hours later, after washing with SF medium, cells were treated for 24 hr with either growth medium, SF medium, or SF medium containing 50 ng/ml VEGF, duplicated for each treatment. Cytoplasmic fractions of the cells were extracted. The amount of DNA fragmentation was then determined according to the manufacturer's instructions. The experiment was repeated six times independently.

Cell migration assay

Cell migration was quantified with a modified transwell method using fluorescence labeling, as previously described (110). Following siRNA-transfection, human RMECs were immediately seeded in 6-well plates at 16 x 10^4 cells per well. Twenty-four hours later, cells were labeled *in situ* with 2 μM calcein AM (Molecular Probes, Eugene, OR) in growth medium for 20 min at 37˚C. After washing, cells were trypsinized and suspended in SF medium. Cells were equally divided into 4 parts and added to 8 μm FALCON® HTS FluoroBlok™ inserts (Becton Dickinson) coated with 0.1% gelatin. VEGF (25 ng/ml) in SF medium was used as a chemoattractant in the lower wells, while SF medium

was added to the control wells, duplicated for each treatment. The plates were incubated for 3 hr at 37˚C. Fluorescence of cells that had migrated through the inserts was measured via a Synergy™ HT multi-detection microplate reader (Bio-Tek, Winooski, VT) in the bottom-read mode using excitation and emission wavelengths of 485 nm and 530 nm, respectively, and a gain of 50. The kinetics of cell migration was monitored every half an hour. Human RMEC migration began almost immediately upon initiation of the experiment and reached a plateau after 2 hr. The fluorescence of cells migrating towards VEGF was recorded 1 hr after the beginning of the experiment. The experiment was repeated three times independently.

Tube formation assay

In vitro formation of tubular structures by human RMECs was studied on a growth factor-reduced Matrigel® matrix (Becton Dickinson) in 48-well plates. Matrigel-coated wells were prepared according to the manufacturer's instructions for the thick-gel method. Following siRNA-transfection, human RMECs were immediately seeded in 6-well plates at 10 x 10^4 cells per well. Twenty-four hours later, cells were trypsinized, and equally divided into 2 parts and suspended in either SF medium or SF medium containing 25 ng/ml VEGF. Cells were then seeded onto the matrigel layers, duplicated for each treatment. After 16 hr of incubation, images of tubes were captured using a DMC digitizing camera (Polaroid) mounted on an IMT-2 inverted microscope (Olympus). Three fields per well were used for quantitative analysis. The digital images were analyzed using Image J software. Capillary-like structures of more than two cell lengths were evaluated and the mean tube length per area of the field was calculated. The

experiment was repeated four times independently.

Data analysis

Although all electroporation parameters were kept constant, the amounts of cells that survived the procedure varied between independent experiments. To avoid further stress, cells were not recounted 24 hr post-transfection. At the beginning of each experiment, RNAi effects contributed to the disparity of cell numbers between different siRNA-transfected cells. Therefore, all results generated using transfected and VEGF-treated samples are presented in relation to the appropriate control sample within each independent experiment.

All experimental data were subjected to the ANOVA statistical test using Stat View software (Abacus Concepts). A value of $p < 0.05$ was considered significant.

4.4 Results

siRNAs mediate specific gene-downregulation of Src, Fyn or Yes in human RMECs

We first confirmed that human RMECs were susceptible to gene specific RNAi with a validated synthetic β-actin siRNA. The knockdown efficiency of β-actin can reach more than 97% 24 hr post-transfection (Figure 4.2). In order to select an siRNA that would efficiently knock down Src in human RMECs, we tested eight sequences correspondent to different regions of Src mRNA (Figure 4.1). Interestingly, the siRNA targeting 5′ UTR induced the most pronounced Src specific protein reduction. Thus, this probe was used in the following experiments and designated as Src siRNA. Using the electroporation

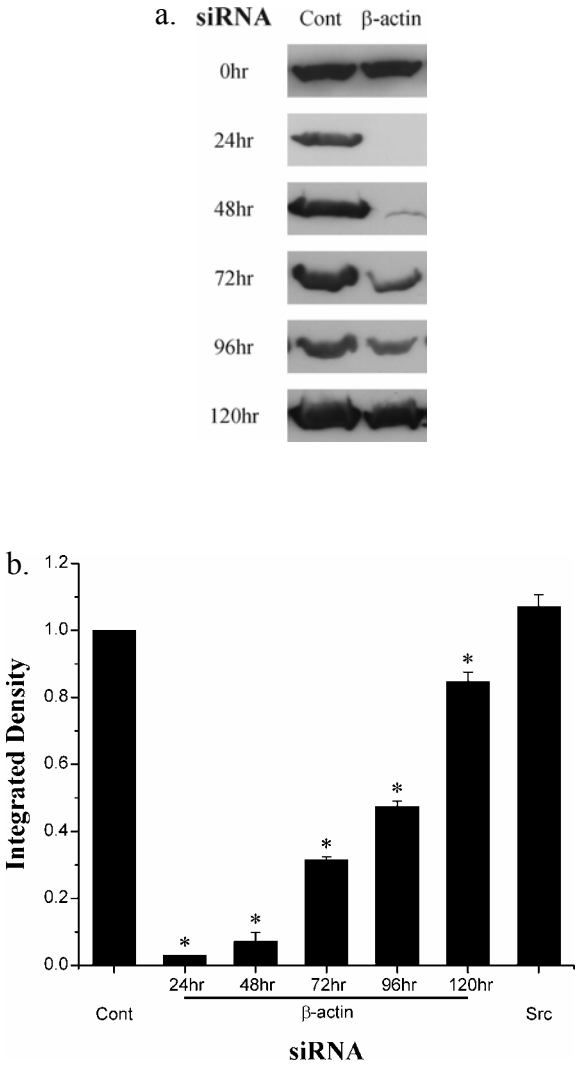

Figure 4.2. Human RMECs are susceptible to synthetic β-actin siRNA-mediated specific gene silencing, which is a transient phenomenon. β-actin and nonsense control siRNAs were transfected at a concentration of 200 nM. a, Western blot analysis of β-actin expression. b, Densitometric analysis shows that β-actin expression was significantly reduced at 24 hr, 48 hr, 72 hr, 96 hr post-transfection ($p < 0.001$) and 120 hr post-transfection ($p < 0.05$) compared to nonsense control siRNA-transfected cells. Cells transfected with Src siRNA (300 nM) showed no reduction of β-actin expression 24 hr post-transfection. Bars represent the mean ± SEM. *, $p < 0.05$.

method, we found that the RNAi effects mediated by synthetic SFK siRNAs and β-actin siRNA were most profound as early as 24 hr post-transfection, and were still significant 72 hr post-transfection. However, the reduction of protein expression was a transient phenomenon, and SFK proteins had returned to control levels by 96 hr post-transfection.

We then tested the knockdown specificity of Src siRNA, the validated Fyn siRNA (109) and Yes siRNA (Ambion) in human RMECs (Figures 4.1, b and c). In a dose titration study using concentrations ranging from 200 nM to 1 μM, we found a concentration of 300 nM as the minimum siRNA concentration for efficient knockdown. Transfection of different siRNAs at concentrations of up to 1 μM showed no toxicity in human RMECs. In Src siRNA-transfected cells, Src expression was specifically reduced by about 66% 24 hr post-transfection, while Fyn and Yes protein levels remained unchanged. In Fyn siRNA-transfected cells, Fyn was effectively knocked down by about 65%, but not Src or Yes. Likewise, Yes siRNA specifically knocked down Yes by about 60%. In cells actively undergoing Src, Fyn, or Yes silencing, we did not observe either nonspecific interference of other untargeted endogenous gene expression, such as Erk1/2 (Figure 4.1b) and β-actin (Figure 4.2b), or significant compensation of the deficient SFK at the protein level by untargeted SFKs.

Simultaneous delivery of Src, Fyn and Yes siRNAs significantly reduced protein expression of Src, Fyn and Yes by 40 - 45% individually ($p < 0.005$) 24 hr post-transfection, as compared to cells transfected with the same amount of nonsense control siRNA. The decrease in protein reduction was consistent with previous work, suggesting that competition between siRNAs in multiple knockdown resulted in lower-level silencing of each gene (105,106). Nonsense control siRNA showed no silencing effect on

any of the proteins tested.

Thus, using RNAi, we selectively knocked down Src, Fyn and Yes to similar extents in human RMECs. These synthetic siRNA-transfected human RMECs maintained typical endothelial morphology and conferred clear phenotypic changes in VEGF-mediated cell events.

Src, Fyn and Yes are all required for VEGF-mediated cell growth in human RMECs

VEGF is a powerful endothelial specific mitogen (57,97). Upon VEGF stimulation, SFKs function upstream of PLC-γ, which eventually leads to the activation of Raf-MEK-Erk pathway and induces cell proliferation (100,111,112). In nonsense control siRNA-transfected human RMECs, 25 ng/ml VEGF induced a 2.2-fold increase in cell growth versus the control medium containing 1% FBS. The induction of proliferation was significantly inhibited by 32 - 53% in cells deficient in individual Src, Fyn, or Yes ($p < 0.05$). In Src, Fyn and Yes triple knockdown cells, VEGF-induced cell growth was impaired by about 56% ($p < 0.005$) (Figure 4.3). The remaining SFK activities which were not completely abolished by RNAi may have contributed in part to the residual cell growth observed. These results showed that Src, Fyn and Yes were all required for VEGF-induced cell proliferation. Each kinase may possess unique functions in VEGF mitogenic signaling that cannot be fully compensated by the other two kinases.

SFK interference does not affect the anti-apoptotic effect of VEGF in human RMECs

To investigate the specific roles of Src, Fyn, or Yes in the VEGF-mediated cell survival pathway, we quantified cell death by determining the enrichment of cytoplasmic

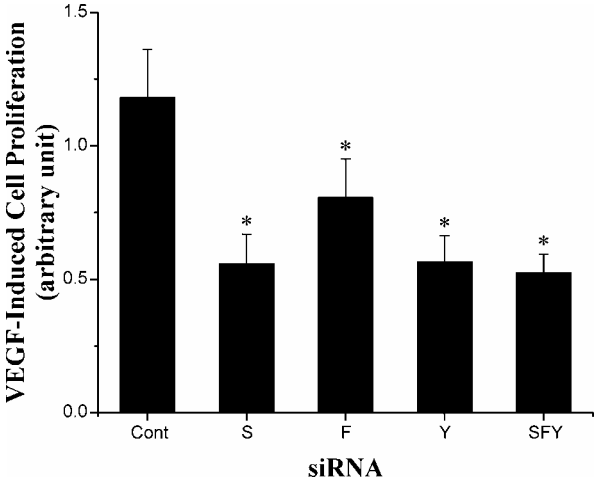

Figure 4.3. Src, Fyn and Yes are all required for VEGF-mediated cell growth in human RMECs. Cell proliferation was quantified with the BrdU incorporation. The absorbance of the VEGF-treated sample was normalized to that of its control sample treated with 1% FBS. VEGF-induced cell proliferation was expressed as an increase of the amount of BrdU incorporation in the VEGF-treated sample compared to that of the 1% FBS-treated control sample (mean ± SEM). *, significantly different from nonsense control siRNA-transfected cells, $p < 0.05$.

mono- and oligonucleosomes due to DNA fragmentation, a late event of apoptosis. In nonsense control siRNA-transfected cells, serum starvation for 24 hr induced a 2.0-fold DNA fragmentation compared to the growth medium condition (Figure 4.4a). In cells subjected to SFK single downregulation by Src, Fyn or Yes siRNA, we did not observe any difference of apoptosis induction by serum deprivation compared to nonsense control siRNA-transfected cells ($p > 0.05$) (Figure 4.4a), despite their significantly impaired cell growth in response to VEGF. Nor did these cells show any significant disruption of the VEGF survival effect ($p > 0.05$) (Figure 4.4b). In addition, Src, Fyn and Yes triple knockdown cells showed no significant change of DNA fragmentation upon serum starvation or VEGF administration compared to nonsense control siRNA-transfected cells ($p > 0.05$) (Figures 4.4, a and b). Thus, at these levels of protein downregulation, Src, Fyn

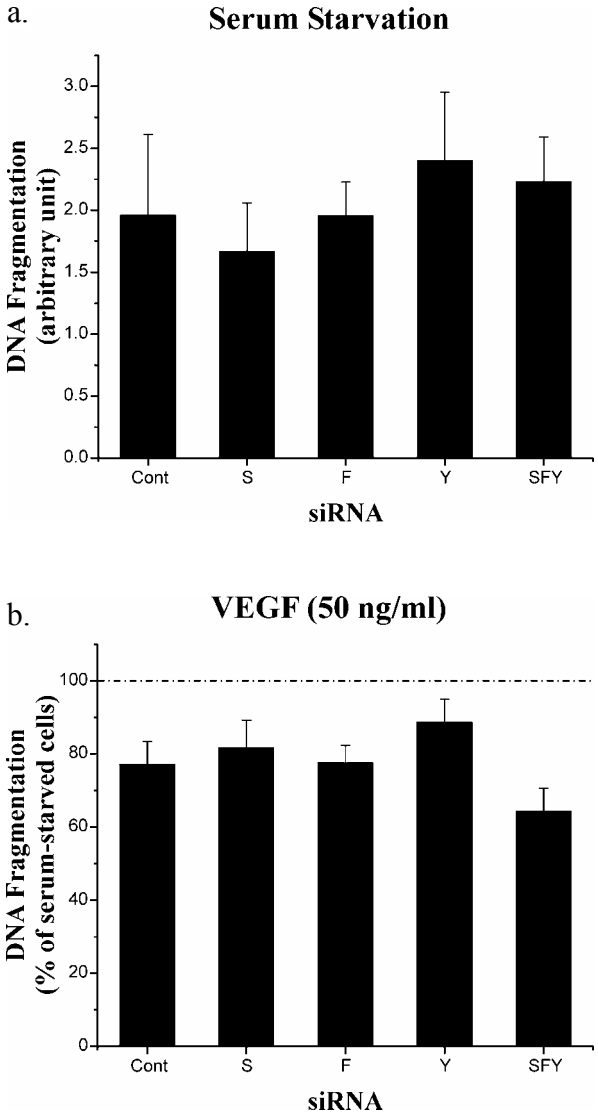

Figure 4.4. SFK interference does not affect the anti-apoptotic effect of VEGF in human RMECs. a, After serum starvation, the amounts of DNA fragments in nonsense control siRNA or SFK siRNA-transfected cells were not significantly different ($p > 0.05$). The absorbance of the SF medium-treated sample was normalized to that of the growth medium-maintained control sample (mean ± SEM). The experiment was repeated three times independently. b, VEGF-mediated cell survival from serum starvation was not significantly different among nonsense control siRNA or SFK siRNA-transfected cells ($p > 0.05$). DNA fragmentation of the VEGF-treated sample was expressed as the fraction of that of the SF medium-treated sample (mean ± SEM). The experiment was repeated six times independently.

and Yes appeared not as important to VEGF survival signaling as to mitogenic signaling.

Src, Fyn and Yes differentially contribute to the modulation of VEGF-mediated cell migration in human RMECs

In addition to its role as a mitogenic and survival factor, VEGF also functions as a chemoattractant and induces endothelial cell migration (38). Interference of Src, Fyn or Yes expression with siRNAs showed differential influences on endothelial chemotaxis towards VEGF (Figure 4.5). There was no significant change of cell motility in Src siRNA-transfected cells compared to nonsense control siRNA-transfected cells. Interestingly, cell migration was significantly increased ($p < 0.01$) in human RMECs transfected with Fyn siRNA, while significantly decreased ($p < 0.05$) in cells transfected with Yes siRNA. Nevertheless, Src, Fyn and Yes triple knockdown cells showed

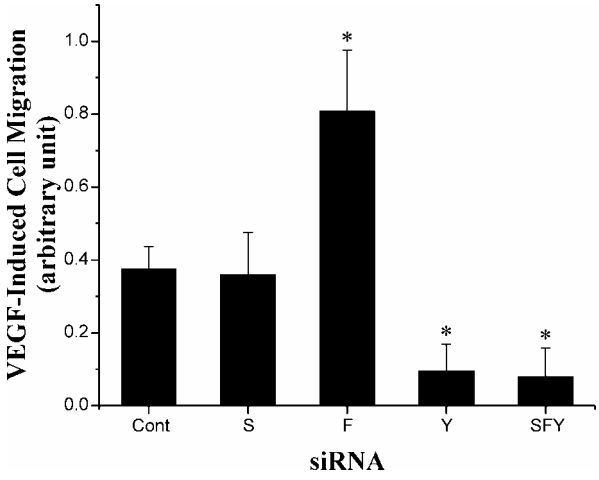

Figure 4.5. Src, Fyn and Yes differentially contribute to the modulation of VEGF-mediated cell migration in human RMECs. The fluorescence (arbitrary unit) from cells migrating towards VEGF was normalized to that of cells migrating towards SF medium. Results were expressed as an increase in VEGF-induced cell migration compared to the random cell migration occurring in SF medium (mean ± SEM). *, significantly different from nonsense control siRNA-transfected cells, $p < 0.05$.

significantly impaired cell migration ($p < 0.05$), which was consistent with a previous finding that blocking SFKs in general inhibited endothelial cell migration (47). Thus, these results revealed differential properties of SFKs in the modulation of VEGF-induced cell migration, i.e. inhibition by Fyn and facilitation by Yes. Due to the incomplete knockdown of protein expression, the role of Src in VEGF-mediated cell migration remains undetermined.

Interfering with Fyn alone or with Src, Fyn and Yes simultaneously perturbs VEGF-mediated tube formation in human RMECs

The roles of Src, Fyn and Yes in VEGF-mediated cell differentiation were assessed with a tube formation assay on growth factor-reduced matrigel (Figure 4.6). Interfering Src or Yes expression failed to disrupt VEGF-induced tube formation. The lack of phenotype did not exclude their possible roles in this cellular event due to the incomplete depletion of targeted proteins. However, the reduction in Fyn resulted in a significant perturbation of VEGF-induced tube formation ($p < 0.02$). Therefore, untargeted Src and Yes did not fully compensate for the deficient function of Fyn in these cells. We also observed significant inhibition of VEGF-induced tube formation in Src, Fyn and Yes triple knockdown cells ($p < 0.05$), even though the protein reduction was less than that in single knockdowns. This finding was consistent with a previous study showing that nonspecific inhibition of SFKs suppressed VEGF-induced angiogenesis in the chick chorioallantoic membrane *in vivo* (46).

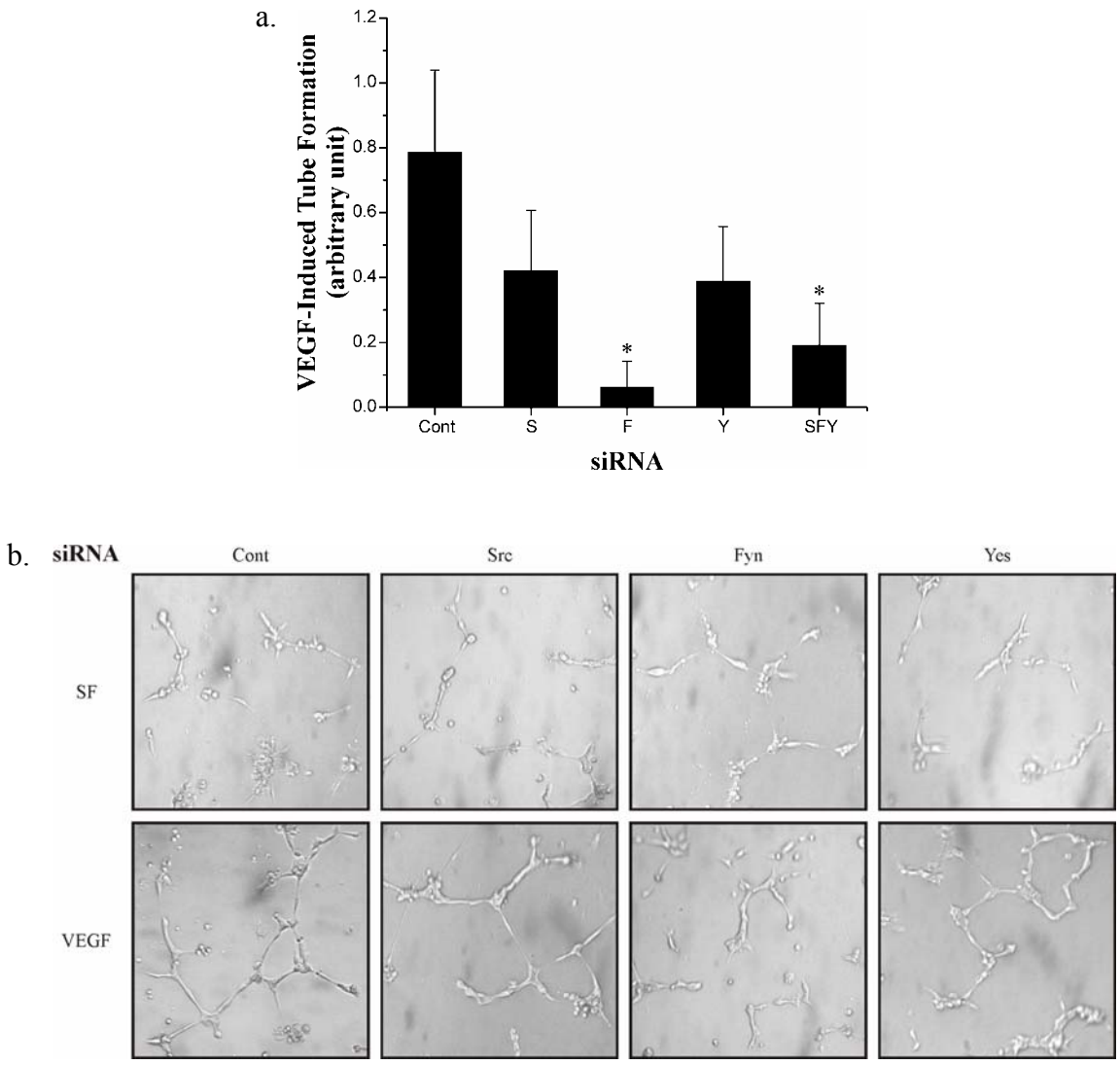

Figure 4.6. Interfering with Fyn alone or with Src, Fyn and Yes simultaneously perturbs VEGF-mediated tube formation in human RMECs. a, Quantitative analysis of VEGF-induced tube formation in siRNA-transfected cells. The mean tube length (μm) of the VEGF-treated sample was normalized to that of the SF medium-treated control sample. Results were expressed as an increase in VEGF-induced tube formation compared to the spontaneous formation of tubes occurring in SF medium (mean ± SEM). *, significantly different from nonsense control siRNA-transfected cells, $p < 0.05$. b, Phase contrast micrographs of formation of tube-like structures in siRNA-transfected cells.

4.5 Discussion

SFK members (e.g. Src, Fyn and Yes) are generally believed to have overlapping functions, but there is emerging evidence that evolutionary pressures may have yielded unique functions of individual family members (46,51). Even though the involvement of SFKs in VEGF-mediated angiogenesis has been clearly demonstrated over the last decade, there has not been an attempt to discriminate the specific roles of individual members. Using RNAi, we have shown that, in addition to their functional redundancy, closely related SFK members Src, Fyn, and Yes each possess functional specificity in VEGF-mediated endothelial cell events. First, Src, Fyn and Yes each play unique roles in VEGF mitogenic signaling. Second, they differentially contribute to the modulation of VEGF-mediated cell migration. Third, Fyn plays a unique role in VEGF-induced tube formation. Nevertheless, human RMECs, deficient in all three SFKs showed significant disturbances in these VEGF-mediated cell events (i.e. proliferation, migration and tube formation). Notably, human RMECs deficient in Fyn showed increased cell migration and decreased tube formation. Tube formation, *per se*, is a complex process, involving multiple steps, such as cell adhesion, extracellular matrix extrusion, cell migration and differentiation (95). It is possible that the roles of SFKs in cellular events other than migration contribute to this discrepancy.

The distinctive functions of Src, Fyn or Yes in VEGF signaling may be due in part to their differential localizations in intracellular compartments (113,114), and consequently distinct association with various upstream activators and downstream substrates. SFKs can be associated not only with plasma membrane, but also with endosomes, the rough endoplasmic reticulum, secretory vesicles and caveolae (114,115). Myristylation and

palmitylation of the N-terminal sequences of SFKs mediate their targeting to membranes. Unlike myristylation, palmitylation is a reversible process (116), which may account for the relocalization of SFKs (113). Notably, the cysteine residue in the likely consensus palmitylation sequence (myr-Gly-Cys-) is present in Fyn and Yes, but not in Src. Additionally, positively charged lysine or arginine residues in the N-terminus of SFKs can provide an electrostatic mechanism to enhance membrane binding. Src, Fyn and Yes differ from each other in these regions (113). Electrostatic charges can also be modulated, for example, by phosphorylation (117). Thus, subcellular targeting of SFKs requires multiple signals and is modifiable, which may confer to each a set of distinctive biological profiles. SFKs can be coupled to and/or activated by many other cellular receptors, such as receptors for platelet-derived growth factor or epidermal growth factor. It can be expected that individual SFKs possess distinctive functions under influence of these receptors as well.

VEGF-induced endothelial cell survival was reported to be mediated by PI 3-kinase/Akt (39,47) and SFKs (46,47). Our data showed that despite significant inhibition of cell proliferation, interference of Src, Fyn or Yes individually or together, failed to disrupt the VEGF anti-apoptotic effect as measured by DNA fragmentation. Apoptosis is an active process, which can be detected by various morphological and biochemical criteria (118). Apoptotic cell surface change is an early event (119) and its occurrence precedes DNA fragmentation (120). A previous report showed that PP2, a selective SFK inhibitor, significantly increased annexin V labeling, a hallmark of apoptotic cell surface change, in serum-starved human umbilical-vein endothelial cells under VEGF protection. However, it did not impair VEGF protection from late apoptotic events, such as cell

detachment and FAK cleavage, as did a PI 3-kinase inhibitor (47). Consistent with this work, our data indicates that SFKs may not participate in late apoptotic events in endothelial cells, although they may influence early apoptotic features (47).

Downregulation of Src, Fyn or Yes individually in human RMECs resulted in differential effects on VEGF-induced cell migration. This suggests that SFKs play important roles in the modulation of the VEGF migration signal. Particularly, VEGF-induced cell migration was significantly increased in cells deficient in Fyn, which indicated an inhibitory effect of Fyn. It is known that VEGFR-1 activation alone fails to induce endothelial cell migration (38,40,121). However, VEGFR-1 activation is sufficient for the migration of monocytes, which naturally express the receptor (122,123). In addition, despite intact VEGFR-2 function, blocking VEGFR-1 alone can abolish VEGF-induced cell migration, which indicates an essential role for VEGFR-1 in cell motility (124). Gille and colleagues showed that the intracellular juxtamembrane region of VEGFR-1, which contained a stretch of three serines, constitutively functioned as a specific repressor of VEGFR-1-mediated VEGF-dependent migration in endothelial cells. Replacement of the juxtamembrane region of VEGFR-1 by that of VEGFR-2 gave VEGFR-1 the competence to induce endothelial cell migration (125). Thus, it has been suggested that there may be an inhibitory pathway in VEGFR-1-mediated migration in endothelial cells, which functions via the intracellular juxtamembrane region. This inhibitory regulation is likely void in monocytes, due to the different composition of the molecular machinery. Fyn has been shown to be associated preferentially with VEGFR-1 (126), and it is phosphorylated upon VEGF stimulation in porcine aortic endothelial cells expressing VEGFR-1, but not in cells expressing VEGFR-2 (38). Combining these facts

with our observation, we propose that Fyn, as a membrane attached protein tyrosine kinase, may be involved in the inhibitory pathway of VEGFR-1-mediated migration in endothelial cells. In addition, silencing Yes resulted in impaired human RMEC migration, which indicates that Yes may function as a positive regulator. This regulation may be through VEGFR-2 or VEGFR-1 at sites other than the intracellular juxtamembrane region. Further work is required to determine the underlying mechanism.

VEGF initiates and promotes pathological angiogenesis and vascular permeability in the retina (2,53,54). SFKs are key components of VEGF signal cascades. Family members Src, Fyn and Yes possess differential roles in the regulation of VEGF-mediated endothelial cell events, such as proliferation, migration, tube formation and vascular permeability. We show that human RMECs, the same cells that undergo dysregulated growth and differentiation in retinopathies, are susceptible to specific-gene silencing by RNAi. Together, these results raise the possibility that SFK member(s) may be selectively targeted, for example by RNAi, for intervention in VEGF-mediated pathological retinal angiogenesis and vascular leakage.

To date, there has been no systematic efficiency study of siRNAs targeting various regions of mRNA. The 5′ or 3′ UTR or regions near the start codon are generally avoided due to abundant regulatory protein binding sites in these regions (104). However, siRNAs targeting the 3′ UTR or a nearby vicinity were shown recently to effectively silence genes in mammalian cells (105). Here, we have shown that an siRNA duplex targeting the 5′ UTR of Src mRNA successfully induced RNA interference, and it appeared to be more efficient than other tested siRNAs targeting the open reading frame. Using siRNAs targeting the 5′ or 3′ UTR to induce RNAi can be advantageous. For example, a plasmid

coding for a target gene or mutants can be introduced without interference, facilitating phenotypic verification or rescue.

While searching for an siRNA which could efficiently knock down Src expression, we noticed that SFKs appeared to be less sensitive to synthetic siRNA-mediated RNAi (maximum knockdown of 60-70%) than β-actin (maximum knockdown of 97%) in human RMECs. We targeted eight sites of Src mRNA using siRNAs, all of which caused some measurable knockdown, and spanning nearly the entire mRNA. However, none of them exerted knockdown effects as profound as that of β-actin siRNA in human RMECs, nor did the previously validated Fyn and Yes siRNAs. Various factors may contribute to this phenomenon, such as cell type, intrinsic protein profiles (e.g. protein abundance and turnover rate) and accessibility of mRNA (127).

Use of vector-based RNAi may achieve better silencing effects and longevity than the synthetic siRNA duplex. However, synthetic siRNAs are less likely to trigger interferon (IFN)-mediated activation of the Jak-Stat pathway and global upregulation of IFN-stimulated genes (128,129), which would confound results. Nevertheless, while our study showed no evidence of general repression of protein synthesis in cells transfected with various siRNAs compared to wild type cells, broad effects of synthetic siRNAs must be considered and caution is warranted in interpreting findings.

In the current work, we demonstrated the use of RNAi to study the biological functions of individual members of a gene family. While incomplete depletion of protein expression may have hampered the depth of our investigation, valuable phenotypic data were derived. We believe that RNAi may be used to interfere specifically in pathogenesis involving multiple, high homology member(s) of a gene family, potentially reducing

therapeutic complications due to nonspecific targeting.

4.6 Acknowledgments

We thank Dr. Abboud J. Ghalayini and Dr. Jin Chen for insightful discussion and suggestion. We thank Dr. Gary W. McCollum for experimental support. We thank Dr. Derya Unutmaz for sharing the Nucleofector™ Device, and Dr. Robbert J. Slebos for sharing the Synergy™ HT multi-detection microplate reader. We thank the Vanderbilt University Medical Center Cell Imaging Shared Resource for training and sharing of microscopes and software.

CHAPTER V

SPECIFIC INVOLVEMENT OF ACTIVATED SRC FAMILY KINASES IN THE PATHOGENESIS OF RETINAL NEOVASCULARIZATION

Xiang Q. Werdich and John S. Penn

Department of Ophthalmology and Visual Sciences

Department of Cell and Developmental Biology

Vanderbilt University School of Medicine, Nashville, TN 37232

This manuscript has been submitted.

5.1 Abstract

VEGF-mediated retinal neovascularization involves both VEGF expression and signaling. Here we showed that *in vitro* SFKs were essential for hypoxia-induced VEGF expression in glial Müller cells and VEGF signaling in RMECs. However, neither process required phosphorylation of the SFK activation loop Tyr416. *In vivo*, in a rat model of OIR, we found a significant increase of retinal SFK Tyr416 phosphorylation, which was specifically associated with pathological angiogenesis. The OIR retinas also expressed significantly higher levels of VEGF than the healthy controls. Using immunohistochemistry and confocal microscopy, we identified Müller cells as the source of the elevated phospho-SFK Tyr416 signal. Intravitreous injection of a selective SFK inhibitor (PP2) significantly reduced retinopathy in the OIR model, indicating that SFKs acted as key regulators in abnormal retinal angiogenesis. Together, these data suggest that SFK activation via a Tyr416-dependent mechanism may be an important factor in the pathogenesis of retinal neovascularization.

5.2 Introduction

Retinal neovascularization is the leading cause of severe vision loss and irreversible blindness in developed countries, affecting people of all ages (1). It is the characteristic pathological event of diverse retinal diseases, such as ROP, retinal vein occlusion, diabetic retinopathy and sickle cell retinopathy. For the pathogenesis of these angiogenic conditions, retinal ischemia and hypoxia have been identified as a major driving force, and hypoxia-inducible VEGF as a crucial stimulator and regulator (2,5,130). In the vertebrate retina, Müller cells are the most abundant glial cells playing active roles in the

maintenance of retinal extracellular homeostasis and the metabolic support of neurons (87). They are the major VEGF secreting cell type in the retina during ischemia-induced neovascularization (11,89). VEGF is a potent vascular endothelial cell mitogen (60). Its high affinity tyrosine kinase receptors, VEGFR-1 (flt-1) and VEGFR-2 (KDR/flk-1), are expressed predominantly in endothelial cells (60). Biologically relevant VEGF-mediated endothelial cell events, such as proliferation, chemotaxis, survival and vascular permeability, are mainly regulated through VEGFR-2 (19,38-40). In the eye, RMECs undergo dysregulated proliferation and differentiation in proliferative retinopathies (2).

As membrane-attached nonreceptor protein tyrosine kinases, broadly expressed SFKs link a variety of extracellular cues to intracellular signal pathways (43). Family members Src, Fyn and Yes are often coexpressed, e.g. in vascular endothelial cells (43-45). Recent studies revealed that SFKs were involved in both hypoxia-induced VEGF expression in cancer cells (18) and VEGF signaling in endothelial cells (46-48). However, their roles in the pathogenesis of VEGF-mediated retinal neovascularization are completely unknown.

SFKs are 52- to 62-kDa proteins consisting of six distinct functional domains: a SH4 domain involved in locating SFKs to cellular membranes, a unique domain, SH3 and SH2 protein-binding domains, a catalytic domain, and a negative regulatory carboxyl terminal tail (43). SFKs have two most important regulatory phosphorylation sites, Tyr527 in the negative regulatory tail and Tyr416 in the activation loop of the catalytic domain. Inactive SFKs are present in a restrained form via the intramolecular interaction of the SH2 domain with phospho-Tyr527 (pY527) and adjacent residues, which is critical for suppressing the kinase activity. The SH3 domain further stabilizes the inactive state by forming intramolecular interactions with amino acids within and adjacent to the

catalytic domain (43). When the intramolecular interactions are disrupted, dissociated pY527 may allow dephosphorylation. Tyr416 then undergoes autophosphorylation, which permits and stabilizes the active conformation, and promotes the intrinsic kinase activity (43,131). Boerner and colleagues showed that despite being present in the pY527-SH2 complex, Src with phospho-Tyr416 (pY416) retained 20% of the catalytic activity and could readily phosphorylate substrates (50). Autophosphorylation of Src at Tyr416 was shown to be directly correlated with its catalytic activity (50). *In vivo*, wild type SFKs are strictly regulated and mainly present in the restrained state (131). By coupling to signal molecules and phosphorylating substrates, SFKs participate in various cell signaling pathways (43).

ROP is a major cause of blindness in infants. The pathogenesis of the disease follows a two-phase course: initial disruption of retinal vascularization and subsequent abnormal vasoproliferation (132). We have developed a rat model of OIR, which mimics the pathophysiological course of human ROP and produces retinopathy representative of the human disease counterpart (71,72).

In this study, we investigated the roles of SFKs in VEGF-mediated retinal angiogenic events both *in vitro* in primary retinal cell cultures and *in vivo* in the rat model of OIR. *In vitro*, regulation of SFK activity via Tyr416 phosphorylation is not required for both VEGF expression under hypoxia in Müller cells and VEGF signaling in RMECs. *In vivo*, SFKs were highly phosphorylated at the activation loop Tyr416 in retinas with pathological retinal angiogenesis, but not in those with only physiological intraretinal vascularization.

5.3 Materials and Methods

Materials

Recombinant human VEGF 165 was purchased from R&D Systems. A selective SFK inhibitor, PP2, and its negative control, PP3, were purchased from Calbiochem (San Diego, CA). Antibodies recognizing SFKs in general, or individual Src, Fyn or Yes, or VEGFR-2 were purchased from Upstate and Santa Cruz Biotechnology. Antibodies recognizing SFK pY416 and phospho-Erk1/2 were purchased from Cell Signaling. Antibodies recognizing SFK pY527 and phospho-FAK Tyr861 (FAK pY861) were purchased from Biosource (Camarillo, CA). Antibodies recognizing vimentin and GFAP were purchased from DAKO. FITC-conjugated goat anti-mouse IgG antibody and RRX-conjugated goat anti-rabbit IgG antibody were purchased from Jackson Immunoresearch Laboratories. HRP-conjugated anti-rabbit and anti-mouse antibodies were purchased from Promega. Unless otherwise specified, all other reagents were purchased from Sigma.

Cell culture

Primary cultures of bovine RMECs (VEC Technologies, Rensselaer, NY) from the 6th to the 10th passage and human RMECs (Cell Systems) from the 5th to the 6th passage were used for *in vitro* studies. Bovine RMECs were routinely cultured in tissue flasks coated with a 50:50 solution of 100 μg/ml fibronectin-100 μg/ml hyaluronic acid in calcium- and magnesium-free PBS (Gibco). Cells were incubated in MCDB-131 complete medium [MCDB-131, 10% FBS, 10 ng/ml epidermal growth factor, 1 μg/ml

hydrocortisone, 100 mg/500 ml Endo Gro (VEC Technologies), 45 mg/500 ml heparin, and 1X antibiotic-antimycotic solution]. Human RMECs were routinely cultured in tissue flasks coated with 0.1% gelatin in PBS and supplied with EGM (Cambrex) supplemented with 10% FBS. Both cell types were cultured in the standard cell culture atmosphere of 5% CO_2 and 95% air in a humidified incubator. When experimental conditions required a serum free medium, MCDB-131 medium containing 1X antibiotic-antimycotic solution was used.

Primary retinal Müller cells were isolated from postnatal day 8 Long-Evans rat pups as previously described (90). The Müller cell identity was confirmed by positive staining for vimentin and negative staining for GFAP. Cells were cultured with DMEM (Gibco) supplemented with 10% FBS (Hyclone) and 1X antibiotic-antimycotic solution. Cells were routinely cultured in the standard cell culture atmosphere (20.9% oxygen; designated as "normoxic condition"). Passages from 3 to 5 were used for *in vitro* experiments.

Western blot analysis

Cells were washed with cold PBS and lysed with cold Buffer I (50 mM Tris-HCl, 150 mM NaCl, 1% NP-40, 0.25% sodium deoxycholate, PH 7.4) containing protease and phosphatase inhibitors (1 mM EDTA, 1 mM PMSF, 1 μg/ml aprotinin, 1 μg/ml leupeptin, 1 μg/ml pepstatin A, 1 mM Na_3VO_4, 1 mM NaF). Retinal tissues were lysed by sonication at 4ºC in Buffer II (50 mM Tris-HCl, 150 mM NaCl, PH 7.4) containing protease and phosphatase inhibitors as above. After centrifugation, the supernatants were collected for protein quantification using a BCA protein assay (Pierce).

Equal amounts of protein samples were resolved by 10% SDS-PAGE minigels (Bio-Rad). Proteins were then transferred to 0.2 μm nitrocellulose membranes (Bio-Rad). After incubation in the blocking buffer, TBS with 0.1% Tween-20 and 5% nonfat dry milk (Bio-Rad), for 30 min at room temperature, membranes were rinsed with TBS and incubated with the primary antibody in the blocking buffer overnight at 4°C. Then, membranes were washed with TBS and incubated with HRP-conjugated anti-rabbit or anti-mouse secondary antibody for 2 hr at room temperature. After thorough washing, the proteins were visualized by enhanced chemiluminescence (Amersham).

Digitized images of Western blots were quantified using Image J software (NIH). Raw densitometric values were normalized against internal controls (i.e. β-actin) and then used for statistical analysis.

Immunoprecipitation

Cell lysates were centrifuged at 12,000 g for 15 min at 4°C. The supernatants were pre-cleared with protein A or G agarose bead slurry (50%; Pierce). Cell extracts, 1 mg per sample, were then incubated with the primary antibody for 2 hr at 4°C with gentle rocking. Immunocomplexes were captured by adding 100 μl protein A or G agarose and gently rocking for 30 min. Beads were then collected by pulse centrifugation (i.e. 10 sec at 10,000 g) and washed with cold Buffer I once and with cold PBS twice. Samples were boiled for 5 min in 2X Laemmli's sample buffer and resolved with 10% SDS-PAGE gels.

Interference of SFK expression with siRNAs

Src siRNA, corresponding to the human Src cDNA sequence

AAGCAACTTGCCCAGCTATGA, and Fyn siRNA, corresponding to human Fyn cDNA sequence AAAGATGCTGAGCGACAGCTA (109), were chemically synthesized with symmetric 3′ dTdT overhangs by Qiagen. Validated human Yes siRNA, β-actin siRNA and nonsense control siRNA were purchased from Ambion.

siRNAs (300 nM) were transfected into 5 x 10^5 human RMECs by electroporation using a human lung microvascular endothelial cell Nucleofector™ kit (Amaxa) and a Nuclefector™ device (Amaxa) according to the manufacturer's instructions. Immediately after electroporation, cells were resuspended in pre-warmed EGM with 10% FBS in the absence of antibiotics. Equal amounts of cells (approximately 80% confluence) were cultured in 12-well plates. Cells began to attach to culture vessels within 1hr after electroporation and, 24 hr later, about 80% of the seeded cells were viable. Cells were then washed with serum free medium, treated with 25 ng/ml VEGF, and lysed for Western blot analysis.

We have characterized the use of these siRNAs in human RMECs and documented in detail elsewhere (Werdich XQ, Penn JS: Differentiation of the roles of Src, Fyn and Yes kinases in VEGF-mediated endothelial cell events by RNA interference. Manuscript submitted). Transfection of Src siRNA (300 nM) alone in human RMECs induced 66% specific downregulation of Src expression, 65% downregulation of Fyn expression by Fyn siRNA (300 nM), and 60% downregulation of Yes expression by Yes siRNA (300 nM) 24 hr post-transfection. Simultaneous transfection of Src, Fyn and Yes siRNAs significantly reduced protein expression of Src, Fyn and Yes by 40 - 45% 24 hr post-transfection. Nonsense control siRNA was used at 300 nM or 900 nM. Transfection of siRNAs at concentrations up to 1 μM showed no toxicity in human RMECs.

Hypoxia exposure of Müller cells

Equal amounts of Müller cells were seeded in 6 cm-Petri dishes and maintained under normoxic conditions. When the cultures reached approximately 80% confluence, cells were washed and each dish supplied with 4 ml of fresh growth medium. In some experiments, PP2 was added at concentrations ranging from 1 μM to 20 μM. Cells were subjected to various hypoxic conditions or normoxia for 24 hr. Anoxic conditions (about 0% oxygen) with a CO_2-enriched environment were generated with BBL™ GasPak Pouch™ system (Becton Dickinson). Normoxic and other hypoxic conditions with oxygen concentrations ranging from 20.9% to 2.5% were generated by using an Isotemp laboratory CO_2 incubator with O_2 control (Kendro Laboratory). Temperature, humidity and CO_2 concentration were controlled and maintained at all times. The culture media and cell lysates were collected for VEGF and protein quantification, respectively. The anoxic condition (about 0% oxygen) was identified as the optimal hypoxic condition for induction of VEGF expression in the primary rat Müller cell culture.

Quantification of VEGF concentration

VEGF concentrations (pg/ml) of Müller cell culture media or retinal lysates were determined using a colorimetric VEGF ELISA assay kit (R&D Systems) according to the manufacturer's instructions. The VEGF concentrations (pg/ml) were then normalized to the total protein concentrations (mg/ml) of Müller cell lysates or retinal lysates, as determined by BCA.

A rat model of OIR and intravitreous injection

For *in vivo* study, we used a well established rat model of OIR (71,72). Briefly, within 4 hr after birth, normalized litters of 16 Sprague-Dawley rat pups were placed with nursing dams in Isolette® infant incubators (Hill-Rom Services, Batesville, IN) with controlled oxygen environments. The animals were exposed to alternating periods of hyperoxia (50% oxygen) and hypoxia (10% oxygen) every 24 hr for 14 days, and then moved to room air. In rat pups, this treatment consistently produced retinopathy representative of human ROP post oxygen exposure (71). In other experiments, animals were exposed to a less extreme variable oxygen regimen with oxygen concentrations of 40 and 15%. Unlike the 50/10% treatment, the incidence of retinopathy in these rats was rare (about 4.8%), and the severity was less than 1 clock hour (72). Therefore, the 50/10% treatment is designated as the OIR model in this manuscript. Age-matched control rats were raised simultaneously in room air.

Some animals were sacrificed at various post exposure days and their retinas were harvested for protein analysis or immunohistochemical staining. Others were subjected to intravitreous injection upon removal to room air. PP2 was used at a final concentration of 10 μM in 0.1% DMSO, and vehicle DMSO was used at a final concentration of 0.1%. Before injection, animals were sedated by methoxyflurane (Pitman-Moore, Mundelein, IL) inhalation. Proparacaine hydrochloride 0.5% (Allergan, Irvine, CA) was topically applied to the cornea. Intravitreous injection of 2.5 μl PP2 (left eyes) or vehicle (right eyes) were administered with a 30-gauge syringe (Hamilton, Reno, NV) according to a procedure described by Shafiee et al (133). Following injection, neomycin/polymyxin B/gramicidin ophthalmic drops (Alcon, Fort Worth, TX) were topically applied. After 6

days in room air (postnatal day 20), animals were sacrificed and retinas were dissected for assessment of retinal neovascularization. Use and treatment of animals conformed to the Declaration of Helsinki principles.

Immunohistochemistry

Deparaffinized 5 μm-thick transverse sections of retinal tissue were antigen-retrieved with DAKO® target retrieval solution (DAKO) according to the manufacturer's instructions. After blocking in SuperBlock® blocking buffer (Pierce), the sections were incubated with the primary antibody in SuperBlock® blocking buffer at 4°C for overnight and then with the FITC- or RRX-conjugated secondary antibody at room temperature for 2 hr. The retinal sections which were incubated in SuperBlock® blocking buffer without the primary antibody served as the negative control. After thorough washing, sections were coverslipped using a ProLong® antifade kit (Molecular Probes). Slides were observed and images were taken with a Zeiss LSM510 confocal microscope (Carl Zeiss Microimaging).

Assessment of retinal neovascularization

Retinal vasculature was stained using a histochemical method for detecting ADPase activity, according to a procedure previously described (134) adapted for our purpose (74). This method stains retinal vascular endothelia and their stem cells in rats of this age (135). The stained retinas were whole-mounted onto slides.

The severity of retinal pathological neovascular development was semi-quantified by the clock-hour method (72,136). Briefly, each retinal surface was divided into twelve

parts (clock hours). Three masked investigators independently evaluated the number of clock hours containing abnormal blood vessel growth. Their assessments were averaged for each retina. The data was expressed in values varying from 0 (no pathology) to 12 (involvement of entire retinal circumference). Counting the number of clock hours occupied by retinal neovascularization is an established unit of clinical assessment of human ROP. Retinas of age-matched room air rats showed no pathology.

Data analysis

Data were analyzed with Stat View software (Abacus Concepts). The ANOVA statistical test was used to analyze parametric data such as VEGF concentration and normalized densitometric values. The non-parametric data for retinal neovascularization obtained by the clock-hour method were analyzed with the Mann-Whitney test. For each test, $p < 0.05$ was considered significant.

5.4 Results

In vitro, regulation of SFK activity via Tyr416 is not required for SFK-mediated VEGF signaling in RMECs

In both bovine and human RMECs cultured in either growth medium (data not shown) or serum free medium (Figure 5.1), we detected a constant level of SFK pY416. These wild type SFKs could actually phosphorylate substrates as measured *in vitro* using a kinase activity assay. VEGF stimulation did not increase the SFK pY416 signal in either cell type in both time course and dose response studies (Figure 5.1, a and b), nor was the *in vitro* catalytic activity changed (data not shown). Furthermore, the pY416

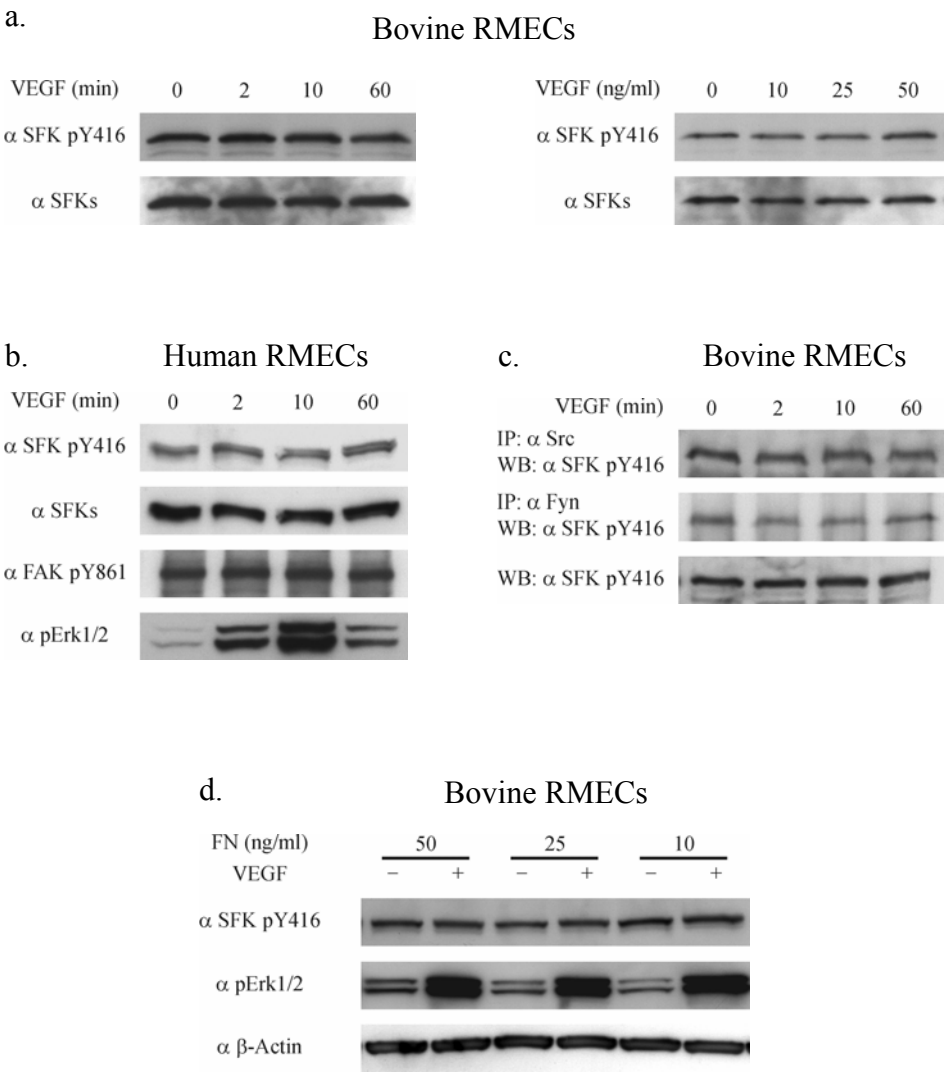

Figure 5.1. *In vitro*, VEGF signaling in RMECs does not increase SFK Tyr416 phosphorylation. Cells were serum-starved overnight. Unless specifically noted, VEGF was used at 25 ng/ml for 10 min. Each experiment was independently repeated at least three times. a, The time course and dose response studies in bovine RMECs. b, A time course study in human RMECs. c, A time course study of individual SFK members Src and Fyn in bovine RMECs. The protein expression level of Yes was lower than that of Src and Fyn, data not shown. d, Representative blots of experiments under modified conditions. Cells were cultured on plates coated with various concentrations of fibronectin (FN).

signal of individual Src, Fyn or Yes did not change (Figure 5.1c). Tyr861 of FAK is a major phosphorylation substrate of SFKs (137). Consistently, FAK pY861 showed no increase upon VEGF stimulation (Figure 5.1b). However, VEGF stimulation did significantly activate SFKs' downstream signal molecules Erk1/2 (100,111,112) (Figure 5.1, b and d). We considered the possibility that the culture conditions were not optimal for SFK quiescence, and that the pre-existing background signal of SFK pY416 may have masked a significant response of SFKs to VEGF stimulation. To address this, we conducted experiments with modified culture and stimulation conditions. These included a broad range of VEGF stimulation times (30 sec to 24 hr), different phosphatase inhibitors (such as pervanadate), and different starvation or surface coating conditions, etc. The results of these experiments were all consistent: VEGF stimulation did not significantly enhance phosphorylation of SFKs at the activation loop Tyr416, nor was the resting state of SFK pY416 (Figure 5.1d) and the kinase activity (data not shown) ever completely quiescent.

Nevertheless, pretreatment with PP2, a selective SFK inhibitor, at various concentrations significantly blocked VEGF-induced phosphorylation of Erk1/2 in both bovine and human RMECs in a dose dependent manner (Figure 5.2a). PP2 binds to the adenosine triphosphate (ATP) pocket of SFKs, and is non-competitive against ATP for the inhibition of SFKs (138). The negative control PP3 exerted no impact on Erk1/2 activation by VEGF (Figure 5.2a).

Using the gene specific RNAi technique, we have efficiently knocked down Src, Fyn and Yes individually or simultaneously in human RMECs (Werdich XQ, Penn JS: Differentiation of the roles of Src, Fyn and Yes kinases in VEGF-mediated endothelial

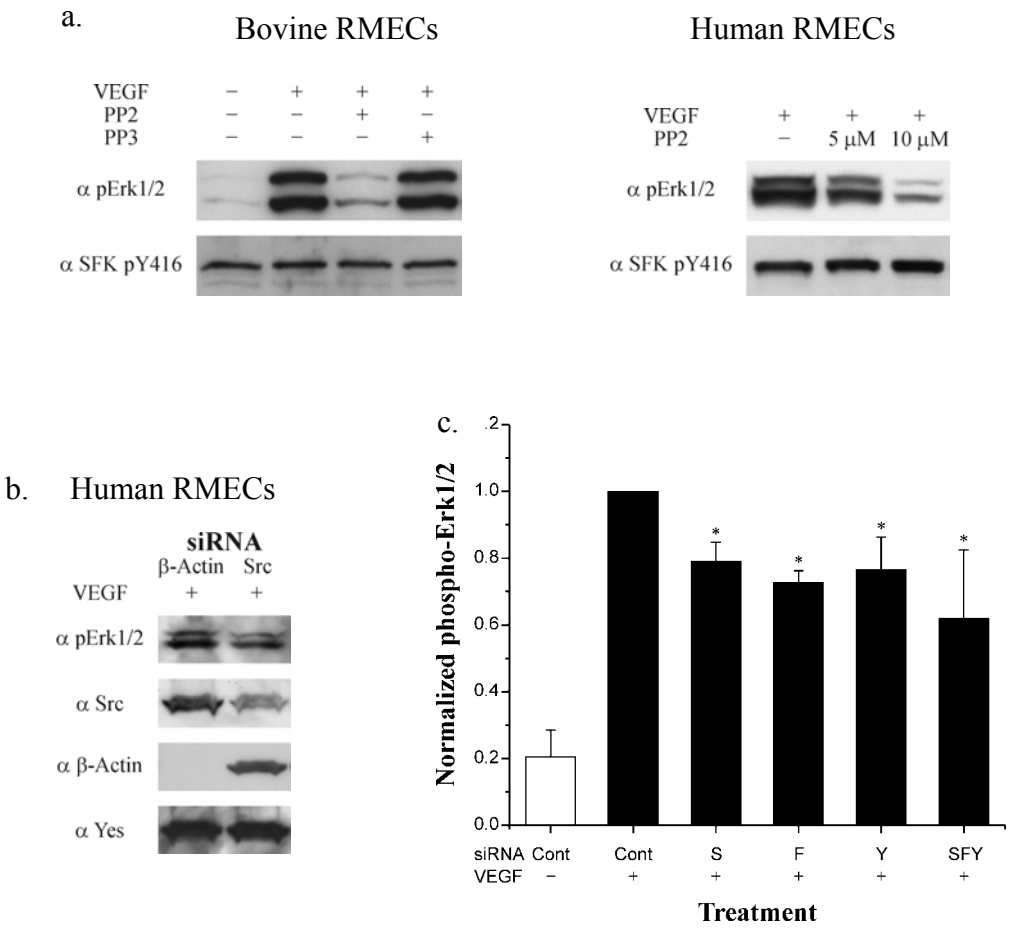

Figure 5.2. *In vitro*, VEGF signaling in RMECs requires SFK activity. Serum-starved cells were treated with 25 ng/ml VEGF for 10 min. a, Inhibition of VEGF-induced Erk1/2 activation by PP2, but not PP3. Unless specifically noted, cells were pre-incubated with 10μM PP2 or PP3 for 2 hours. The experiment was independently repeated four times. b, Inhibition of VEGF-induced Erk1/2 activation by specific downregulation of Src using RNAi. c, Quantitative analysis of the effects of specific downregulation of Src, Fyn, or Yes by RNAi on VEGF-induced Erk1/2 activation. The experiment was independently repeated three times. *, significantly different from VEGF-treated control cells which were transfected with the nonsense control siRNA, $p < 0.05$. Cont, nonsense control; S, Src; F, Fyn; Y, Yes; SFY, Src, Fyn and Yes.

cell events by RNA interference. Manuscript submitted). VEGF-induced phosphorylation of Erk1/2 was significantly reduced in cells deficient in individual Src, Fyn, or Yes, and in cells deficient in all three SFKs ($p < 0.05$) (Figure 5.2, b and c). The remaining activities of SFKs which were not completely abolished by RNAi, may have contributed, at least in part, to the remaining Erk1/2 activation. Therefore, gene specific downregulation of SFKs by RNAi in human RMECs confirmed that SFKs were indeed required for VEGF signaling through the Raf-MEK-Erk pathway, and that Src, Fyn and Yes all contributed.

In addition, we observed that VEGF stimulation induced rapid and substantial recruitment of SFKs to VEGFR-2 in both bovine and human RMECs. In human RMECs, two minutes after stimulation, the amount of VEGFR-2-associated SFKs was significantly increased by 1.8-fold, and 10 min post stimulation by 2.0-fold (Figure 5.3).

Thus, SFKs were important molecular components of VEGF signal cascades. However, SFK activation via Tyr416 phosphorylation was not required for VEGF signaling in RMECs.

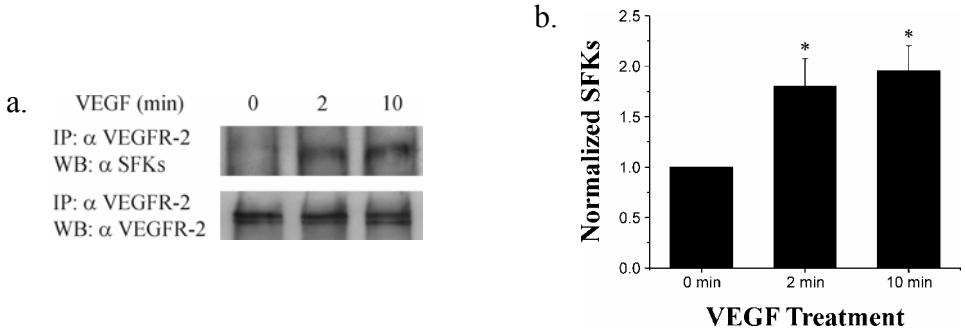

Figure 5.3. *In vitro*, VEGF signaling in RMECs induces recruitment of SFKs to VEGFR-2. Serum-starved human RMECs were treated with 25 ng/ml VEGF. The experiment was independently repeated five times. a, Representative Western blots. b, Quantitative analysis of Western blots. *, $p < 0.02$.

In vitro, regulation of SFK activity via Tyr416 is not required for SFK-mediated VEGF expression under hypoxia in Müller Cells

Müller cells are the predominant VEGF-secreting cell type in the retina during ischemia-induced hypoxia (11,89). *In vitro*, primary rat Müller cells secreted VEGF spontaneously even under normoxic culture conditions (i.e. 20.9% oxygen), which constituted a higher oxygen concentration than that normally found in the retina (8). In fresh growth medium, VEGF concentration was below the detection sensitivity of the ELISA assay. After 24 hr incubation, we found VEGF in the rat Müller cells culture medium at a level of 215.32 ± 56.47 pg/mg (VEGF concentration normalized to total protein concentration). Exposure of the cells to hypoxia (0% oxygen) induced 2.4-fold increase in VEGF production after 24 hr ($p < 0.05$) (Figure 5.4a). We did not observe any significant change in cell morphology under hypoxia.

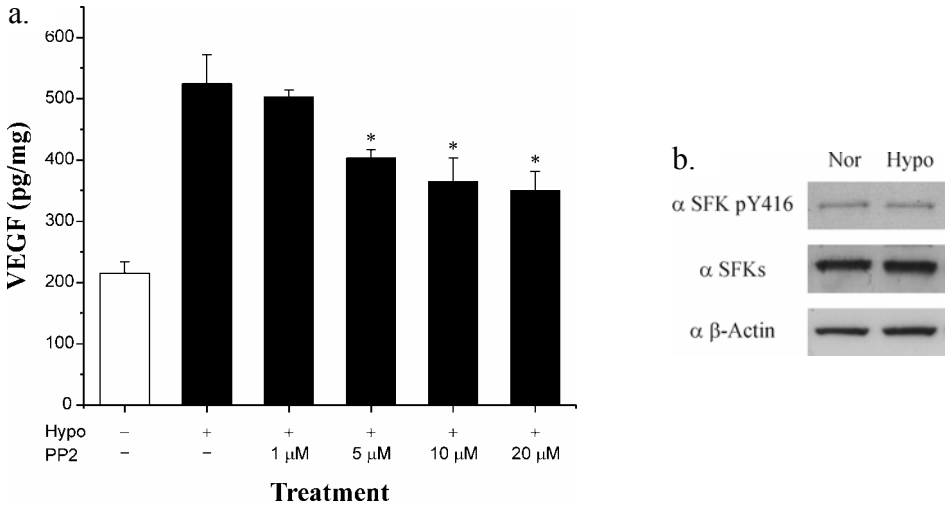

Figure 5.4. *In vitro*, regulation of SFK activity via Tyr416 is not required for SFK-mediated VEGF expression under hypoxia in Müller cells. Nor, normoxia; Hypo, hypoxia (0% oxygen). Each experiment was independently repeated at least three times. a, VEGF induction by hypoxia in Müller cells and its inhibition by PP2. *, significantly different from cells treated with hypoxia alone, $p < 0.02$. b, Wertern blot analysis (24 hr incubation).

Using Western blot analysis, we consistently detected the pY416 signal of SFKs in Müller cells cultured under normoxic conditions (Figure 5.4b). Exposure of the cells to hypoxia did not increase the SFK pY416 signal (Figure 5.4b), despite a significantly increased VEGF production (Figure 5.4a). The time course study and exposure of cells to other hypoxic conditions (2.5 to 10% oxygen) revealed no change either (data not shown).

In order to clarify the role of SFKs in the hypoxia-induced VEGF production pathway, we cultured Müller cells under hypoxic conditions (0% oxygen) in the presence of PP2. PP2 did, in fact, significantly reduce VEGF production in a dose dependent manner (Figure 5.4a). Control treatments with DMSO alone or with the negative control PP3 at the same concentration resulted in no change on VEGF production.

Therefore, while SFKs were clearly required for VEGF production under hypoxia, regulation of SFK activity via a Tyr416-dependent mechanism was not.

In vivo, significantly increased retinal SFK Tyr416 phosphorylation correlates with elevated retinal VEGF levels in a rat model of OIR

The OIR model (50/10% oxygen treatment) consistently produced retinopathy in rat pups (Figure 5.5b). The retinal VEGF expression was significantly increased at all tested post-exposure ages compared to room air controls ($p < 0.05$) (Figure 5.6a). Upon removal to room air, oxygen-treated animals showed the highest retinal VEGF level with a 6.6-fold increase compared to their room air controls. VEGF expression dropped later during the first day post-exposure and then gradually increased, before dropping again as measured on day 6 post-exposure. We hypothesize that the substantially elevated retinal VEGF expression at the end of the oxygen exposure resulted mainly from the oxygen

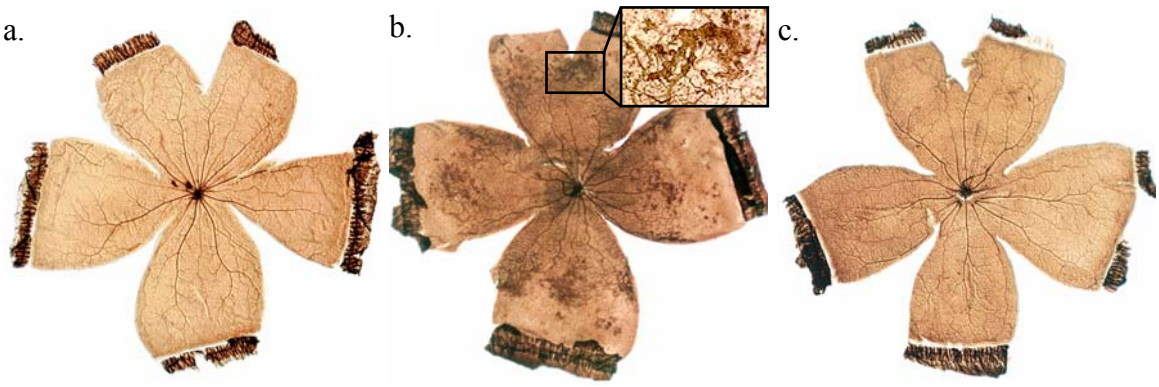

Figure 5.5. Demonstration of the retinal vasculature. Rat retinas were harvested on day 6 post oxygen exposure (postnatal day 20) and stained for ADPase activity. a, A retina of room air control animals. b, An OIR (50/10% oxygen treatment) retina. The insert shows the vascular pathology at a higher magnification. c**,** A retina from the 40/15% oxygen treatment group.

treatment (30). The subsequent VEGF increase during the post-exposure period in room air was also due to ischemia-induce hypoxia in non-perfused retinal tissue (11).

Using Western blot analysis, we found that phosphorylation of the SFK activation loop Tyr416 was significantly increased in OIR retinas compared to room air controls, when measured on various post-exposure days (Figure 5.6b). Upon removal of animals to room air, SFK pY416 was observed at the highest level which later gradually tailed off, a pattern which was consistent with the retinal VEGF profile. We did not see a decreased SFK pY527 signal in these retinas compared to the room air controls (Figure 5.6b). SFK protein levels showed no significant different between OIR retinas and room air controls (Figure 5.6b). Tyr861 of FAK, a substrate of SFKs, was highly phosphorylated in OIR retinas with a profile similar to that of SFK pY416 (Figure 5.6b). Retinal phospho-Erk1/2 showed only a modest difference between oxygen-treated samples and room air controls.

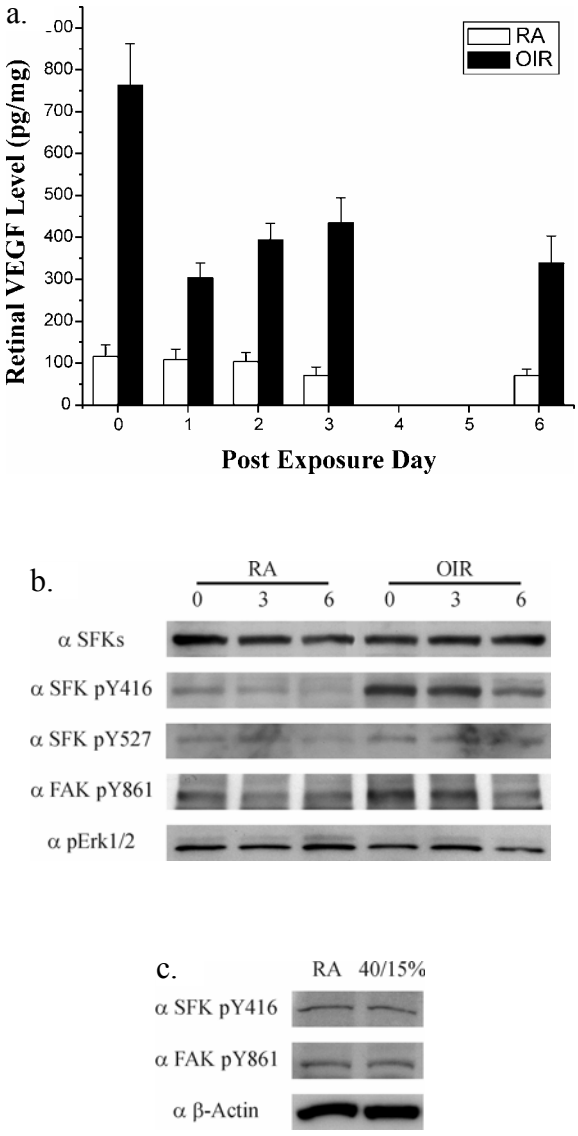

Figure 5.6. *In vivo*, significantly increased retinal SFK Tyr416 phosphorylation correlates with elevated retinal VEGF levels in a rat model of OIR. Each experiment was independently repeated at least three times. a, The retinal VEGF profile in OIR rats (n = 36) and room air controls (RA, n = 17). Retinal VEGF of OIR rats was significantly higher than that of controls on all tested ages, $p < 0.05$. b**,** The SFK profile in the OIR retinas. Retinas were harvested on post exposure day 0, 3 and 6. c**,** The SFK profile in the 40/15% retinas. Retinas were harvested on post exposure day 0 (postnatal day 14).

In a previous study, we demonstrated that the higher amplitude of the fluctuating inspired oxygen resulted in higher incidence and severity of retinopathy in rat pups (72). An oxygen regimen cycling between 40 and 15% oxygen constituted the maximum oxygen variation without producing retinopathy in rat pups (Figure 5.5c). Nevertheless, immediately after oxygen exposure, these retinas showed an average avascular area which was 14% of the total retina area, while room air controls were fully vascularized. There was also a 2.7-fold increase in the retinal VEGF level compared to the room air control (72,139). Unlike OIR retinas, we did not observe any increase of the SFK pY416 signal or phosphorylation of FAK Tyr861 in these retinas compared to room air controls (Figure 5.6c).

Thus, significantly increased phosphorylation of the SFK activation loop Tyr416 was specifically seen in the OIR retina.

Immunohistochemical staining pattern of the elevated SFK pY416 signal in the OIR retina is consistent with Müller cell localization

To further investigate the cellular source of the elevated retinal SFK pY416 signal seen in Western blots, we performed an immunohistochemical analysis of retinal transverse sections using confocal microscopy. In the OIR retina harvested immediately after removing animals to room air, many cell somas located in the middle region of the inner nuclear layer (INL) displayed increased SFK pY416 staining, as compared to the age-matched room air control (Figure 5.7a). Longitudinally, they resided in the peripheral retina, approximately extending from the location of the retinal vascular frontier towards the retinal margin (data not shown). These immunoreactive cell bodies displayed an irregular shape with processes projecting from the main trunk, as shown in the insert of

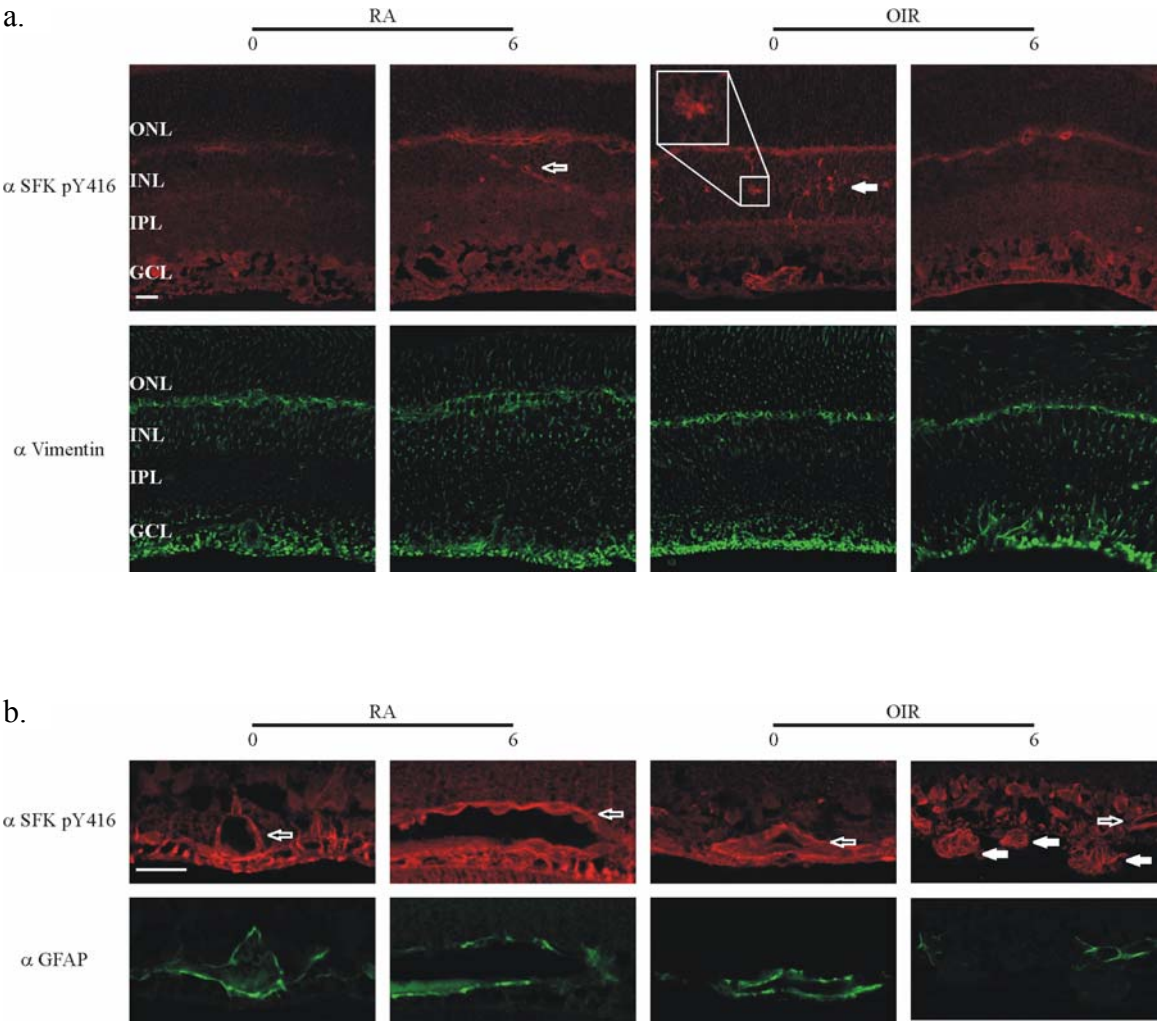

Figure 5.7. *In vivo*, immunohistochemical analysis of the SFK pY416 signal in the retina. Retinas were harvested on post exposure day 0 and 6. ONL, outer nuclear layer; INL, inner nuclear layer; IPL, inner plexiform layer; GCL, ganglion cell layer. Bar, 20 μm. a**,** The staining pattern of the increased SFK pY416 signal in OIR retinas consistent with Müller cell localization (the white arrow). Adjacent slides were stained for vimentin. The black arrow with white edge denotes normal retinal blood vessels, which grew from the superfacial network towards the deep network. b**,** The staining pattern of SFK pY416 in the normal intraretinal vessels (the black arrow with white edge) and pathological preretinal vascular tufts (the white arrow). Adjacent slides were stained for GFAP.

Figure 5.7a. The location and morphology of these cells identified them as Müller cells (140). The increased SFK pY416 signal in the INL trended to subside during the post exposure period, which was consistent with the Western blot profile of SFK pY416. Vimentin-staining revealed radially oriented processes of Müller cells spanning nearly the entire depth of the retina which supported our assumptions concerning the SFK pY416-positive cells. There was no significant difference in the vimentin-staining pattern among retinas derived from OIR rats and room air controls.

We also observed that the normal intraretinal vascular beds, including both superficial and deep networks, were positively stained for SFK pY416 (Figure 5.7, a and b). The staining intensity was consistent among tissues harvested from OIR rats and from room air controls on various post-exposure days (Figure 5.7b). On day 6 post exposure, abnormal blood vessel growth was seen in OIR retinas but not in room air controls. Those vessels penetrated the inner limiting membrane (ILM), grew into the vitreous, and formed preretinal neovascular tufts. These tufts were mainly composed of hyperplastic endothelial cells (72), which were also positively stained by the SFK pY416 antibody (Figure 5.7b). There was no significant difference in the intensity of SFK pY416 staining in intraretinal blood vessels and preretinal neovascular tufts. GFAP staining showed astrocytes which were restricted to the nerve fiber layer (NFL) (Figure 5.7b, lower panel). During the development of the superficial retinal vascular network, astrocytes function as a guide for endothelial cell migration and are closely associated with blood vessels (93). However, in OIR retinas, they failed to accompany the proliferating endothelial cells into preretinal neovascular tufts.

Intravitreous injection of PP2 significantly reduced retinopathy in a rat model of OIR

The importance of SFKs in retinal neovascularization is evidenced by our *in vitro* and *in vivo* findings. *In vitro* experiments identified 10 μM PP2 as an optimum concentration for inhibiting SFK-mediated VEGF induction by hypoxia in Müller cells and VEGF signaling in RMECs. In OIR rats, intravitreous injection of PP2 (10 μM) upon removing animals to room air significantly inhibited retinopathy by 33% compared to the vehicle control injection. The severity of retinopathy semi-quantified by the clock-hour method showed a median of 4 with a range of 2-7.5 for the PP2-injected eyes, and a median of 6 with a range of 2-10 for the vehicle-injected eyes, $p < 0.01$ (Figure 5.8a). The size of the retinal area involving pathological neovascularization was also markedly reduced, as shown in Figure 5.8b.

5.5 Discussion

Our results clearly demonstrated that SFKs are involved in VEGF-mediated retinal neovascularization. *In vitro*, SFKs were required for both VEGF expression under hypoxia in Müller cells and VEGF signaling in RMECs. *In vivo*, in a rat model of OIR, the activation loop Tyr416 of SFKs was highly phosphorylated, which paralleled significantly increased retinal VEGF. Our immunohistochemical analysis revealed that the elevated SFK pY416 signal originated from Müller cells, which have previously been shown to constitute a predominant source of VEGF secretion during the pathogenesis of retinopathy (11,89). A significant inhibition of retinopathy by intravitreous injection of a selective SFK inhibitor, PP2, in the OIR rats confirmed that SFKs were key regulators of the abnormal retinal blood vessel growth.

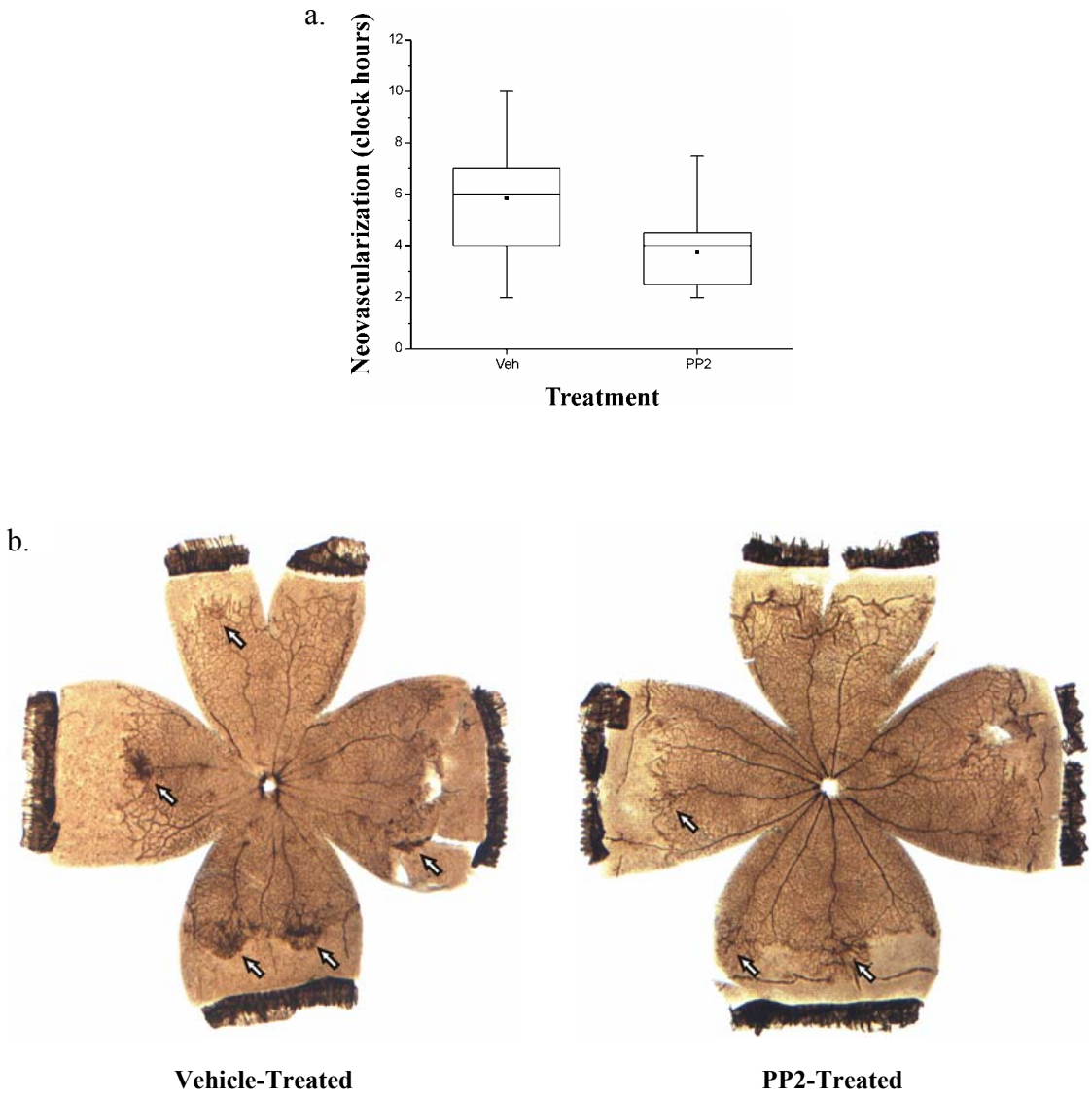

Figure 5.8. *In vivo*, intravitreous injection of PP2 significantly reduces retinal neovascularization in a rat model of OIR. PP2, 10 μM; vehicle, 0.1% DMSO in sterile PBS. Animals, n = 17. a, Demonstration of the severity of retinopathy (clock hours) by box graph. The black dot denotes the mean; the line within the box denotes the median; the vertical bar denotes the range. The two treatments were significantly different from each other at $p < 0.01$. b, Demonstration of the severity of retinopathy with ADPase-stained retinas. Arrows denote preretinal neovascularization.

In quiescent bovine and human RMEC cultures, we showed that VEGF stimulation could activate SFKs' downstream signal molecules-Erk1/2 (100,111,112) without increasing SFK Tyr416 phosphorylation and their intrinsic catalytic activity under various experimental conditions. Consistently, our *in vivo* data showed that the SFK pY416 signal was equivalently detected in intraretinal vessels and preretinal vascular tufts in OIR and normal retinas, even though the VEGF level in OIR retinas was significantly higher than that in room air controls. Thus, Tyr416-dependent SFK activation is not required for SFK-mediated VEGF signaling in RMECs both *in vitro* and *in vivo*.

In the retina, Müller cells are the main storage site for glycogen, principally obtaining ATP through glycolysis and consuming little oxygen (88). They are highly resistant to hypoxia and hypoglycemia which allows them to function normally in a perturbed environment, such as during ischemia. Our *in vitro* data showed that VEGF expression under hypoxia in Müller cells required SFK activity, which, however, was not correlated to an increase in Tyr416 phosphorylation. This finding was consistent with our *in vivo* data from rats treated with the 40/15% oxygen regimen. During the post exposure period, there was a continuous process of hypoxia-induced retinal VEGF expression and intraretinal vascularization. However, we did not observe any increase of the SFK pY416 signal in these retinas compared to age-matched room air controls, in which the retinal vasculature has fully developed. Therefore, Tyr416-dependent SFK activation is not required for SFK-mediated VEGF expression under hypoxia in Müller cells both *in vitro* and *in vivo*.

It is generally believed that upon stimulation, the catalytic activity of cellular SFKs is increased via phosphorylation of Tyr416 (43). This would allow them to phosphorylate substrates and participate in various signaling events, as previously shown in hypoxic induction of VEGF in U87 glioma cells and kidney 293 cells (18), or in platelet-derived growth factor signaling in various cell types (109,141). Conversely, our data show that regulation of SFK activity via a Tyr416-dependent mechanism was not always required for SFK signaling. Specifically, we found that SFK-mediated VEGF expression under hypoxia in Müller cells and VEGF signaling in RMECs could occur without an increase of Tyr416 phosphorylation. *In vivo*, SFKs may exist in four possible forms dependent on the phosphorylation states of Tyr527 and Tyr416 (131). It has been shown that Src, which is unphosphorylated at Tyr416, has a basal kinase activity and can readily phosphorylate substrates (142). In addition, the phospho-Tyr416 form of Src, even being in the intramolecular SH2-pY527 complex, retains about 20% of its catalytic activity and can phosphorylate substrates (50). In quiescent Müller cells and RMECs, we consistently detected a SFK pY416 signal. This indicates that at least a fraction of cellular SFKs is phosphorylated at Tyr416. In fact, these wild type SFKs could actually phosphorylate substrates (e.g. enolase) *in vitro*. We believe that both the SFK basal kinase activity and the pY416-related regulatory activity may have contributed to the kinase activity. We propose that, in some circumstances, wild type SFKs retain a baseline kinase activity, which is physiologically relevant. This baseline kinase activity is sufficient for signal transduction through SFKs. Takahashi and Shibuya reported that SFKs were not activated by VEGF in sinusoidal endothelial cells using an *in vitro* kinase assay (143), while others demonstrated that SFKs were, indeed, required for VEGF signal pathways in human

umbilical vein endothelial cells using SFK inhibitors or a kinase-deleted Src mutant (47,48). Cary and colleagues showed that although Src kinase activity was necessary for integrin-signaling in fibroblasts, it did not need to be upregulated by phosphorylation of Tyr416 (142).

However, under some pathological conditions, SFKs can indeed become highly activated via phosphorylation of Tyr416. In OIR retinas, we consistently observed a significantly increased SFK pY416 signal compared to the retinas from the 40/15% oxygen treatment group and the room air control group. We suspect that this Tyr416-dependent SFK activation may be involved in the pathophysiological course of OIR. It is not yet clear why and how SFKs are activated at Tyr416. SFK activation in Müller cells can be a direct consequence of retinal ischemia and oxygen insult, or an indirect response to severely stressed neurons during and post oxygen exposure. Since SFKs were activated only in the retinas of the 50/10% treatment group, but not in those of the moderate 40/15% treatment group, there may be a threshold for hypoxia and ischemia tolerance in the retinal tissue. Consequently, severe disturbances of the retinal physiological environment lead to SFK activation and retinopathy.

Although there is no direct link between activated SFKs and excessive VEGF production by Müller cells in the OIR retina, several lines of evidence support this hypothesis. First, SFK activation in OIR retinas was correlated with drastically increased retinal VEGF levels post oxygen exposure. Second, SFKs were activated in the somas of Müller cells, where increased VEGF expression has been localized in the ischemic retina (11,89,93). Third, the distribution of cells with increased levels of SFK pY416 approximated the peripheral avascular retinal region. More significantly, in U87 glioma

cells, overexpression of Src resulted in increased VEGF transcription under hypoxia. Transfection with v-Src constitutively increased the VEGF mRNA level even in the absence of hypoxia (18). In addition, activated SFKs in Müller cells may participate in other undefined pathophysiological events. For example, glial cells have been shown to influence the blood-brain barrier properties(144). However, it remains possible that SFK activation in the OIR retina is a consequence rather than a cause of pathological or physiological events.

Significant increase of SFK expression and/or catalytic activity has been observed in a variety of tumors. This elevated SFK activity was shown to be correlated with the stage and metastatic potential of some neoplasia, which identified the activated SFKs as potential targets for intervention in turmorigenesis (145). Here, we report that significantly increased phosphorylation of the activation loop Tyr416 of SFKs was associated with the pathogenesis of retinopathy in a rat model of OIR, but not in the physiological intraretinal vascularization. The mechanism of SFK activation at Tyr416 and its roles in the pathophysiological course warrant further characterization. Ultimately, this may lead to a discrimination of important molecular and cellular differences between physiological retinal vascular development and pathological retinal neovascularization. The detailed knowledge of SFK activation and subsequent abnormal cellular functions may facilitate rational design of therapeutic strategies which selectively target pathological events and minimize the unfavorable impact on physiological cellular functions.

5.6 Acknowledgments

We thank Dr. Gary W. McCollum for experimental support. We thank Dr. Derya Unutmaz for sharing the Nucleofector™ Device. We thank the VUMC Cell Imaging Shared Resource for the training and sharing of microscopes and software.

CHAPTER VI

CONCLUDING REMARKS

Hypoxia inducible VEGF plays a major role in initiation and mediation of retinal neovascularization in various diseases such as ROP. We have developed a rat model of OIR which mimics the pathophysiological course of human ROP. Exposure of newborn rat pups to alternating periods of hyperoxia and hypoxia can interrupt the development of normal retinal vasculature and lead to tissue ischemia. Retinal glial Müller cells are the major VEGF secreting cell type during the pathophysiological course of OIR. Dysregulated retinal VEGF signaling disturbs the delicate balance of pro-angiogenic and anti-angiogenic factors. It results in abnormal RMEC proliferation and differentiation. SFKs are important molecular components of the VEGF expression pathway during hypoxia in Müller cells and of VEGF signal cascades in RMECs.

Although SFKs have been indicated as candidate tyrosine kinases upstream of HIF-1 in the hypoxia-induced gene expression pathway (14), the underlying molecular mechanism is largely unknown. Hypoxia exposure of primary rat Müller cell cultures may serve as a ready venue for studies of this signal pathway *in vitro*. The proteins associated with SFKs in this signal cascade may be identified using immunoprecipitation or the yeast two-hybrid system. The SFK substrates may be identified using the method of KESTREL (kinase substrate tracking and elucidation) (146).

In vitro, we demonstrated that SFK members Src, Fyn and Yes have differential functions in regulation of VEGF-mediated endothelial cell proliferation, migration and

tube formation. Previously, Eliceiri and colleagues also showed that Src and Yes, but not Fyn were involved in VEGF-mediated vascular permeability (46). Together, these raise the possibility that SFK member(s) may be selectively targeted for inhibition of VEGF-mediated pathological events. Our data strongly motivate further investigation of the molecular mechanism of each signal cascade involved. Future work can first focus on the clear-cut finding shown in Figure 4.5. The involvement of Fyn in the inhibitory pathway of VEGFR-1-mediated endothelial cell migration is hypothetical. Initial experiments should answer the question of whether or not there is a link between the two inhibitory pathways. Evidence may be found by studying the effects of Fyn downregulation on VEGFR-1-mediated cell migration using, for example, porcine aortic endothelial cell lines which stably express wild type or mutant VEGFR-1 (38,125). To reveal the underlying molecular mechanism, both binding activity and catalytic activity of Fyn should be considered, since one may participate in a signal event independent of the other. Mutational analysis is highly recommended, which will facilitate pinpointing the functional region(s), in turn providing valuable information about molecular mechanisms.

Unlike VEGF induction by hypoxia in U87 glioma cells or PDGF signaling, VEGF induction by hypoxia in Müller cells and VEGF signaling in RMECs do not require activation of SFKs by phosphorylation of Tyr416, although SFKs are clearly required. Apparently, the baseline kinase activity of wild type SFKs in these cells can phosphorylate substrates sufficiently to propagate signals. Since the SFK pY416 signal is detected in quiescent wild type cells, at least some fraction of cellular SFKs is phosphorylated at Tyr416. Although there is considerable structural information available for the inactive “closed” conformation of SFKs, it remains unclear how they may

assemble into active signaling complexes with substrates and regulators. In addition, SFKs possess three distinct functions, the basal kinase activity of the kinase domain, the regulated kinase activity via phosphorylation of Tyr416, and SH2 and SH3 binding functions. Each of them may play functionally unique roles in SFK-mediated signal transduction pathways (142). In order to define the molecular mechanism of SFK-mediated signal pathways, the following Src mutants will be of value: the kinase dead mutant (K295R), the unregulatable kinase mutant (Y416F), SH2 or SH3 domain mutants (T215W or D99N) (142).

In vivo, our data showed that significant SFK activation via phosphorylation of Tyr416 was specifically involved in the pathogenesis of OIR, but not in physiological intraretinal vascularization. Many more questions need to be addressed, such as: how are SFKs activated *in vivo* in the OIR model? what other ischemic retinopathies involve SFK activation? what are the roles of activated SFKs in the pathogenesis of retinopathy? Overexpression of v-Src or the constitutively active Src mutant (Y527F) in primary Müller cell cultures would not only confirm the role of activated SFKs on VEGF transcription, but also provide useful information about other physiological events in Müller cells which may be altered during an increased SFK activity. Coculture analysis of Müller cells and retinal neurons, and retinal tissue culture analysis may provide valuable information about the impact of neurons on the cellular functions of Müller cells under hypoxia.

Further characterization of the roles of SFKs in retinal neovascularization will facilitate rational design of therapeutic strategies targeting the SFK-mediated pathological events for inhibition.

REFERENCES

1. Lee P, Wang CC, Adamis AP. Ocular neovascularization: an epidemiologic review. *Surv Ophthalmol* 1998, 43:245-269

2. Campochiaro PA. Retinal and choroidal neovascularization. *J Cell Physiol* 2000, 184:301-310

3. Miller JW. Vascular endothelial growth factor and ocular neovascularization. *Am J Pathol* 1997, 151:13-23

4. Harris A, Bingaman DP, Ciulla TA, and Martin BJ: Retinal and choroidal blood flow in health and disease. Retina. Edited by Ryan SJ. St. Louis, Mosby, 2001, pp. 68-88

5. Michaelson I. The mode of development of the vascular system of the retina with some observations on its significance for certain retinal diseases. *Trans Ophthalmol Soc UK* 1948, 68:137-180

6. Ashton N. Retinal vascularization in health and disease: Proctor Award Lecture of the Association for Research in Ophthalmology. *Am J Ophthalmol* 1957, 44:7-17

7. Shweiki D, Itin A, Soffer D, Keshet E. Vascular endothelial growth factor induced by hypoxia may mediate hypoxia-initiated angiogenesis. *Nature* 1992, 359:843-845

8. Aiello LP, Northrup JM, Keyt BA, Takagi H, Iwamoto MA. Hypoxic regulation of vascular endothelial growth factor in retinal cells. *Arch Ophthalmol* 1995, 113:1538-1544

9. Shima DT, Adamis AP, Ferrara N, Yeo KT, Yeo TK, Allende R, Folkman J, D'Amore PA. Hypoxic induction of endothelial cell growth factors in retinal cells: identification and characterization of vascular endothelial growth factor (VEGF) as the mitogen. *Mol Med* 1995, 1:182-193

10. Miller JW, Adamis AP, Shima DT, D'Amore PA, Moulton RS, O'Reilly MS, Folkman J, Dvorak HF, Brown LF, Berse B, . Vascular endothelial growth factor/vascular permeability factor is temporally and spatially correlated with ocular angiogenesis in a primate model. *Am J Pathol* 1994, 145:574-584

11. Pierce EA, Avery RL, Foley ED, Aiello LP, Smith LE. Vascular endothelial growth factor/vascular permeability factor expression in a mouse model of retinal neovascularization. *Proc Natl Acad Sci USA* 1995, 92:905-909

12. Aiello LP, Avery RL, Arrigg PG, Keyt BA, Jampel HD, Shah ST, Pasquale LR, Thieme H, Iwamoto MA, Park JE, . Vascular endothelial growth factor in ocular

fluid of patients with diabetic retinopathy and other retinal disorders. *N Engl J Med* 1994, 331:1480-1487

13. Okamoto N, Tobe T, Hackett SF, Ozaki H, Vinores MA, LaRochelle W, Zack DJ, Campochiaro PA. Transgenic mice with increased expression of vascular endothelial growth factor in the retina: a new model of intraretinal and subretinal neovascularization. *Am J Pathol* 1997, 151:281-291

14. Guillemin K, Krasnow MA. The hypoxic response: huffing and HIFing. *Cell* 1997, 89:9-12

15. Bunn HF, Poyton RO. Oxygen sensing and molecular adaptation to hypoxia. *Physiol Rev* 1996, 76:839-885

16. Semenza GL, Wang GL. A nuclear factor induced by hypoxia via de novo protein synthesis binds to the human erythropoietin gene enhancer at a site required for transcriptional activation. *Mol Cell Biol* 1992, 12:5447-5454

17. Wang GL, Jiang BH, Semenza GL. Effect of protein kinase and phosphatase inhibitors on expression of hypoxia-inducible factor 1. *Biochem Biophys Res Commun* 1995, 216:669-675

18. Mukhopadhyay D, Tsiokas L, Zhou XM, Foster D, Brugge JS, Sukhatme VP. Hypoxic induction of human vascular endothelial growth factor expression through c-Src activation. *Nature* 1995, 375:577-581

19. Ferrara N, Gerber HP, LeCouter J. The biology of VEGF and its receptors. *Nat Med* 2003, 9:669-676

20. Ferrara N, Henzel WJ. Pituitary follicular cells secrete a novel heparin-binding growth factor specific for vascular endothelial cells. *Biochem Biophys Res Commun* 1989, 161:851-858

21. Tischer E, Mitchell R, Hartman T, Silva M, Gospodarowicz D, Fiddes JC, Abraham JA. The human gene for vascular endothelial growth factor. Multiple protein forms are encoded through alternative exon splicing. *J Biol Chem* 1991, 266:11947-11954

22. Houck KA, Ferrara N, Winer J, Cachianes G, Li B, Leung DW. The vascular endothelial growth factor family: identification of a fourth molecular species and characterization of alternative splicing of RNA. *Mol Endocrinol* 1991, 5:1806-1814

23. Shima DT, Kuroki M, Deutsch U, Ng YS, Adamis AP, D'Amore PA. The mouse gene for vascular endothelial growth factor. Genomic structure, definition of the transcriptional unit, and characterization of transcriptional and post-transcriptional regulatory sequences. *J Biol Chem* 1996, 271:3877-3883

24. Park JE, Keller GA, Ferrara N. The vascular endothelial growth factor (VEGF) isoforms: differential deposition into the subepithelial extracellular matrix and bioactivity of extracellular matrix-bound VEGF. *Mol Biol Cell* 1993, 4:1317-1326

25. Houck KA, Leung DW, Rowland AM, Winer J, Ferrara N. Dual regulation of vascular endothelial growth factor bioavailability by genetic and proteolytic mechanisms. *J Biol Chem* 1992, 267:26031-26037

26. Carmeliet P, Ng YS, Nuyens D, Theilmeier G, Brusselmans K, Cornelissen I, Ehler E, Kakkar VV, Stalmans I, Mattot V, Perriard JC, Dewerchin M, Flameng W, Nagy A, Lupu F, Moons L, Collen D, D'Amore PA, Shima DT. Impaired myocardial angiogenesis and ischemic cardiomyopathy in mice lacking the vascular endothelial growth factor isoforms VEGF164 and VEGF188. *Nat Med* 1999, 5:495-502

27. Ng YS, Rohan R, Sunday ME, Demello DE, D'Amore PA. Differential expression of VEGF isoforms in mouse during development and in the adult. *Dev Dyn* 2001, 220:112-121

28. Stalmans I, Ng YS, Rohan R, Fruttiger M, Bouche A, Yuce A, Fujisawa H, Hermans B, Shani M, Jansen S, Hicklin D, Anderson DJ, Gardiner T, Hammes HP, Moons L, Dewerchin M, Collen D, Carmeliet P, D'Amore PA. Arteriolar and venular patterning in retinas of mice selectively expressing VEGF isoforms. *J Clin Invest* 2002, 109:327-336

29. Ishida S, Usui T, Yamashiro K, Kaji Y, Amano S, Ogura Y, Hida T, Oguchi Y, Ambati J, Miller JW, Gragoudas ES, Ng YS, D'Amore PA, Shima DT, Adamis AP. VEGF164-mediated inflammation is required for pathological, but not physiological, ischemia-induced retinal neovascularization. *J Exp Med* 2003, 198:483-489

30. McColm JR, Geisen P, Hartnett ME. VEGF isoforms and their expression after a single episode of hypoxia or repeated fluctuations between hyperoxia and hypoxia: relevance to clinical ROP. *Mol Vis* 2004, 10:512-520

31. de Vries C, Escobedo JA, Ueno H, Houck K, Ferrara N, Williams LT. The fms-like tyrosine kinase, a receptor for vascular endothelial growth factor. *Science* 1992, 255:989-991

32. Terman BI, Dougher-Vermazen M, Carrion ME, Dimitrov D, Armellino DC, Gospodarowicz D, Bohlen P. Identification of the KDR tyrosine kinase as a receptor for vascular endothelial cell growth factor. *Biochem Biophys Res Commun* 1992, 187:1579-1586

33. Millauer B, Wizigmann-Voos S, Schnurch H, Martinez R, Moller NP, Risau W, Ullrich A. High affinity VEGF binding and developmental expression suggest Flk-1 as a major regulator of vasculogenesis and angiogenesis. *Cell* 1993, 72:835-846

34. Peters KG, de Vries C, Williams LT. Vascular endothelial growth factor receptor expression during embryogenesis and tissue repair suggests a role in endothelial differentiation and blood vessel growth. *Proc Natl Acad Sci U S A* 1993, 90:8915-8919

35. Shibuya M, Yamaguchi S, Yamane A, Ikeda T, Tojo A, Matsushime H, Sato M. Nucleotide sequence and expression of a novel human receptor-type tyrosine kinase gene (flt) closely related to the fms family. *Oncogene* 1990, 5:519-524

36. Terman BI, Carrion ME, Kovacs E, Rasmussen BA, Eddy RL, Shows TB. Identification of a new endothelial cell growth factor receptor tyrosine kinase. *Oncogene* 1991, 6:1677-1683

37. Matthews W, Jordan CT, Gavin M, Jenkins NA, Copeland NG, Lemischka IR. A receptor tyrosine kinase cDNA isolated from a population of enriched primitive hematopoietic cells and exhibiting close genetic linkage to c-kit. *Proc Natl Acad Sci U S A* 1991, 88:9026-9030

38. Waltenberger J, Claesson-Welsh L, Siegbahn A, Shibuya M, Heldin CH. Different signal transduction properties of KDR and Flt1, two receptors for vascular endothelial growth factor. *J Biol Chem* 1994, 269:26988-26995

39. Gerber HP, McMurtrey A, Kowalski J, Yan M, Keyt BA, Dixit V, Ferrara N. Vascular endothelial growth factor regulates endothelial cell survival through the phosphatidylinositol 3'-kinase/Akt signal transduction pathway. Requirement for Flk-1/KDR activation. *J Biol Chem* 1998, 273:30336-30343

40. Gille H, Kowalski J, Li B, LeCouter J, Moffat B, Zioncheck TF, Pelletier N, Ferrara N. Analysis of biological effects and signaling properties of Flt-1 (VEGFR-1) and KDR (VEGFR-2). A reassessment using novel receptor-specific vascular endothelial growth factor mutants. *J Biol Chem* 2001, 276:3222-3230

41. Matsumoto T, Claesson-Welsh L. VEGF receptor signal transduction. *Sci STKE* 2001, 2001:RE21

42. Cross MJ, Dixelius J, Matsumoto T, Claesson-Welsh L. VEGF-receptor signal transduction. *Trends Biochem Sci* 2003, 28:488-494

43. Thomas SM, Brugge JS. Cellular functions regulated by Src family kinases. *Annu Rev Cell Dev Biol* 1997, 13:513-609

44. Bull HA, Brickell PM, Dowd PM. Src-related protein tyrosine kinases are physically associated with the surface antigen CD36 in human dermal microvascular endothelial cells. *FEBS Lett* 1994, 351:41-44

45. Kiefer F, Anhauser I, Soriano P, Aguzzi A, Courtneidge SA, Wagner EF. Endothelial cell transformation by polyomavirus middle T antigen in mice lacking Src-related kinases. *Curr Biol* 1994, 4:100-109

46. Eliceiri BP, Paul R, Schwartzberg PL, Hood JD, Leng J, Cheresh DA. Selective requirement for Src kinases during VEGF-induced angiogenesis and vascular permeability. *Mol Cell* 1999, 4:915-924

47. Abu-Ghazaleh R, Kabir J, Jia H, Lobo M, Zachary I. Src mediates stimulation by vascular endothelial growth factor of the phosphorylation of focal adhesion kinase at tyrosine 861, and migration and anti-apoptosis in endothelial cells. *Biochem J* 2001, 360:255-264

48. Eliceiri BP, Puente XS, Hood JD, Stupack DG, Schlaepfer DD, Huang XZ, Sheppard D, Cheresh DA. Src-mediated coupling of focal adhesion kinase to integrin alpha(v)beta5 in vascular endothelial growth factor signaling. *J Cell Biol* 2002, 157:149-160

49. Brugge JS, Erikson RL. Identification of a transformation-specific antigen induced by an avian sarcoma virus. *Nature* 1977, 269:346-348

50. Boerner RJ, Kassel DB, Barker SC, Ellis B, DeLacy P, Knight WB. Correlation of the phosphorylation states of pp60c-src with tyrosine kinase activity: the intramolecular pY530-SH2 complex retains significant activity if Y419 is phosphorylated. *Biochemistry* 1996, 35:9519-9525

51. Lowell CA, Soriano P. Knockouts of Src-family kinases: stiff bones, wimpy T cells, and bad memories. *Genes Dev* 1996, 10:1845-1857

52. Paul R, Zhang ZG, Eliceiri BP, Jiang Q, Boccia AD, Zhang RL, Chopp M, Cheresh DA. Src deficiency or blockade of Src activity in mice provides cerebral protection following stroke. *Nat Med* 2001, 7:222-227

53. Lutty GA, McLeod DS, Merges C, Diggs A, Plouet J. Localization of vascular endothelial growth factor in human retina and choroid. *Arch Ophthalmol* 1996, 114:971-977

54. Vinores SA, Youssri AI, Luna JD, Chen YS, Bhargave S, Vinores MA, Schoenfeld CL, Peng B, Chan CC, LaRochelle W, Green WR, Campochiaro PA. Upregulation of vascular endothelial growth factor in ischemic and non-ischemic human and experimental retinal disease. *Histol Histopathol* 1997, 12:99-109

55. Gao G, Li Y, Zhang D, Gee S, Crosson C, Ma J. Unbalanced expression of VEGF and PEDF in ischemia-induced retinal neovascularization. *FEBS Lett* 2001, 489:270-276

56. Bouck N. PEDF: anti-angiogenic guardian of ocular function. *Trends Mol Med* 2002, 8:330-334

57. Leung DW, Cachianes G, Kuang WJ, Goeddel DV, Ferrara N. Vascular endothelial growth factor is a secreted angiogenic mitogen. *Science* 1989, 246:1306-1309

58. Ferrara N, Houck K, Jakeman L, Leung DW. Molecular and biological properties of the vascular endothelial growth factor family of proteins. *Endocr Rev* 1992, 13:18-32

59. Kim KJ, Li B, Winer J, Armanini M, Gillett N, Phillips HS, Ferrara N. Inhibition of vascular endothelial growth factor-induced angiogenesis suppresses tumour growth in vivo. *Nature* 1993, 362:841-844

60. Ferrara N, Davis-Smyth T. The biology of vascular endothelial growth factor. *Endocr Rev* 1997, 18:4-25

61. Adamis AP, Miller JW, Bernal MT, D'Amico DJ, Folkman J, Yeo TK, Yeo KT. Increased vascular endothelial growth factor levels in the vitreous of eyes with proliferative diabetic retinopathy. *Am J Ophthalmol* 1994, 118:445-450

62. Bullard LE, Qi X, Penn JS. Role for extracellular signal-responsive kinase-1 and -2 in retinal angiogenesis. *Invest Ophthalmol Vis Sci* 2003, 44:1722-1731

63. Tombran-Tink J, Chader GG, Johnson LV. PEDF: a pigment epithelium-derived factor with potent neuronal differentiative activity. *Exp Eye Res* 1991, 53:411-414

64. Tombran-Tink J, Shivaram SM, Chader GJ, Johnson LV, Bok D. Expression, secretion, and age-related downregulation of pigment epithelium-derived factor, a serpin with neurotrophic activity. *J Neurosci* 1995, 15:4992-5003

65. Dawson DW, Volpert OV, Gillis P, Crawford SE, Xu H, Benedict W, Bouck NP. Pigment epithelium-derived factor: a potent inhibitor of angiogenesis. *Science* 1999, 285:245-248

66. Stellmach V, Crawford SE, Zhou W, Bouck N. Prevention of ischemia-induced retinopathy by the natural ocular antiangiogenic agent pigment epithelium-derived factor. *Proc Natl Acad Sci U S A* 2001, 98:2593-2597

67. Volpert OV, Zaichuk T, Zhou W, Reiher F, Ferguson TA, Stuart PM, Amin M, Bouck NP. Inducer-stimulated Fas targets activated endothelium for destruction by anti-angiogenic thrombospondin-1 and pigment epithelium-derived factor. *Nat Med* 2002, 8:349-357

68. Ashton N, WARD B, SERPELL G. Role of oxygen in the genesis of retrolental fibroplasia; a preliminary report. *Br J Ophthalmol* 1953, 37:513-520

69. Hardy P, Dumont I, Bhattacharya M, Hou X, Lachapelle P, Varma DR, Chemtob S. Oxidants, nitric oxide and prostanoids in the developing ocular vasculature: a basis for ischemic retinopathy. *Cardiovasc Res* 2000, 47:489-509

70. Foos RY. Chronic retinopathy of prematurity. *Ophthalmology* 1985, 92:563-574

71. Penn JS, Henry MM, Tolman BL. Exposure to alternating hypoxia and hyperoxia causes severe proliferative retinopathy in the newborn rat. *Pediatr Res* 1994, 36:724-731

72. Penn JS, Henry MM, Wall PT, Tolman BL. The range of PaO2 variation determines the severity of oxygen-induced retinopathy in newborn rats. *Invest Ophthalmol Vis Sci* 1995, 36:2063-2070

73. Lutty GA, McLeod DS. A new technique for visualization of the human retinal vasculature. *Arch Ophthalmol* 1992, 110:267-276

74. Penn JS, Tolman BL, Lowery LA. Variable oxygen exposure causes preretinal neovascularization in the newborn rat. *Invest Ophthalmol Vis Sci* 1993, 34:576-585

75. Robbins SG, Rajaratnam VS, Penn JS. Evidence for upregulation and redistribution of vascular endothelial growth factor (VEGF) receptors flt-1 and flk-1 in the oxygen-injured rat retina. *Growth Factors* 1998, 16:1-9

76. McLeod DS, Taomoto M, Cao J, Zhu Z, Witte L, Lutty GA. Localization of VEGF receptor-2 (KDR/Flk-1) and effects of blocking it in oxygen-induced retinopathy. *Invest Ophthalmol Vis Sci* 2002, 43:474-482

77. Saito Y, Omoto T, Cho Y, Hatsukawa Y, Fujimura M, Takeuchi T. The progression of retinopathy of prematurity and fluctuation in blood gas tension. *Graefes Arch Clin Exp Ophthalmol* 1993, 231:151-156

78. Cunningham S, Fleck BW, Elton RA, McIntosh N. Transcutaneous oxygen levels in retinopathy of prematurity. *Lancet* 1995, 346:1464-1465

79. York JR, Landers S, Kirby RS, Arbogast PG, Penn JS. Arterial oxygen fluctuation and retinopathy of prematurity in very-low-birth-weight infants. *J Perinatol* 2004, 24:82-87

80. Kinsey VE, Arnold HJ, Kalina RE, Stern L, Stahlman M, Odell G, Driscoll JM, Jr., Elliott JH, Payne J, Patz A. PaO2 levels and retrolental fibroplasia: a report of the cooperative study. *Pediatrics* 1977, 60:655-668

81. Patz A. Clinical and experimental studies on retinal neovascularization. *Am J Ophthalmol* 1982, 94:715-743

82. Kalina RE, Karr DJ. Retrolental fibroplasia. Experience over two decades in one institution. *Ophthalmology* 1982, 89:91-5, 103

83. Reynaud X, Dorey CK. Extraretinal neovascularization induced by hypoxic episodes in the neonatal rat. *Invest Ophthalmol Vis Sci* 1994, 35:3169-3177

84. Penn JS, Tolman BL, Henry MM. Oxygen-induced retinopathy in the rat: relationship of retinal nonperfusion to subsequent neovascularization. *Invest Ophthalmol Vis Sci* 1994, 35:3429-3435

85. Ashton N, COOK C. Direct observation of the effect of oxygen on developing vessels: preliminary report. *Br J Ophthalmol* 1954, 38:433-440

86. Simpson DA, Murphy GM, Bhaduri T, Gardiner TA, Archer DB, Stitt AW. Expression of the VEGF gene family during retinal vaso-obliteration and hypoxia. *Biochem Biophys Res Commun* 1999, 262:333-340

87. Newman E, Reichenbach A. The Muller cell: a functional element of the retina. *Trends Neurosci* 1996, 19:307-312

88. Winkler BS, Arnold MJ, Brassell MA, Puro DG. Energy metabolism in human retinal Muller cells. *Invest Ophthalmol Vis Sci* 2000, 41:3183-3190

89. Robbins SG, Conaway JR, Ford BL, Roberto KA, Penn JS. Detection of vascular endothelial growth factor (VEGF) protein in vascular and non-vascular cells of the normal and oxygen-injured rat retina. *Growth Factors* 1997, 14:229-241

90. Hicks D, Courtois Y. The growth and behaviour of rat retinal Muller cells in vitro. 1. An improved method for isolation and culture. *Exp Eye Res* 1990, 51:119-129

91. Sarthy VP, Brodjian SJ, Dutt K, Kennedy BN, French RP, Crabb JW. Establishment and characterization of a retinal Muller cell line. *Invest Ophthalmol Vis Sci* 1998, 39:212-216

92. Conn G, Bayne ML, Soderman DD, Kwok PW, Sullivan KA, Palisi TM, Hope DA, Thomas KA. Amino acid and cDNA sequences of a vascular endothelial cell mitogen that is homologous to platelet-derived growth factor. *Proc Natl Acad Sci U S A* 1990, 87:2628-2632

93. Stone J, Itin A, Alon T, Pe'er J, Gnessin H, Chan-Ling T, Keshet E. Development of retinal vasculature is mediated by hypoxia-induced vascular endothelial growth factor (VEGF) expression by neuroglia. *J Neurosci* 1995, 15:4738-4747

94. Folkman J. Angiogenesis in cancer, vascular, rheumatoid and other disease. *Nat Med* 1995, 1:27-31

95. Griffioen AW, Molema G. Angiogenesis: potentials for pharmacologic intervention in the treatment of cancer, cardiovascular diseases, and chronic inflammation. *Pharmacol Rev* 2000, 52:237-268

96. Senger DR, Galli SJ, Dvorak AM, Perruzzi CA, Harvey VS, Dvorak HF. Tumor cells secrete a vascular permeability factor that promotes accumulation of ascites fluid. *Science* 1983, 219:983-985

97. Connolly DT, Heuvelman DM, Nelson R, Olander JV, Eppley BL, Delfino JJ, Siegel NR, Leimgruber RM, Feder J. Tumor vascular permeability factor stimulates endothelial cell growth and angiogenesis. *J Clin Invest* 1989, 84:1470-1478

98. Alon T, Hemo I, Itin A, Pe'er J, Stone J, Keshet E. Vascular endothelial growth factor acts as a survival factor for newly formed retinal vessels and has implications for retinopathy of prematurity. *Nat Med* 1995, 1:1024-1028

99. De VC, Escobedo JA, Ueno H, Houck K, Ferrara N, Williams LT. The fms-like tyrosine kinase, a receptor for vascular endothelial growth factor. *Science* 1992, 255:989-991

100. He H, Venema VJ, Gu X, Venema RC, Marrero MB, Caldwell RB. Vascular endothelial growth factor signals endothelial cell production of nitric oxide and prostacyclin through flk-1/KDR activation of c-Src. *J Biol Chem* 1999, 274:25130-25135

101. Zachary I. VEGF signalling: integration and multi-tasking in endothelial cell biology. *Biochem Soc Trans* 2003, 31:1171-1177

102. Elbashir SM, Harborth J, Lendeckel W, Yalcin A, Weber K, Tuschl T. Duplexes of 21-nucleotide RNAs mediate RNA interference in cultured mammalian cells. *Nature* 2001, 411:494-498

103. Tijsterman M, Ketting RF, Plasterk RH. The genetics of RNA silencing. *Annu Rev Genet* 2002, 36:489-519

104. Elbashir SM, Harborth J, Weber K, Tuschl T. Analysis of gene function in somatic mammalian cells using small interfering RNAs. *Methods* 2002, 26:199-213

105. McManus MT, Haines BB, Dillon CP, Whitehurst CE, van PL, Chen J, Sharp PA. Small interfering RNA-mediated gene silencing in T lymphocytes. *J Immunol* 2002, 169:5754-5760

106. Holen T, Amarzguioui M, Wiiger MT, Babaie E, Prydz H. Positional effects of short interfering RNAs targeting the human coagulation trigger Tissue Factor. *Nucleic Acids Res* 2002, 30:1757-1766

107. Parrish S, Fleenor J, Xu S, Mello C, Fire A. Functional anatomy of a dsRNA trigger: differential requirement for the two trigger strands in RNA interference. *Mol Cell* 2000, 6:1077-1087

108. Tuschl T, Elbashir SM, Harborth J, Weber K. The siRNA user guide. *http://www rockefeller edu/labheads/tuschl/sirna html* 2004,

109. Ding Q, Stewart J, Jr., Olman MA, Klobe MR, Gladson CL. The pattern of enhancement of Src kinase activity on platelet-derived growth factor stimulation of

glioblastoma cells is affected by the integrin engaged. *J Biol Chem* 2003, 278:39882-39891

110. Rodriguez-Nieto S, Gonzalez-Iriarte M, Carmona R, Munoz-Chapuli Rn, Medina MA, Quesada AR. Antiangiogenic activity of aeroplysinin-1, a brominated compound isolated from a marine sponge. *FASEB J* 2001,01-0427fje

111. Guo D, Jia Q, Song HY, Warren RS, Donner DB. Vascular endothelial cell growth factor promotes tyrosine phosphorylation of mediators of signal transduction that contain SH2 domains. Association with endothelial cell proliferation. *J Biol Chem* 1995, 270:6729-6733

112. Xia P, Aiello LP, Ishii H, Jiang ZY, Park DJ, Robinson GS, Takagi H, Newsome WP, Jirousek MR, King GL. Characterization of vascular endothelial growth factor's effect on the activation of protein kinase C, its isoforms, and endothelial cell growth. *J Clin Invest* 1996, 98:2018-2026

113. Resh MD. Myristylation and palmitylation of Src family members: the fats of the matter. *Cell* 1994, 76:411-413

114. Robbins SM, Quintrell NA, Bishop JM. Myristoylation and differential palmitoylation of the HCK protein-tyrosine kinases govern their attachment to membranes and association with caveolae. *Mol Cell Biol* 1995, 15:3507-3515

115. Kaplan KB, Swedlow JR, Varmus HE, Morgan DO. Association of p60c-src with endosomal membranes in mammalian fibroblasts. *J Cell Biol* 1992, 118:321-333

116. Magee AI, Gutierrez L, McKay IA, Marshall CJ, Hall A. Dynamic fatty acylation of p21N-ras. *EMBO J* 1987, 6:3353-3357

117. Walker F, deBlaquiere J, Burgess AW. Translocation of pp60c-src from the plasma membrane to the cytosol after stimulation by platelet-derived growth factor. *J Biol Chem* 1993, 268:19552-19558

118. Majno G, Joris I. Apoptosis, oncosis, and necrosis. An overview of cell death. *Am J Pathol* 1995, 146:3-15

119. Fadok VA, Voelker DR, Campbell PA, Cohen JJ, Bratton DL, Henson PM. Exposure of phosphatidylserine on the surface of apoptotic lymphocytes triggers specific recognition and removal by macrophages. *J Immunol* 1992, 148:2207-2216

120. Willingham MC. Cytochemical methods for the detection of apoptosis. *J Histochem Cytochem* 1999, 47:1101-1110

121. Rousseau S, Houle F, Kotanides H, Witte L, Waltenberger J, Landry J, Huot J. Vascular endothelial growth factor (VEGF)-driven actin-based motility is mediated by VEGFR2 and requires concerted activation of stress-activated protein kinase 2

(SAPK2/p38) and geldanamycin-sensitive phosphorylation of focal adhesion kinase. *J Biol Chem* 2000, 275:10661-10672

122. Barleon B, Sozzani S, Zhou D, Weich HA, Mantovani A, Marme D. Migration of human monocytes in response to vascular endothelial growth factor (VEGF) is mediated via the VEGF receptor flt-1. *Blood* 1996, 87:3336-3343

123. Clauss M, Weich H, Breier G, Knies U, Rockl W, Waltenberger J, Risau W. The vascular endothelial growth factor receptor Flt-1 mediates biological activities. Implications for a functional role of placenta growth factor in monocyte activation and chemotaxis. *J Biol Chem* 1996, 271:17629-17634

124. Kanno S, Oda N, Abe M, Terai Y, Ito M, Shitara K, Tabayashi K, Shibuya M, Sato Y. Roles of two VEGF receptors, Flt-1 and KDR, in the signal transduction of VEGF effects in human vascular endothelial cells. *Oncogene* 2000, 19:2138-2146

125. Gille H, Kowalski J, Yu L, Chen H, Pisabarro MT, Davis-Smyth T, Ferrara N. A repressor sequence in the juxtamembrane domain of Flt-1 (VEGFR-1) constitutively inhibits vascular endothelial growth factor-dependent phosphatidylinositol 3'-kinase activation and endothelial cell migration. *EMBO J* 2000, 19:4064-4073

126. Chou MT, Wang J, Fujita DJ. Src kinase becomes preferentially associated with the VEGFR, KDR/Flk-1, following VEGF stimulation of vascular endothelial cells. *BMC Biochem* 2002, 3:32

127. McManus MT, Sharp PA. Gene silencing in mammals by small interfering RNAs. *Nat Rev Genet* 2002, 3:737-747

128. Bridge AJ, Pebernard S, Ducraux A, Nicoulaz AL, Iggo R. Induction of an interferon response by RNAi vectors in mammalian cells. *Nat Genet* 2003, 34:263-264

129. Sledz CA, Holko M, de Veer MJ, Silverman RH, Williams BR. Activation of the interferon system by short-interfering RNAs. *Nat Cell Biol* 2003, 5:834-839

130. Ashton N. Retinal vascularization in health and disease. *Am J Ophthalmol* 1957, 44:7-17

131. Roskoski R, Jr. Src protein-tyrosine kinase structure and regulation. *Biochem Biophys Res Commun* 2004, 324:1155-1164

132. Smith LE. Pathogenesis of retinopathy of prematurity. *Semin Neonatol* 2003, 8:469-473

133. Shafiee A, Penn JS, Krutzsch HC, Inman JK, Roberts DD, Blake DA. Inhibition of retinal angiogenesis by peptides derived from thrombospondin-1. *Invest Ophthalmol Vis Sci* 2000, 41:2378-2388

134. McLeod DS, Lutty GA, Wajer SD, Flower RW. Visualization of a developing vasculature. *Microvasc Res* 1987, 33:257-269

135. Penn JS, Tolman BL, Bandyopadhyay A, Mauldin DV. Retinal Vasoformation in the Rat As Illustrated by Adenosine Diphosphatase Staining. *Investigative Ophthalmology & Visual Science* 1991, 32:1147

136. Zhang S, Leske DA, Holmes JM. Neovascularization grading methods in a rat model of retinopathy of prematurity. *Invest Ophthalmol Vis Sci* 2000, 41:887-891

137. Calalb MB, Zhang X, Polte TR, Hanks SK. Focal adhesion kinase tyrosine-861 is a major site of phosphorylation by Src. *Biochem Biophys Res Commun* 1996, 228:662-668

138. Karni R, Mizrachi S, Reiss-Sklan E, Gazit A, Livnah O, Levitzki A. The pp60c-Src inhibitor PP1 is non-competitive against ATP. *FEBS Lett* 2003, 537:47-52

139. Werdich XQ, McCollum GW, Rajaratnam VS, Penn JS. Variable oxygen and retinal VEGF levels: correlation with incidence and severity of pathology in a rat model of oxygen-induced retinopathy. *Exp Eye Res* 2004, 79:623-630

140. Newman EP: Glia of the retina. Retina. Edited by Ryan SJ. St. Louis, Mosby, 2001, pp. 89-103

141. Rosenfeldt HM, Hobson JP, Maceyka M, Olivera A, Nava VE, Milstien S, Spiegel S. EDG-1 links the PDGF receptor to Src and focal adhesion kinase activation leading to lamellipodia formation and cell migration. *FASEB J* 2001, 15:2649-2659

142. Cary LA, Klinghoffer RA, Sachsenmaier C, Cooper JA. Src catalytic but not scaffolding function is needed for integrin-regulated tyrosine phosphorylation, cell migration, and cell spreading. *Mol Cell Biol* 2002, 22:2427-2440

143. Takahashi T, Shibuya M. The 230 kDa mature form of KDR/Flk-1 (VEGF receptor-2) activates the PLC-gamma pathway and partially induces mitotic signals in NIH3T3 fibroblasts. *Oncogene* 1997, 14:2079-2089

144. Janzer RC, Raff MC. Astrocytes induce blood-brain barrier properties in endothelial cells. *Nature* 1987, 325:253-257

145. Tsygankov AY, Shore SK. Src: regulation, role in human carcinogenesis and pharmacological inhibitors. *Curr Pharm Des* 2004, 10:1745-1756

146. Knebel A, Morrice N, Cohen P. A novel method to identify protein kinase substrates: eEF2 kinase is phosphorylated and inhibited by SAPK4/p38delta. *EMBO J* 2001, 20:4360-4369